Rui Tiago Pinto dos Santos Beleza de Seabra Assessment of a Gothic steel church: San Sebastian Church

Portugal | 2016

ADVANCED MASTERS IN STRUCTURAL ANALYSIS
OF MONUMENTS AND HISTORICAL CONSTRUCTIONS

Master's Thesis

Rui Tiago Pinto dos Santos Beleza de Seabra

Assessment of a Gothic steel church: San Sebastian Church

University of Minho

Czech university of Prague

Education and Culture

Erasmus Mundus

ADVANCED MASTERS IN STRUCTURAL ANALYSIS
OF MONUMENTS AND HISTORICAL CONSTRUCTIONS

Master's Thesis

Rui Tiago Pinto dos Santos Beleza de Seabra

Assessment of a Gothic steel church: San Sebastian Church

This Masters Course has been funded with support from the European Commission. This publication reflects the views only of the author, and the Commission cannot be held responsible for any use which may be made of the information contained therein.

Portugal | 2016

DECLARATION

Name:	Rui Tiago Pinto dos Santos Beleza de Seabra
Email:	ruisantosseabra@gmail.com

Title of the Msc Dissertation:	Assessment of a Gothic steel church: San Sebastian Church
Supervisor(s):	Nuno Mendes, Paulo Lourenço
Year:	2016

I hereby declare that all information in this document has been obtained and presented in accordance with academic rules and ethical conduct. I also declare that, as required by these rules and conduct, I have fully cited and referenced all material and results that are not original to this work.

I hereby declare that the MSc Consortium responsible for the Advanced Masters in Structural Analysis of Monuments and Historical Constructions is allowed to store and make available electronically the present MSc Dissertation.

University:	University of Minho
Date:	September 1, 2016
Signature:	_____

This page is left blank on purpose.

To my parents…

This page is left blank on purpose.

ACKNOWLEDGEMENTS

Along this hard Journey last year, I met a lot of people that taught me important values. I hope to carry these values along my life. These people, and my Friends, changed my life in many ways, and without them, this Journey would have been much harder. To all of them, my deepest acknowledgement!

First, I would like to express my gratitude to my supervisor, Professor Nuno Mendes, for his patience, support and dedication to my thesis. I also would like to thank him for the knowledge on dynamic monitoring he taught me. I am sure that if I have the opportunity to do something like that in the future, I will apply his teachings. I want to thank him for the help he gave me in the Philippines during the dynamic testing. And also for the relaxing dinners and for the Adventure of the return.

Second, my acknowledgement goes to Professor Paulo Lourenço, co-supervisor of this thesis, for his practical view on the approach to Civil Engineering and conservation of historical constructions. I also would like to thank him for his help, precise and precious advices.

My gratitude to Tina Paterno and Alfonso Ancheta, for their kindness, help during the dynamic testing in Manila. I will never forget their hospitality.

My gratitude also goes to Giorgos Karanikoloudis, for his infinite (and beyond…) patience with his advices on how to work with DIANA software.

My gratitude to all PhD students at the University of Minho, for their warm welcome. They were important to the adaptation to the University.

I also thank all of the SAHC colleagues of this Masters.

I thank all the SAHC professors for the transmitted knowledge. Among them, I would like to refer Prof. Petr Kabele, for teaching me that with simple things, complex things turn simple; Prof. Climent Molins, for teaching me how to look at ancient structures in a different way, and to think outside the box; Prof. Petr Štemberk, for his particular way to approach Civil Engineering and the way he passes his knowledgement and enthusiasm to the students; Prof Pere Roca, for the invaluable transmitted knowledge.

I thank to Hugo Matos, Diogo Augusto, Luís Silva, Paulo Neto, Ricardo Marinho, Vítor Pascoal, Ana Ramos, Vera Azevedo, for their Friendship for Life!

I thank to Carlos Rodrigues, to whom I am grateful for the given opportunity, for his good will, for the patience he had with me and for his life teachings.

Finally, to the Professors of my life, the Engineers of my life, my Parents for being a lamp, a light on my path. I wholeheartedly dedicate to them this work. Without their extreme effort and work throughout the years, and their persistence on making me take this Masters, I would never have had the chance to do it.

Erasmus Mundus Programme

This page is left blank on purpose.

This page is left blank on purpose.

This page is left blank on purpose.

ABSTRACT

Philippines is a country where the structures built there have to be resistant to seismic action. Buildings built nowadays take into consideration this aspect, and specific rules are given in order to provide the structures with the resistance enough to resist the generated forces in an earthquake. However, buildings built in the past did not take into account these horizontal forces. In the past, people was aware about the existence of earthquakes, but it was not aware on their impact on the structural behaviour of the structures. Nowadays, with technological advances, seismic activity is now better characterized, and the safety of heritage buildings can be assessed by means of numerical models. This safety can also be assessed by means of historical surveying, NDT tests and dynamic testing. Both numerical models and experimental results are important, since they allow to conclude on the influence of the damage on the structure.

In this thesis the following approach was used., First, the structure was described (either historically and structurally), the material properties were also analysed and past interventions were presented.

Then, two numerical models were subjected to vertical and horizontal loads. Finally, the corrosion effects were also studied by reducing the thickness of the steel plates that compose the columns of the structure. The results showed that for a 40% corrosion damage, the horizontal capacity of the structure reduced 22%, and the vertical capacity for the same level of corrosion damage decreased 20%. It was also possible to conclude that the studied part of the structure had a high capacity for horizontal loads. The capacity of the two models is higher than the reference values for acceleration.

This page is left blank on purpose.

RESUMO

As Filipinas são um país no qual as estruturas que são construídas têm de apresentar resistência à ação sísmica. Os edifícios atuais construídos nos últimos anos têm em consideração este aspeto, e o seu dimensionamento cumpre regras específicas que impedem que colapsem quando submetidos às forças horizontais do sismo. Contudo, os edifícios antigos não eram dimensionados de forma a resistir a este tipo de forças. No passado, as sociedades estavam alertadas para a possibilidade da ocorrência de sismos, mas não estavam cientes do impacto no comportamento estrutural que um evento deste tipo causa. Nos dias de hoje, e devido aos avanços no conhecimento cientifico e tecnológico, a atividade sísmica é caracterizada de forma mais precisa, e desta forma, a segurança dos edifícios patrimoniais pode ser avaliada através de modelos numéricos. Além disso, deve-se também fazer um levantamento histórico do edifício, e efectuar ensaios não destrutivos. A modelação numérica e o diagnóstico são fundamentais, pois permitem concluir sobre o estado de conservação, o dano existente e o desempenho da estrutura.

Esta tese seguiu a seguinte abordagem: Primeiro, descreveu-se a estrutura em estudo (quer do ponto de vista histórico, quer do ponto de vista estrutural), e foram analisadas as propriedades dos materiais e as intervenções efetuadas no passado. De seguida, foram preparados dois modelos numéricos e, posteriormente foram submetidos às cargas verticais e horizontais. Por último, foram avaliados os efeitos da corrosão, reduzindo a espessura das chapas de aço dos pilares de forma uniforme em toda a estrutura. Os resultados permitiram concluir que para um nível de corrosão de 40%, a capacidade da estrutura reduzia 22%; e para a capacidade vertical, para o mesmo nível de corrosão, a capacidade da estrutura reduzia 20%. Foi ainda possível concluir que a parte em estudo da estrutura tem uma elevada capacidade para resistir a forças horizontais. Para ambos os modelos, os valores da capacidade eram superiores aos valores de referência da aceleração.

This page is left blank on purpose.

TABLE OF CONTENTS

FIGURE INDEX

1. INTRODUCTION

1.1 Motivation

The San Sebastian Church is located in the city center of Manila. Dating from 1891, the church is integrated in the district of Quiapo, and it is in the Tentative List for the World Heritage Site by UNESCO. The church also assumes an important cultural value, since in the country there are few neo-gothic churches, and it belongs to the Spanish colonial era.

Philippines is a country located in the Pacific ring of fire, which is known for the strong seismic activity, and over its long history, the country had endured through strong earthquakes. The church that is object of study of this thesis is not the original one. Originally the church was made out of masonry, until the priest responsible for the church asked Genaro Palacios to rebuild a church that would be “anti-tremors”. Nowadays, the church does not present damage due to seismic activity, but it presents severe damage due to water infiltration that must be addressed, and its impact also has to be studied.

That is why due to its history, cultural significance, structural typology and current state, that it turns out of importance to study the San Sebastian structural behavior.

1.2 Objectives of the work

The current thesis pretends to study the behaviour of a part of the San Sebastian church, located in the capital city of the Philippines, Manila. This study will comprehend a description of the building, a summary on all the performed tests there and a structural analysis of a part of the structure.

In order to study the structure behaviour, several tasks were done:

- Historical surveying was carried out in order to understand the structure.
- An analysis on the data given by the report was performed
- The vertical and horizontal stability of a part of the structure was evaluated taking into account all of the information that was given by the conditions assessment report.

For a proper analysis of the structure, and since the steel that was part of the columns presented damage due to corrosion effects, a study on the effects of different levels of corrosion on the structural behaviour was also performed.

1.3 Thesis Outline

The present thesis is composed by six chapters. In general, it comprises the historical survey, the dynamic testing, and the structural analysis. Chapter 2 describes the structure. Chapter 3 presents all the testing performed in the structure. Chapters 4 and 5 are dedicated to the numerical models. A synopsis of each chapter is given below.

The first chapter gives a brief introduction to the studied topic and points out the relevance and importance that this case study assumes, and the motivations for the choice of this theme.

The second chapter comprehends a full characterization of the building, both historical and structural. Columns, towers, dome, foundations, roof framing system, walls and floors are here described. Much of these descriptions were provided by the Assessment Conditions Report provided by the Church Foundation. Material properties are also presented, and a description of past interventions is provided.

The third chapter approaches all the performed in-situ tests. All the studies regarding the column cross-section reductions, ground penetrating radar, rotation measurements, temperature and humidity measurements are presented. The dynamic identification testing that was performed during the visit is also presented.

The fourth chapter presents the assumptions that were assumed for the modelling of the structure, particularly, boundary conditions, material properties and the type of elements used. A validation of the numerical models with a linear static analysis for the self-weight is also presented. Since two numerical models were done, a presentation of each model is given in this chapter.

The fifth chapter presents all of the performed numerical analysis (vertical and horizontal loading) for the two considered models. A study on the vertical and horizontal capacity of the structure as function of the corrosion damage is also presented.

The sixth chapter presents a summary on all the conclusions that were obtained by this thesis and future works are also proposed.

2. THE DESCRIPTION OF THE SAN SEBASTIAN CHURCH

2.1 Historical review

The San Sebastian Church is located in the capital city of the Philippines, Manila, in Plaza del Carmen Square, and in the San Rafael Street. In the next Figures (Figure 1 and Figure 2), an aerial view of the location of the church, and a photo of it can be seen.

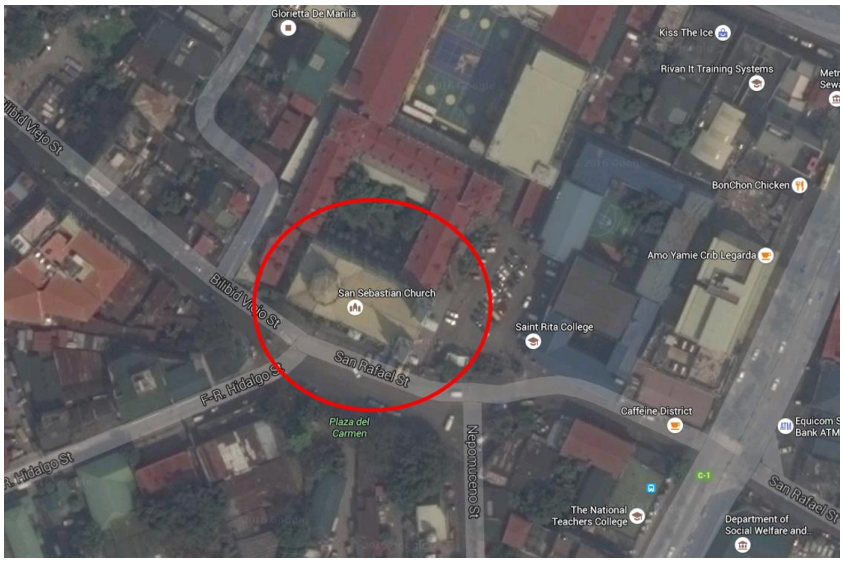

Figure 1 – Aerial view with the location of the church.

Figure 2 - The San Sebastian Church.

The original San Sebastian Church, is not the one we can observe nowadays. The first version of the church was built in 1621 in a land (Figure 3) that was donated to the religious order of the Augustinian

Recollects by Don Bernardino de Castillo Maldonado y Rivera, Maestro de Campo of the Royal Infantry Battalion and commander of Fort Santiago, and his wife, Doña Maria Enriquez de Céspedes.

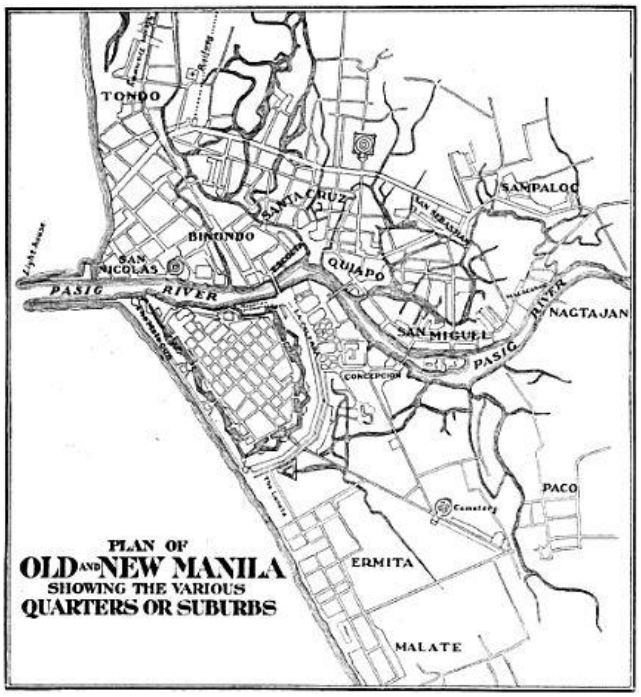

Figure 3 – Map of Manila at the time of the construction(Leggio 2012).

The land was donated to the Order with the condition that in it a church and a convent dedicated to San Sebastian would be built (Romanillos 2001). It is said the church housed the first image of Our Lady of Mount Carmel. It is because of this fact that this church is considered as the national shrine of the Carmelite devotion in the Philippines, and therefore, emphasizing the importance it represents for the locals. The Order of Augustinian Recollects is the entity that is responsible for the church, since 1621. The first church was inaugurated on the May 5, 1621, and was described by historians and story-tellers as “curious,” “well built,” and of “medium” size (Romanillos 2001). However, this church did not last for long. In 1639, it was looted and damaged in the Sangley Uprising (the second rebellion led by mixed Chinese and indigenous/Indio Filipino ancestries). Years later, in 1645, a devastating earthquake, known as the San Andreas earthquake, completely destroyed the church. This earthquake is regarded as the most destructive earthquake throughout the whole Spanish occupation.

Soon after the earthquake, the Recollect monks demolished what was left of the church, and started to build a larger, and more decorated church on the same place (Salvatierra 1993, p21). Made of masonry, the second church is said to consist on “one nave with a transept which served as the main church, and a very spacious presbytery with ten large glass windows facing the street, five doors, confessionals made of tindalo, the pews of molave and tindalo. (Romanillos 2001).

This church proved to be more resistant than the previous one, lasting for at least ten major earthquakes, before undergoing an extensive renovation and expansion, which added two rows of columns in the centre of the nave and raised the height of the church in 1859-61. Two years after these interventions, a devastating earthquake occurred in Manila, causing major damage in Manila Cathedral and in the Saint Augustin Church (Romanillos 2001). The San Sebastian church was no exception, and again the Recollects wasted no time, and started to rebuild a new church. The church was opened to public on January 20, 1867. This version of the church lasted for 13 years before being severely damaged by the earthquake of 1880, where the walls were severely damaged. The timber members were also being severely attacked by termites and weevils (Romanillos 2001). The damage was so much that the Head of Civil Works for the Colonial Government of Spain, Genaro Palacios, had no other choice, but to classify the condition of it as a life safety issue. Palacios, a Spanish engineer specialized in seismic engineering assumed the responsibility of the design and the construction of it. Palacios said that the new church, made in steel, would be stronger, but lighter than masonry, making it “ideal for tremors”. It was said that it would be earthquake proof, termite-proof, and, they assumed, fire-proof.

The Philippines are located in one of the most intense world areas in what concerns seismic activity. This area is called the Pacific Ring of Fire, where there is a frequent and strong seismic activity. This is the reason why the most predominant architectural style is the baroque style, due to their limited height. It is, therefore, reasonable to say that this structure has an important cultural value, since in the country there are few neo-gothic churches, and it belongs to the Spanish colonial era. Other relevant features are:

-It is the first and only fully prefabricated metal structure in the Philippines, and possibly in all Asia.

-It is one of the last churches in the Philippines that kept its original design, interior finishes and materials.

The design of the building was the result of a close collaboration between Palacios and the Recollect monks from Manila and Madrid, and lasted for three years. As soon as the design was finished and approved, a bid concerning the steel production work was started and sent to companies in Spain, England, France and Belgium.

The bid was won by the company that proposed the lowest price, the Belgian company *Société Anonyme de Travaux Publics*, that was known for working on many large-scale structural steel projects (Figure 4). Despite being famous for bridge construction, the company also constructed some buildings such as the *Museo Nacional de Ciencias Naturales*, in Madrid, Spain.

Figure 4 – Blueprint for Palacios' church design (Leggio 2012).

It was common at that time, that the items, before being shipped, were first assembled in the factory to ensure that any defective parts would not be dispatched, allowing all parts to fit in each ship. The same happened to this case. Each piece was weighted, described and measured before being sent off. All pieces arrived in Manila between June 1888 and August 1890 (Figure 5).

Figure 5 – Assembly of a part of the basilica in a factory (Conservation and Development Foundation 2014).

Each piece was shipped already primed (the first primer was red lead in linseed oil). After the first primer, a second primer (white lead in oil paint) was applied, ready to receive the decorative trompe l'oeil finish locally. All columns were pre-assembled and shipped as vertical segments, and each four sides of them were fully riveted, to be stacked and spliced together locally (Figure 6). The decorative parts would be fastened in-situ. At that time, an impressive amount of 1500 tons of steel and cast iron parts, along with the stained glass arrived in Quiapo (the district where the church is located). The basilica was constructed by Filipino workers, artisans and craftsmen, together with an international crew, as follows:

- Foundations: Magin Pers French;

- Foreman: Frederick Sawyer, British;

- Assembly: Peter Brakel and Didier Carpentier, Belgian;

- Floors: Quentin, Chinese;

-Stained glass imported from Henri Oidtman, Germany;

- Interior finishes: Academia de *Dibujo, Pintura y Arte*, a local art school under the leadership of Lorenzo Rocha.

In-situ, all of these parts were screwed, bolted and riveted. In order to hide the industrial nature of the building, the columns were covered by mouldings, cornices, and fluting. The seams and joints were filled with putty in order to make surfaces look like carved stone.

Figure 6 – Construction of the Steel Church (Conservation and Development Foundation 2014).

For the final appearance, both interior and exterior were faux finished to look like stone. Interior surfaces still have the original faux stone veining, false joints, and trompe l'oeil of statues of saints and martyrs in niches.

The interiors, made with the trompe l'oeil technique are unique, and make this church assume larger historical relevance. They are one of the last surviving original interior finishes of a church in the country. This church might also be the last one in the country, where the metal finish pretends to imitate another material. When the survey carried out by the San Sebastian Basilica Conservation and Development Foundation Inc. took place, many remains of the time that it was constructed were found, hidden in places that the builders thought they were never going to be found.

The church took a decade to build, and on August 15, 1891, the steel church was inaugurated. In the meantime, Pope Leo XIII in 1890, declared it a basilica (Figure 7).

Figure 7 – The San Sebastian Church in 1900.

In 1973, the church was declared a National Historical Landmark, and a National Cultural Treasure in 2011. It was also on the World Monuments Fund Watch list in 1998 and 2010. The church is in the Tentative List for the World Heritage Site by UNESCO.

2.2 Description of the building

2.2.1 General description

The San Sebastian Church is located next to a College that is ruled by the religious community of the Recollect Brothers. Figure 8 presents an aerial view of the church.

Figure 8 – General view of the Church.

The church has a length of 52.7m and it is 24.5m wide. There are two towers, with 48m height. In the altar area, there is a dome with 30m height. The dome has approximately 10m width in each direction. It has a total number of 57 columns. All of the columns are made out of rectangular hollow sections (RHS), with a regular size of 600mm x 600mm each. When the required section is higher, the columns are made out of several hollow sections connected by steel plates and rivets. The maximum number of RHS's it reaches is five, in the tower area in the main façade corners.

Inside the church (Figure 9), there is a choir loft that has the total width of the church and the length of the first three columns. There is also on this level an extension of the floor that extends for 6m. This choir loft is made entirely out of steel as well, but the finishing at this level is made out of timber. The floor is made out of a grid of beams oriented both in the longitudinal and transversal direction. The longitudinal beams have 50mm width, and 140mm height, and span the full length of the three columns. The transversal beams have 100m width and 150mm height.

Figure 9 – Interior of the church.

There are two types of steel being used in this church, depending on the location, and its requirements from the structural point of view. The most demanding areas from the structural point of view, like columns and walls are made out of mild steel, and the less demanding elements are made of cast iron. There is also an important factor helping to the deterioration of the columns that was an intervention made out in the 1980's, where concrete was applied in the columns. Since concrete is, in general, a porous material and cement does not adhere very well to metal, the metal started to corrode due to the presence of water accumulation.

2.2.2 Columns

The interior columns consist of a rectangular hollow shape, and based on historical documentation, they have isolated concrete foundations. Figure 10 illustrates the appearance and the constitution of the columns inside.

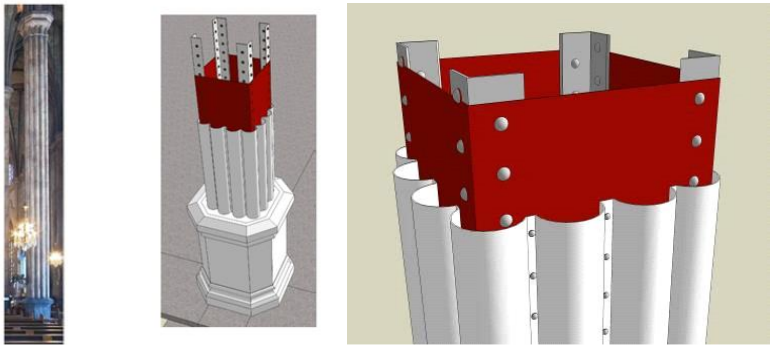

a) b)

Figure 10 – Interior columns: a) photo of a column; b) drawing showing the interior of the columns.

The most common column dimension is 600x600mm, as stated before, with the exception of the four column supporting the dome that are slightly larger with 800x800mm and some narrower columns that flank the rose windows with 600x400mm. The columns (see Figure 11) are made with sheet profiles with 5mm thickness, and in the corners, there are some angle bars with 5mm thickness that connect the four steel plates.

Figure 11 – Exterior column.

The external columns are connected laterally by I-beams and cross braces, which are inside the cavity of the walls. Historic records allow to say that the columns were shipped as 6 meter section, and then they were assembled and joined vertically in Quiapo. The different sections were connected with internal splice plates. The columns in the towers are connected both by plates and angle cleats at the 4th and 5th floor. Cavity wall columns have a floor plate at floor level, which act as stiffeners.

2.2.3 Towers

The towers have a total height of 48m, and the height of their steeple is 18 meters. The roof angle of the towers is approximately 75 degrees. The framing system that sustains the roof has several components, namely (Figure 12):

- A central column,
- Hip rafters,
- Purlins,
- Diagonal cross braces.

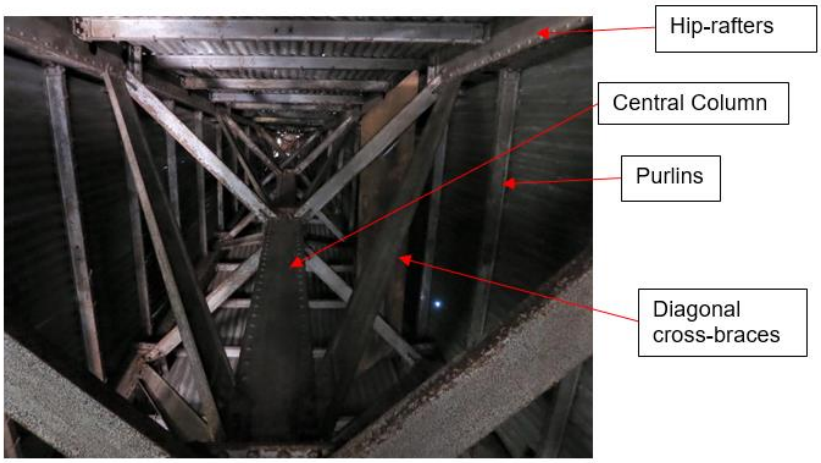

Figure 12 – The inside of the towers and their components.

The central column is the element that connects the tower's structure to the steeple structure. It is a column, for which the cross-section changes each 2.75m, ending at the upper third section. The purlins, like the hip rafters, decrease in size, and they finish their column-like aspect at the upper third and continue as I-beams.

Therefore, the last third of the roof is mainly a lightweight structure composed of flat and angle bars. The hip rafter is attached to a projecting plate at the base, which in turn is attached to the tower's 4th floor corner columns. Figure 13 shows that the central column in fact does not go until the top of the towers.

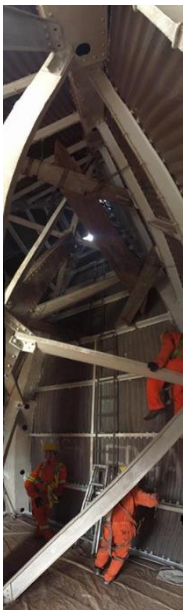

Figure 13 – The upper part of the towers.

In the towers, where the bells are located, and where one can access the roof, there is a floor that originally was made on steel and timber, but now seems to be made of a concrete slab applied directly into a galvanized sheet deck (Figure 14a and b) and a set of I-beams. Furthermore, the slab is directly in contact with the columns and the walls. According to drawings, the thickness of the slab is 155mm.

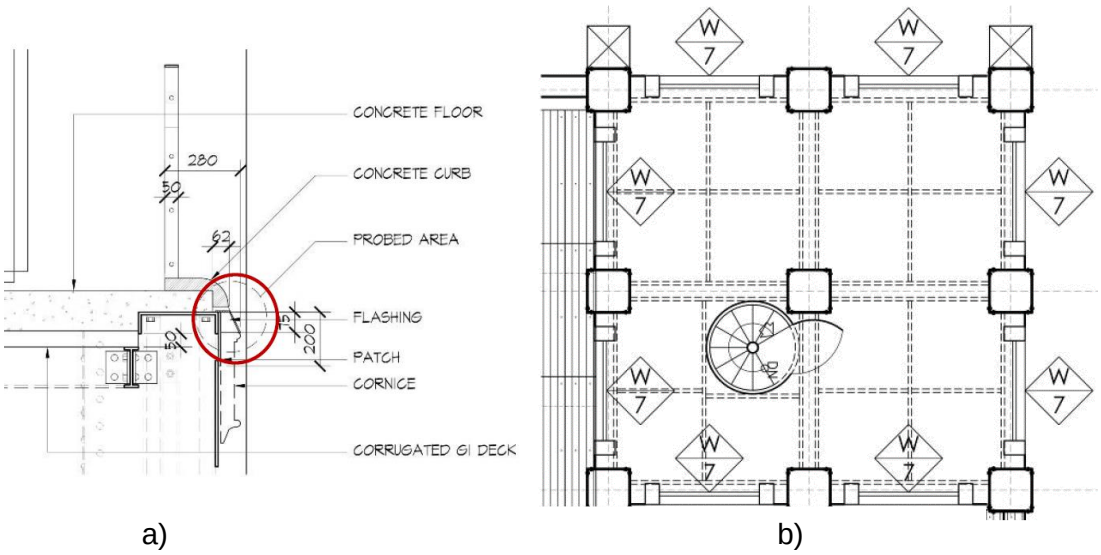

Figure 14 - Details of the concrete slab of the towers: a) Cross-section of the floor; b) Plan of the towers.

The towers at the belfry level have four openings. Each opening has a wrought iron guard rail mounted on a concrete curb and fastened to fenestration jambs. Walls have in the inside braced single-ply steel sheets riveted or bolted to angle bars. On the other façades, cast iron bells are mounted on the jambs. On the east façade, cast iron bells are mounted to the jambs.

2.2.4 Dome

The dome is composed by four columns that support each 25% of the load. The columns that are in the dome are 200mm larger than the other columns. The columns in this area seem to be in good condition, since there is no evidence of the accumulation of water at the base of the columns. The dome is the area where less information is available, since the access is limited. The Philippines Conservation Institute has yet to analyse this area and quantify the damage, and also clarify the dimensions of the elements present.

2.2.5 Foundations

According to historical documents the columns are constructed over the foundations of the previous churches. They rest on a metal base plate, which is bolted to a 0.8m height concrete footing. It is believed that some timber chocks were used between the bolts and plates to tighten the bolt's

connection as the moisture would make them expand. Figure 15 presents a historical drawing containing a representation of the foundations.

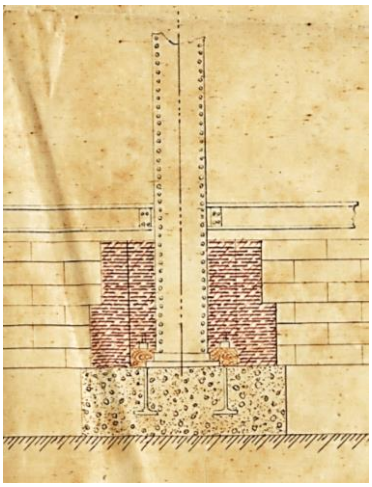

Figure 15 – The foundations of the Church.

All columns were tarred from the bottom to the ground level. The columns were then surrounded by a layer of bricks that left a space between the wall and the column. The column base was surrounded by a brick encasement, with 2.30m x 1.20m x 0.575m at the bottom and 2.00m x 0.60m x 0.425m at the top, which left a space between the wall and the column. The columns and inner brick were then plastered with hydraulic mortar, and the space was filled with hydraulic cement. The column height from the base plate to the ground floor is 2.30m based on camera inspections. According to the GPR scans and views from the column cavities, the brick encasement was never built (Conservation and Development Foundation 2014).

Historical documentation, confirmed by observations on the only dry wall column cavity, indicates that all of the outer columns are connected by a beam at the floor level at 0.4m from the ground floor. Below this, there is grid wall of either volcanic tuff or timber. Over this, tie beams, 0.5m below ground level, were laid in a grid pattern. Some specimens of the floor allowed to conclude that the old timber floor girders were supported by brick pedestals. A brick retaining wall surrounds the perimeter.

2.2.6 Roof framing systems

The roof framing system can be divided in two different types, depending on their location on the structure. One of the types is the one present on the third row of columns from the main façade and the other one is on the successive frames until the dome (Figure 16 and Figure 17).

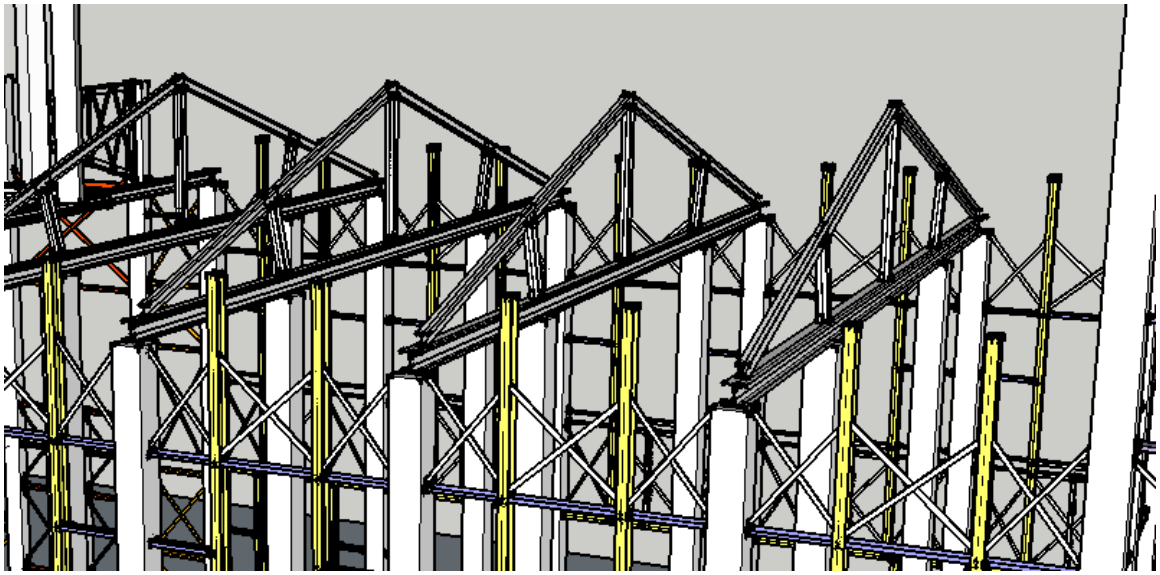

Figure 16 – Roof frames in the nave.

The first type of frame is characterized by having a tie-beam at 1.30m from the top. The horizontal tie-beam is an I profile with 250mm height and 170mm width. All the remaining elements are equal to the first frame but they do not have the tie-beam in the middle. Supporting the cross vaults (Figure 18), there are some elements made out of three pairs of bars. One of these bars is a diagonal bar with a height of 80mm and a thickness of 5mm. The vertical and horizontal bars also have 80mm height, with the same thickness as the diagonal one.

Figure 17 – Front frame.

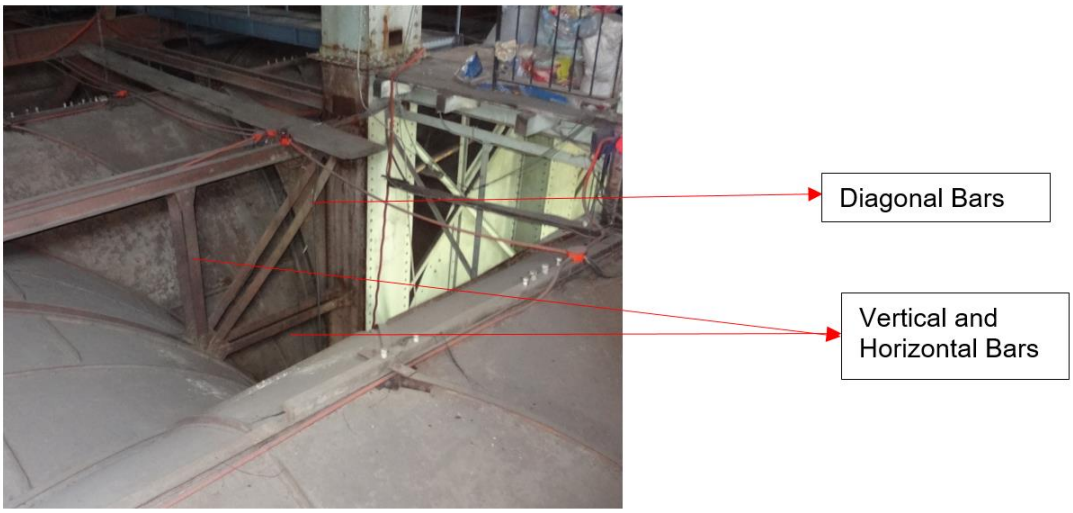

Figure 18 – The supporting elements of the vaults.

The roofs are made of corrugated galvanized sheets that are fastened to purlins beneath with J-bolts. It can be seen some wrought-iron grilles on the ridge of the nave roof, at the perimeter of nave and dome roofs. Below this, there is an accessible attic, where the roof framing system is.

2.2.7 Walls

The walls can be divided into two types. The first type is the one that is present in public spaces, composed of two leafs, with a frame in the middle. The second one is the one that is present on private accessible spaces, such as the attics and the towers, composed only by one leaf and the frame.

The wall panels consist of 3 mm rolled mild steel plates with an average size of 1.5m x 2m. Between the columns and hidden within the cavity walls, some structural members such as cross braces and beams are present. The cross braces are the structural elements that support the columns in tension. The columns are connected to each other by horizontal I-beams and C-channels on top, midsection, floor and footing levels. Each wall panel is riveted to these members, with angle bars, which also act as stiffeners for the wall. This makes the walls contributing to the resistance of the whole structure. On top of these walls there was a C-profile that in the drawings is named as the Roof beam. Inside the walls, some vertical bars, connecting the different levels of horizontal beams, can be observed forming this way the interior structural wall frame.

The cross-section of the main angle bar that connects horizontally the columns to the windows is a section with 80mm width, 80mm height and 9mm thickness.

The cross-section of the T-bar is a T-section with 100mm width, 75mm height and 9mm thickness.

The cross-section of the cross bracing angle bar is an L section with 60mm height, 60mm width and 9mm thickness.

The cross-section of the vertical and horizontal frames corresponds to an I-section with 190mm width, 295mm height and a thickness of 15mm. These elements connect the beams and the columns inside the walls to each other.

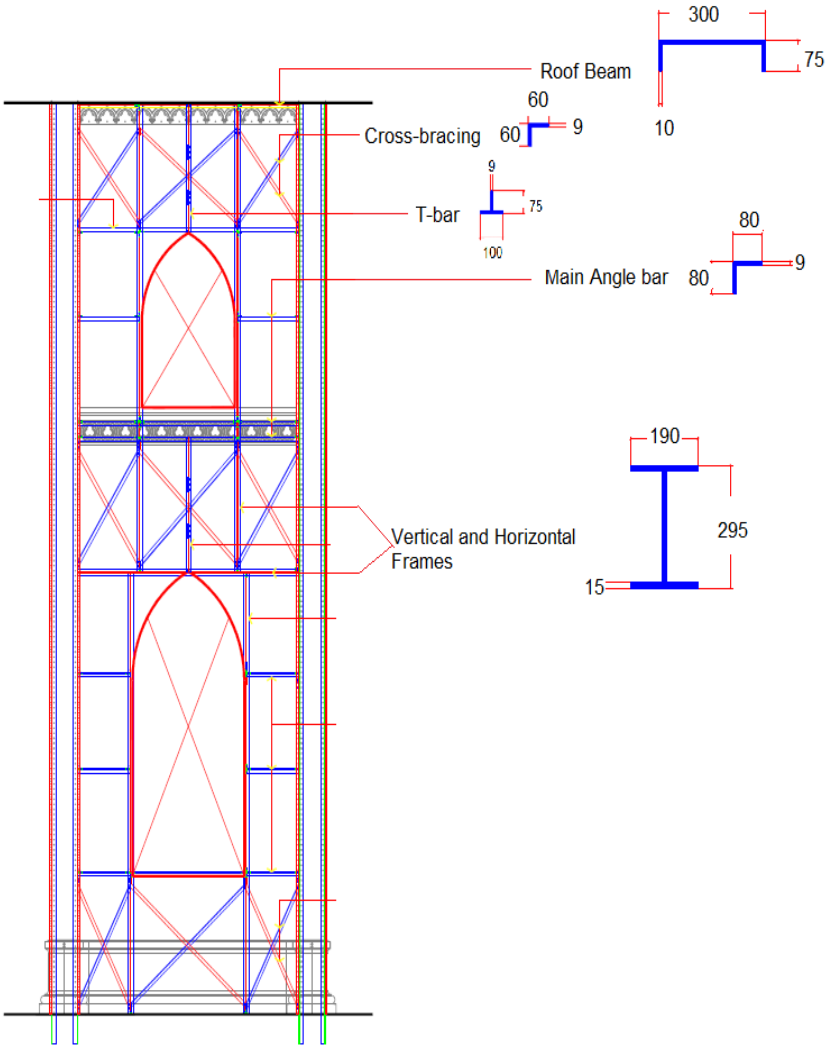

Figure 19 – Wall elements and sections.

Figure 20 presents the angle bar section above the clerestory, which corresponds to an L section with 75mm width, 75mm height and 10mm thickness.

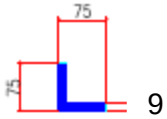

Figure 20 – Cross-Section of the angle bars above the clerestory. Dimensions in millimetres

In Figure 21 and Figure 22 the inside of the walls are shown, where the cross-bracings, the angle bars and the vertical frames can be observed.

Figure 21 – Side vies of the interior of the walls.

Figure 22 – Interior of the walls (Top View).

2.2.8 Floors

The original floor, made of Tindalo hardwood, was replaced by the current Machuca tile floor, an early handmade cement tile from the Philippines. There was also a crawl space beneath, that was filled with sandy soil and a layer of what seems a lime-based cement (Figure 23).

Figure 23 – Crawl space beneath the floor.

The floor in the altar is made in marble, and it is the original one, with the exception of the tiles located in the south end. These were replaced when the altar was extended southward in 1962 (Figure 24).

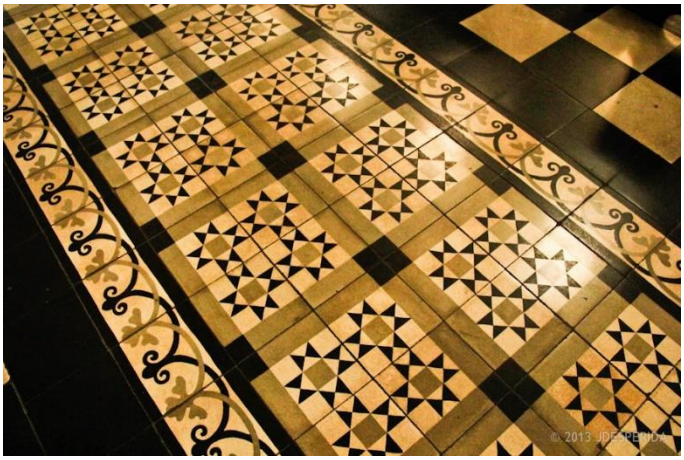

Figure 24 – Tile floor of the church.

2.3 Material properties

Metals have been used for the construction of buildings many years ago. Figure 25 shows one example of application, the Hanging Gardens of Babylon, where the linings were made of this material. They were put in the base of the walls to separate the soil from the structure to retain moisture.

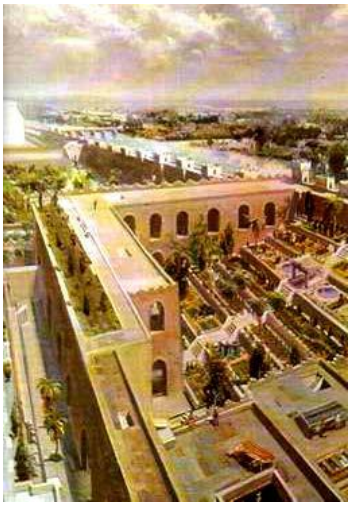

Figure 25 – The Hanging Gardens of Babylon.

Iron started to be used, although, not before the industrial revolution, in structural elements. There are three types of iron, known as, wrought iron, cast iron and steel.

Wrought iron has a very small carbon content, and was used for thousands of years, mainly for elements that needed more resistance. It is a brittle material, but has a very high hardness. In order to manufacture it, many methods were used, namely: bloomer process, indirect process, and puddling and faggoting.

One example of this type of metal construction is the iron pillar in Delhi, India, presented in Figure 26. This masterpiece has 7.21 m high, and it is 98% made of wrought iron.

Figure 26 – Iron pillar in Delhi, India

There are several types of cast iron, such as, grey cast iron, white cast iron and ductile cast iron. It is usually known to be a brittle material, and its application is not suitable for members that will be in a sharp edge, or a high degree of flexibility is needed.

Cast iron is appropriate for elements subjected to high compression loads, but it is not so appropriate for members under tension. It was obtained by melting pig iron (Figure 27) in small furnaces known as cupolas or in reverberatory furnaces.

Figure 27 – A piece of pig iron.

Metals were also used in abundance in ancient masonry and timber structures, for example in anchor ties.

After this early use, the iron started to be used as the main structural element in the late 19th century, as many bridges in the world from this time are an example, made with wrought and cast iron. An example of its application is the Luis I bridge in Porto, Portugal (Figure 28).

Figure 28 – Luis I bridge, in Porto, Portugal.

Soon after, metals started to be used as a material for regular buildings. Many small churches made of corrugated, galvanized steel, as the San Sebastian Church, were used in the United Kingdom, before their permanent masonry structure was built. While San Sebastian Basilica is a marvel of art and architecture, it is not unique in its all-metal composition. The 19th and 20th century were times where metal was used for houses and also for worship buildings. These were known to be very cheap and to be easily transportable. Due to their economy and flexibility in design and transport, metals also started to be widely used by missionaries in the West side of the USA since the 1830's. These churches were not very complex, being small in size, with a capacity of 100 to 500 people. Curiously, there is a report from September 1844 of a church that was made in England and sent to Jamaica for construction. (Leggio 2012) This author states: *"A church has been sent out to Jamaica, as a specimen, as many of the kind are likely to be required. The pilaster supports are of cast iron, on which are fixed the frame-roof, of wrought iron, of an ingenious construction combining great strength with simplicity of arrangement; the whole is covered with corrugated iron and the ceiling formed of paneled compartments, covered with felt, to act as a non-conductor of heat. The body of the church is 65 feet by 40; the chancel, 24 by 12: a robing-room and vestry are attached. The windows are glazed with plate-glass, one eight of an inch in thickness; the two chancel windows and four others are of stained glass."* The industrial revolution led to an increase of population in the cities, and caused the expansion of towns across the countries. These towns were normally close to the industries, and fast to assemble. Religious buildings expanded as well, since the steel construction was inexpensive and fast to assemble

(Mornement and Holloway 2007). Across the world, there are other churches also in all-metal. One is located in Grecia, Costa Rica. It is the *Iglesia de la Nuestra Senora de las Mercedes* (Figure 29), which is very similar in appearance to San Sebastian Church from the outside. Another example is the baroque style church of Saint Stephen, in Istanbul, made entirely out of steel and iron components, completed in 1898. Its parts were prefabricated in Vienna between 1893 and 1896. But no church was as decorated as the San Sebastian, where the metal tried to simulate the appearance of stone.

Figure 29 - *Nuestra Senora de las Mercedes* Church.

One aspect that must be determined for a proper structural analysis and assessment is the strength of the material. Not so much is known about the material properties of these churches, but a study performed by Drdacky et al. (2013) allowed to obtain the strength of the steel of a Turkish church. Among all the tested specimens, the yield strength was varying from 280 to 317MPa, and the rupture strength was 388 to 417MPa, with 7% carbon content.

In the San Sebastian Church, the carbon content is low, varying from 0.003% to 0.04%. The toughest material, that is the one with the highest carbon content, is present in bolts, cross braces and wall plates. The softest one is present in columns and nuts.

The mild steel present in the San Sebastian Church has a yield strength of 326MPa and a tensile strength of 375MPa (Ivanova, Ganev, and Drdácký 2013).

Another important aspect to characterize the steel in the church is the thermal coefficient, that, as previous research, it is said to be 0.023 in the walls and 0.046 in the columns (Conservation and Development Foundation 2014).

2.4 Past interventions

Philippines is a country where the rainfall is something to take into account when designing the gutter systems. Philippines climate is variable, ranging from tropical rainforest, tropical savanna, tropical monsoon, or humid sub-tropical. It is known by its high temperatures, very high humidity and plenty of rainfall. Philippines is also known for its monsoons. This phenomenon consists on a large-scale sea breeze that occurs when the temperature in land is much warmer or cooler than the temperature of the ocean. Associated to this phenomenon, a large amount of rain falls. At the time of construction of the structure, this was not taken into account, leading to damage that is seen nowadays. It is said that even for the time of its construction, the drainage system was not enough to drain all the water. Only later, some interventions were carried out with the intention of minimizing the damage.

Therefore, one past intervention consisted on patching holes in the roof gutter with sealant. Additionally, some PVC gutters and hoses were installed to allow water from the roof pipes to be properly drained and conducted to the ground.

In addition, the nave gutter was one of the elements that needed to be repaired more urgently. These elements were mechanically cleaned with the help of a brushing cup (Figure 30). After being properly cleaned, the elements were cold-galvanized with zinc-rich-paint. The same intervention was performed in the corner gutters, but in these, the used material was fiberglass-reinforced plastic.

Figure 30 – Gutter being mechanically cleaned.

One intervention to be noted was done in the pinnacles, where concrete was poured to avoid the water dropping to the inside of the columns. Such intervention, according to information provided by the parish, was performed in the 1980's (Figure 31). The pinnacles also had to be intervened, where some plates had to be fixed, since they were detaching rapidly.

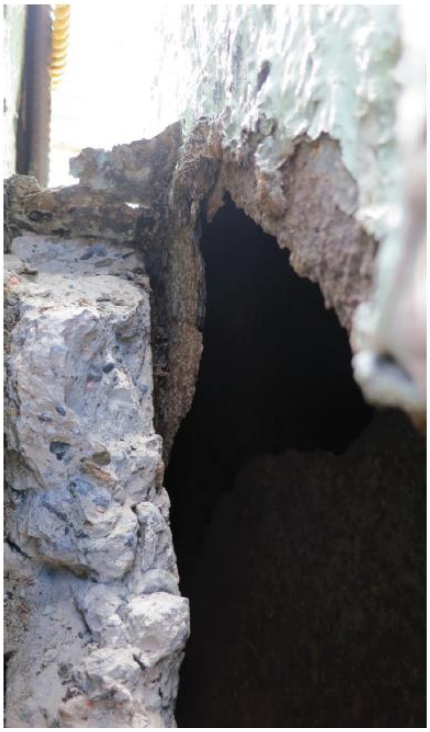

Figure 31 – Concrete applied on the pinnacle valleys.

Some patch repairs were performed with the intention of sealing previous leaks, but now they are leaking again. Assuming these repairs were not properly done, and they are leaking since their application, it is reasonable to say that leaks are causing damage for at least 25 years, when the last repair was performed.

In the west steeple, a large number of downspouts were disconnected, causing a large amount of water to go to the belfry floor.

The interior suffered less interventions, but was subjected to a major intervention. The choir loft initially was not like as observed presently. In the beginning, the choir loft was located in the first three sets of columns (Figure 32a). This change happened in the 1930's, when a pipe organ needed to be installed in the east end of the choir loft, which became possible by extending this part of the choir in the direction of the altar (Figure 32b). The organ hides a part of a window, which was punched to channel the organ's blower pipe. This addition becomes perceptible, because the floor pattern for each part is different. The original choir floor has alternating planks of lighter and darker wood, unlike the new part.

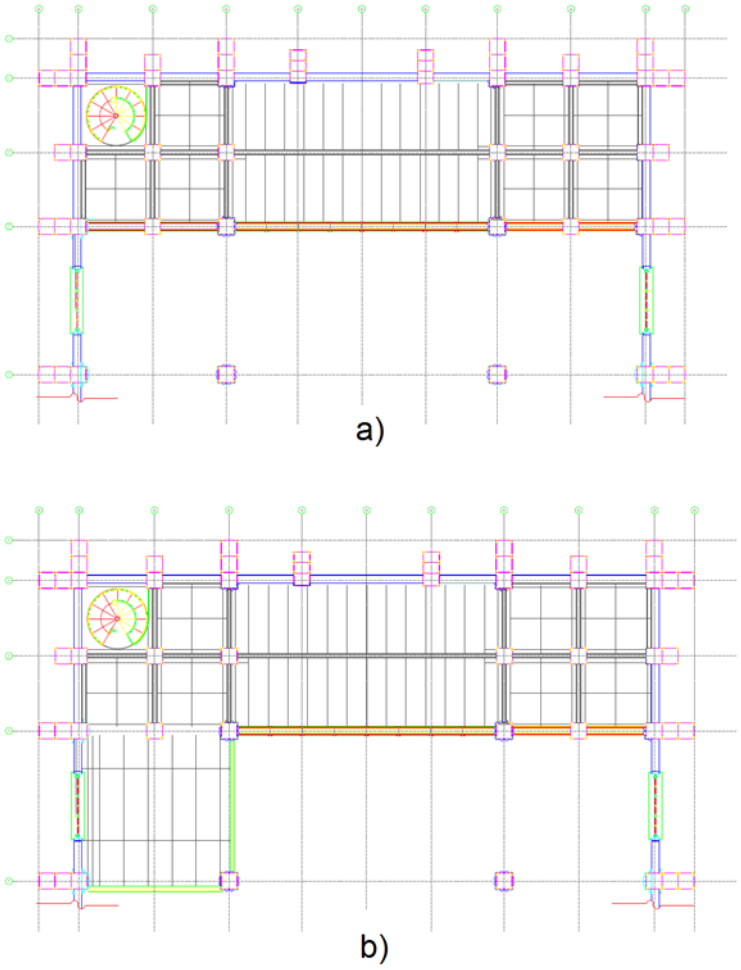

Figure 32 – Plans of the choir loft: a) choir loft before intervention; b) choir loft after intervention.

3. IN-SITU TESTING

The following chapter pretends to compile all of the information that was obtained through the different types of tests that were performed on the structure. Some of the tests were performed by the Save San Sebastian Basilica Conservation and Development Foundation Inc. For a proper interpretation of the damage, the results for the different tests are here presented and summarized, namely the column cross-section reduction evaluation, the GPR scans, the Inclinometers, the temperature and humidity. Furthermore, the University of Minho carried out the dynamic identification tests (Mendes, Seabra, and Lourenço 2016).

3.1 Column cross-section reduction

In the past, a study regarding the cross-section reduction from the columns was performed (Conservation and Development Foundation 2014). This proved to be a major step towards a proper and effective retrofitting of the structure. The damage pattern was also obtained and a first condition assessment was performed. It was possible to assess the structural integrity of the structure and to compare it to the initial condition.

After a visual inspection performed using an endoscopic camera, which took pictures every 50cm, it was possible to assess the existing damage. By the analysis of all images, some critical damage was found, and its cause was evaluated. The evaluation of the damage concluded that the major cause was water accumulation at the base, leading to significant material loss in the column plates. The water infiltrates on the columns located in the corners. This lead to moderate corrosion and damage on the bracing system. The column cross-section reduction might also have been caused by previous concrete repairs, causing large losses in the pinnacles plates.

In order to perform the condition assessment, the size of each column was measured and documented. The distance of the damage to the ground floor was also measured, in order to characterize the damage pattern along the column height. The procedure consisted on measuring the damaged perimeter of the cross-section, which was then multiplied by the thickness of the plate to obtain the area that was lost. The thickness of the plates was determined using the ultrasonic thickness gauging. This value was then divided by the theoretical area of the undamaged column, and the percentage of loss was determined. Considering the material loss and the column's condition, a grouping considering the cross-section loss was proposed. The columns were divided into groups, namely, with cross-sectional loss lower and higher than 60%.

For the group of columns that had less than 60% damage (the number of assessed columns was 51), the average value for the cross-sectional loss measured by direct measurement was 13%; the cross-sectional loss measured by ultrasonic thickness gauging was 10%; the total cross-sectional losses for the columns in good conditions is 23%. For the group of columns with more than 60% damage, (the

number of assessed columns was 5) the average value for the cross-sectional loss measured by direct measurement was 66%; the cross-sectional loss measured by ultrasonic thickness gauging was 10%; the total cross-sectional loss for the columns in bad conditions was 76%. In some columns, it is possible to see some deformation, mainly represented by warping. This pattern was attributed to past seismic and wind loads.

Examples of the column condition assessment of the thickness are presented in Figure 33 and Figure 34. These studies were carried out in 2014 and, current damage can be larger(Figure 33 and Figure 34). The pink colour in Figure 33 indicates the bulging damage. The identified damage in this column was bulging of the column/plate corner where the rivets attach the pipe moulding to the column.

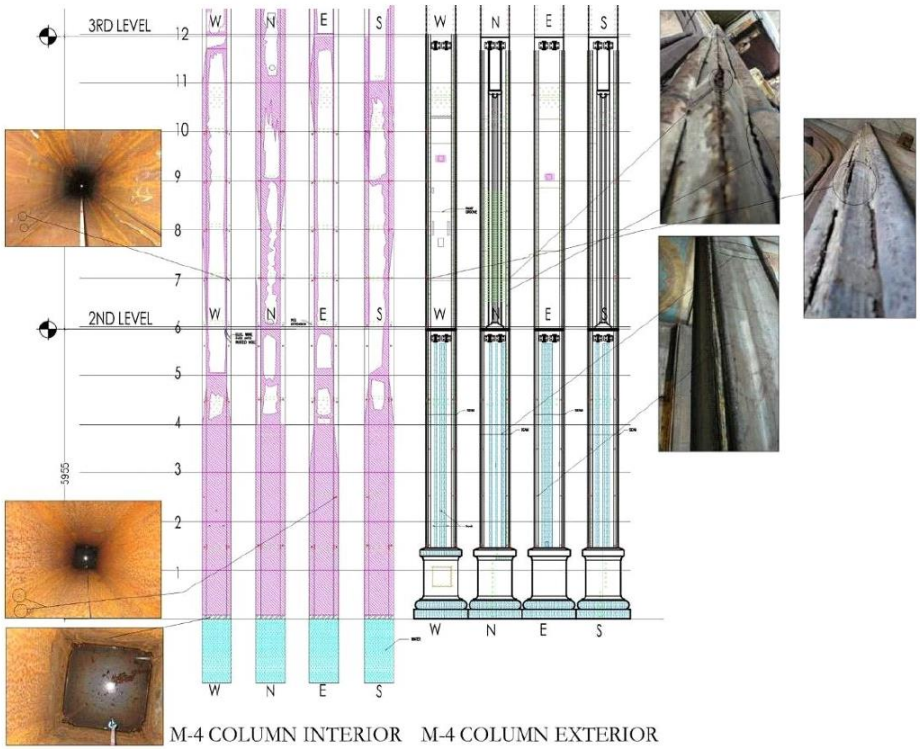

Figure 33 – Damage pattern in the lower part of column M-4.

Figure 34 – Bulging at the column.

Some splaying of the corner is believed to have been caused by rust jacking. There is rust at 12m height on all sides of the column, and some water has accumulated at the base. Heavy rust is present at the angle bar and in the column plate.

In column M-4, but at a higher level, bulging at column plate is found, but in small quantities. From 24m higher, this condition gets worst, mainly because rivets are not being protected by pipe mouldings and are exposed. Open corners were heavily repaired with putty. Corrosion is mainly located between the angle bar and the column plate.

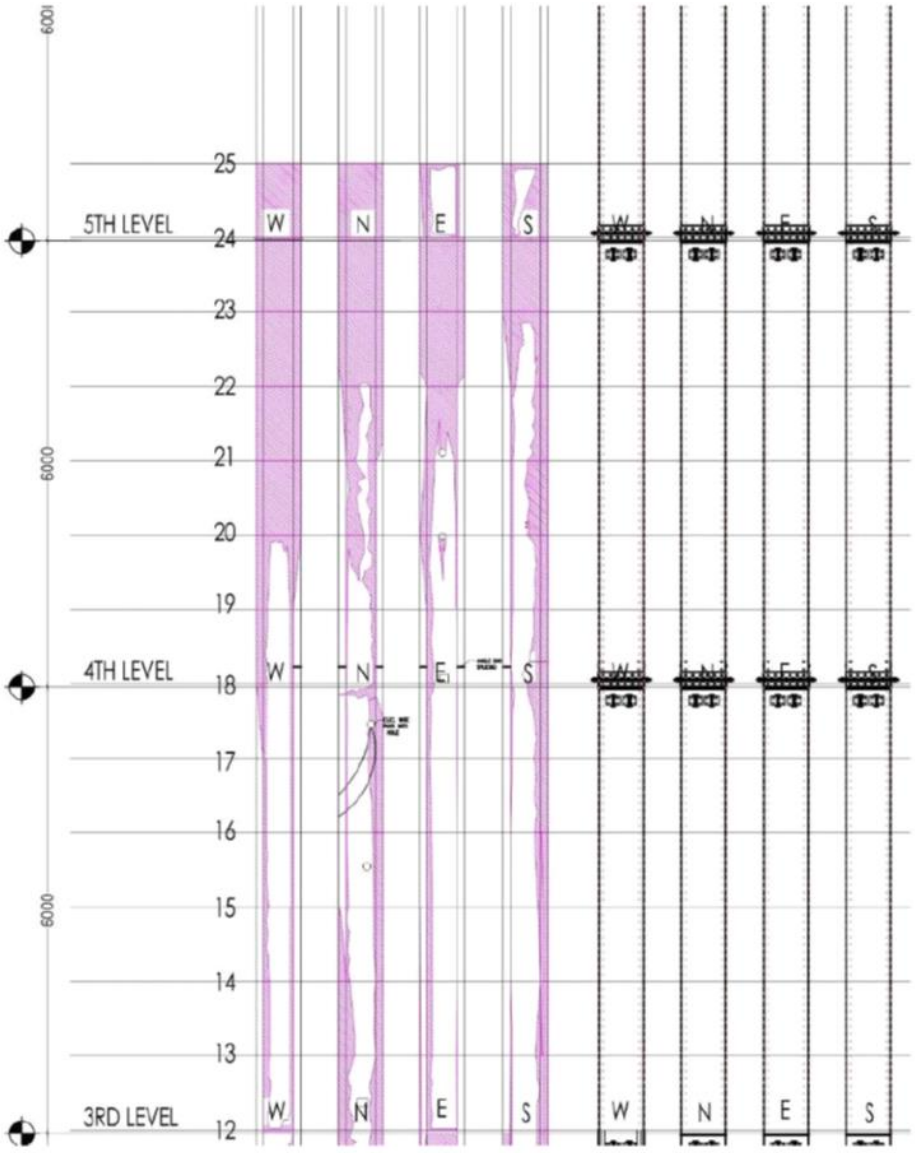

Figure 35 - Damage pattern in the upper part of column M-4.

Figure 36 presents a plan with a photo of the inside of the columns of the structure. It is possible to observe that the higher damage in columns occurs in the outer ones. The inside columns are almost undamaged.

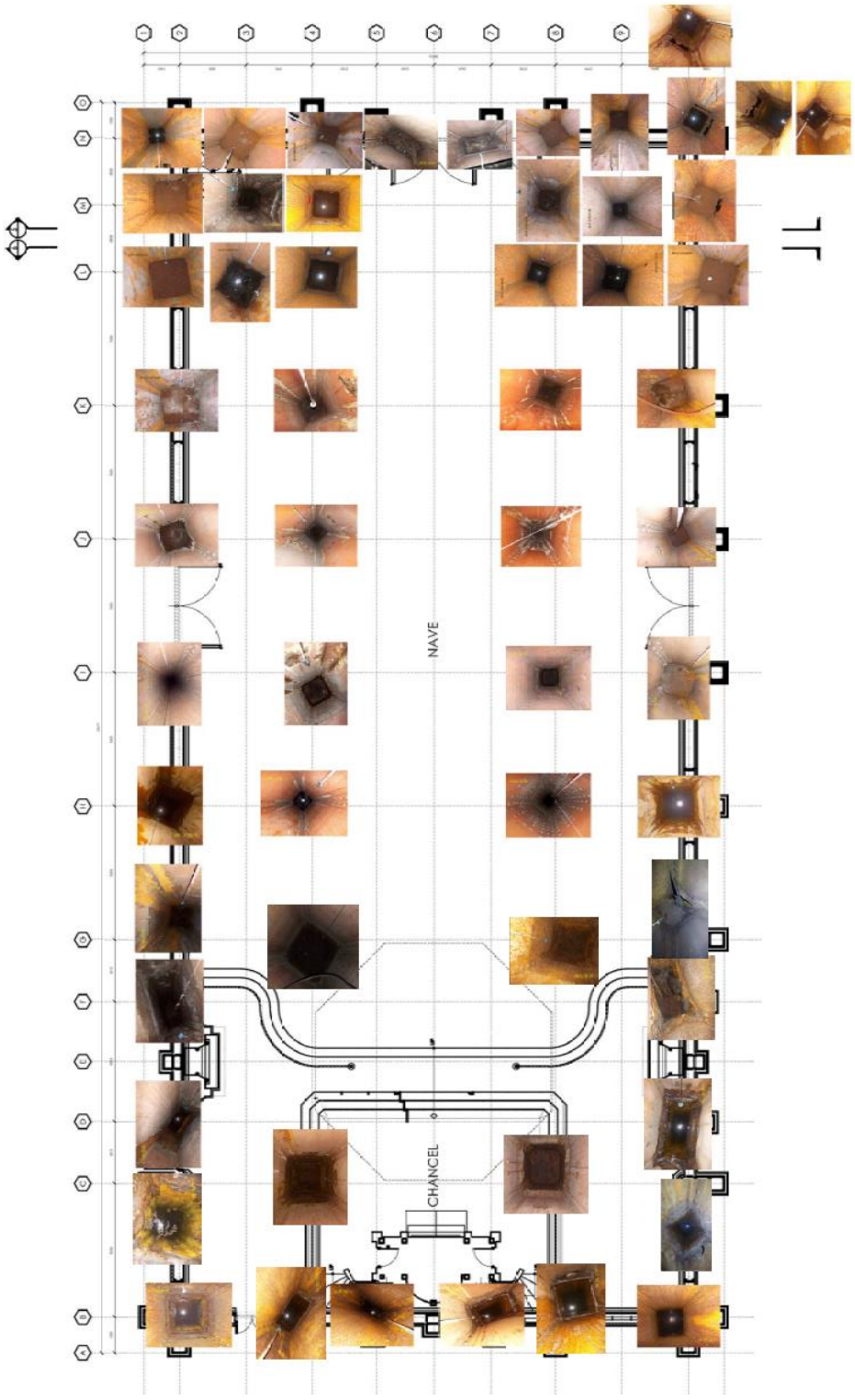

Figure 36 – Plan of the structure with photos of the column's interior.

3.2 Ground penetrating radar

GPR is a method that is used to detect objects, changes in material, voids or cracks that are beneath some object (Figure 37). Historically, GPR in the beginning was focused on mapping structures on the ground, however nowadays its application range has spread to many applications, including structural assessment (Daniels 2004).

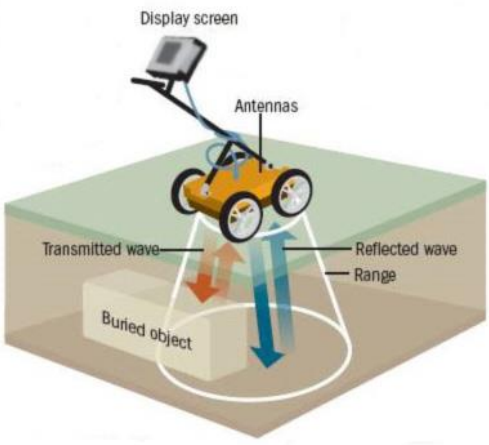

Figure 37 – GPR functioning system (http://bchazmat.com/bchazmat-services/ground-penetrating-radar-gpr/).

In the San Sebastian Church, GPR was used for many purposes. The first objective was to determine if there was any steel tie beams connecting the columns; the second objective was to infer on the presence of a concrete block or brick pedestal at the base of the steel columns; the third objective was to determine if the drainage pipes along the exterior walls were aligned; the fourth objective was to see if there was any cellar under the sanctuary; and, finally, the fifth objective was to check how the subsurface conditions were.

According to the Final Condition Assessment Report performed between March 31 and July 1, 2014 (Conservation and Development Foundation 2014) there were two GPR survey campaigns performed. The first campaign was conducted on October 30, 2013; and the second one was performed on January 29, and February 6-7, 2014. The total amount of scan lines was 146 (This amount takes into account all tests, inside and outside). The conclusions presented here are for the different frequencies of the GPR scanning process. Three scanners were used, depending on the frequencies adopted. One was a Noggin 100, for a frequency of 100MHz; other one was a Noggin 250, for a frequency of 250MHz; the last one was a Conquest SL, for a frequency of 1GHz.

The 100MHz allowed to find that at a depth of 0.25m there are drainage lines that start at the interior corners of the two towers, converging in the central area of the church, and go to the outside of the church by the entrance (Figure 38). Some metal objects were also found in the subsoil, however, the accuracy of results is not the best one, since some air wave reflections might have affected the results.

It was also possible to realize that the top of the tie beams might be at a depth of 0.60m, since the hyperbola apex is located at this level. Nevertheless, this test also allowed to include other metallic objects that seem to be out of place, taking into account the position of the columns and tie-beams (Conservation and Development Foundation 2014).

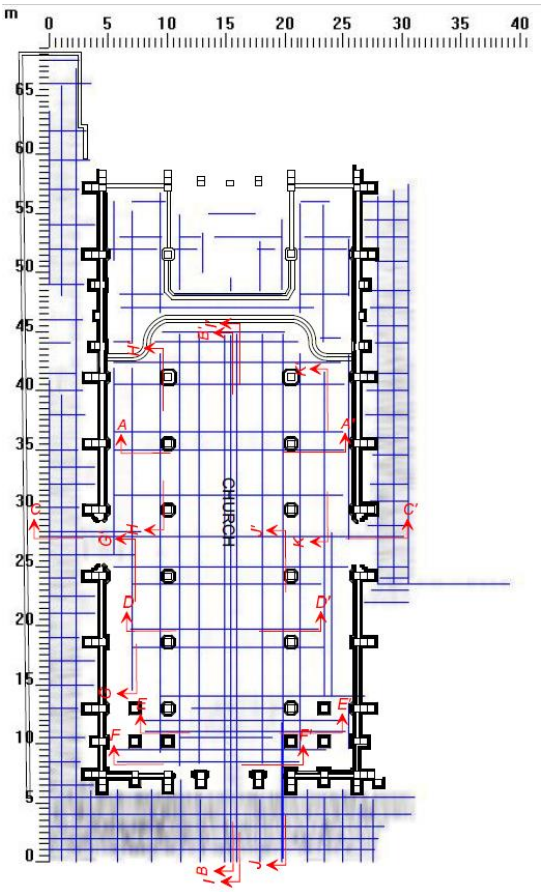

Figure 38 – 100MHz GPR scan lines.

In order to have a higher image resolution, a second set of tests was performed, with a 250MHz frequency. These tests helped to confirm the existence of the drainage lines along the lateral walls. These tests also helped to conclude that there are some metallic objects located near the surface. Moreover, some objects were found spaced approximately every 0.50m, at a depth of 15 to 20cm that might correspond to the previous floor joints that were part of the original wooden floor of the church.

A third set of tests was performed using a frequency of 1GHz, which was used in specific areas to have higher image definition, to properly characterize them. These tests were performed to locate old floor joints under the nave tiles, and allowed to conclude that there is a possibility of its existence spaced every 0.35m at a depth of 0.15m. However, the continuity and uniformity of these elements around the columns is not perceptible. It was also tried to locate concrete or brick pedestals, and confirm drainage line along the walls. No pedestal was detected and the drainage line was detected. Another purpose for

this new campaign was to check if the church was linked to the adjacent building, and the conclusion is that the two buildings are not connected. There is only an area filled with rubble or gravel infill.

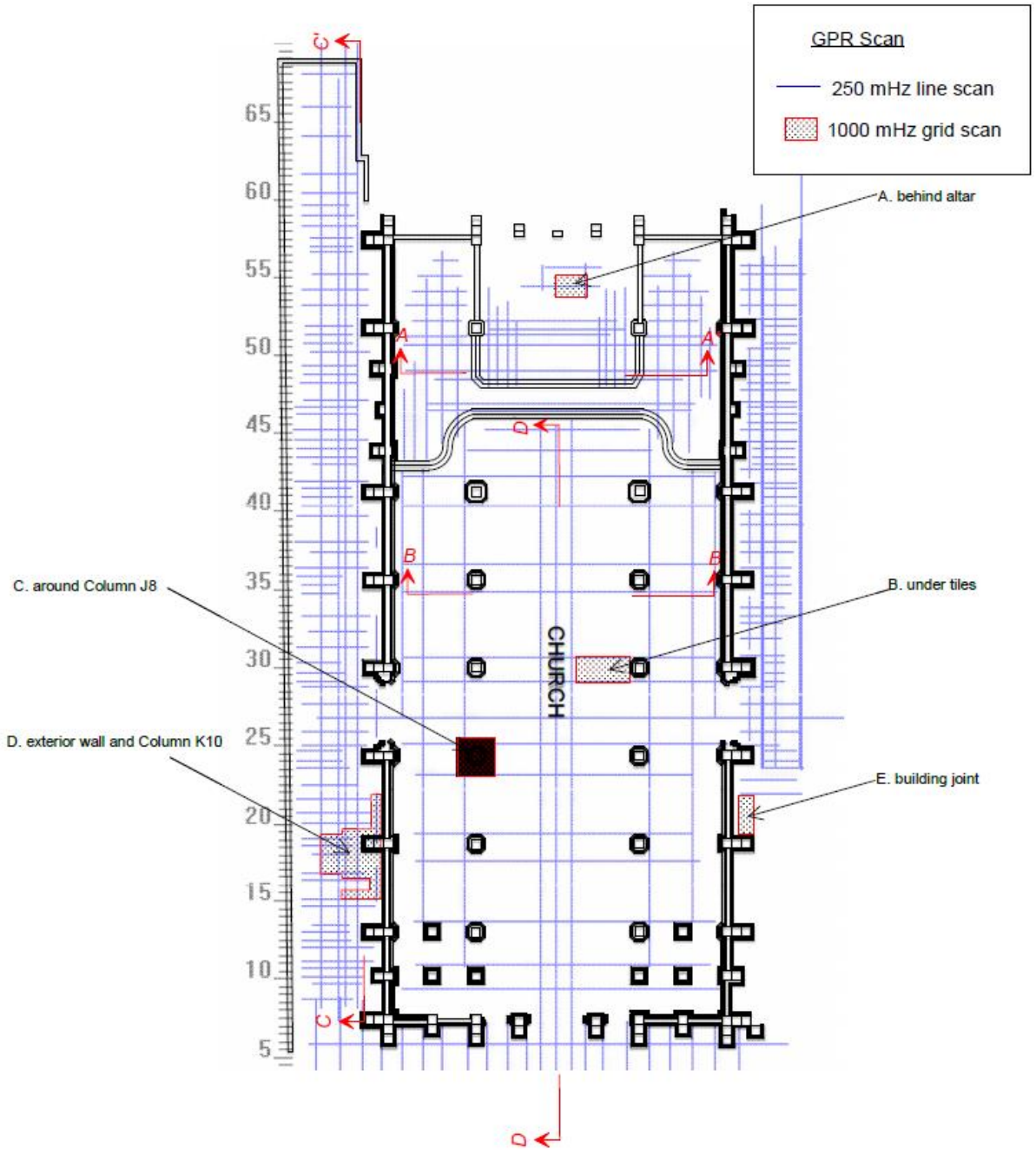

Figure 39 – 250 and 1000MHz scan lines.

Throughout all the campaigns performed with the GPR, there was a very interesting discovery. In one of the scans performed on the courtyard, it seems that there are some parts of an ancient wall with thickness equal to 2m, possibly from an old version of the church, approximately 4m below the surface.

This finding is extremely interesting from the historical point of view, since it allows to help the historians and archaeologists to try to reproduce what might had been the previous versions of the older churches.

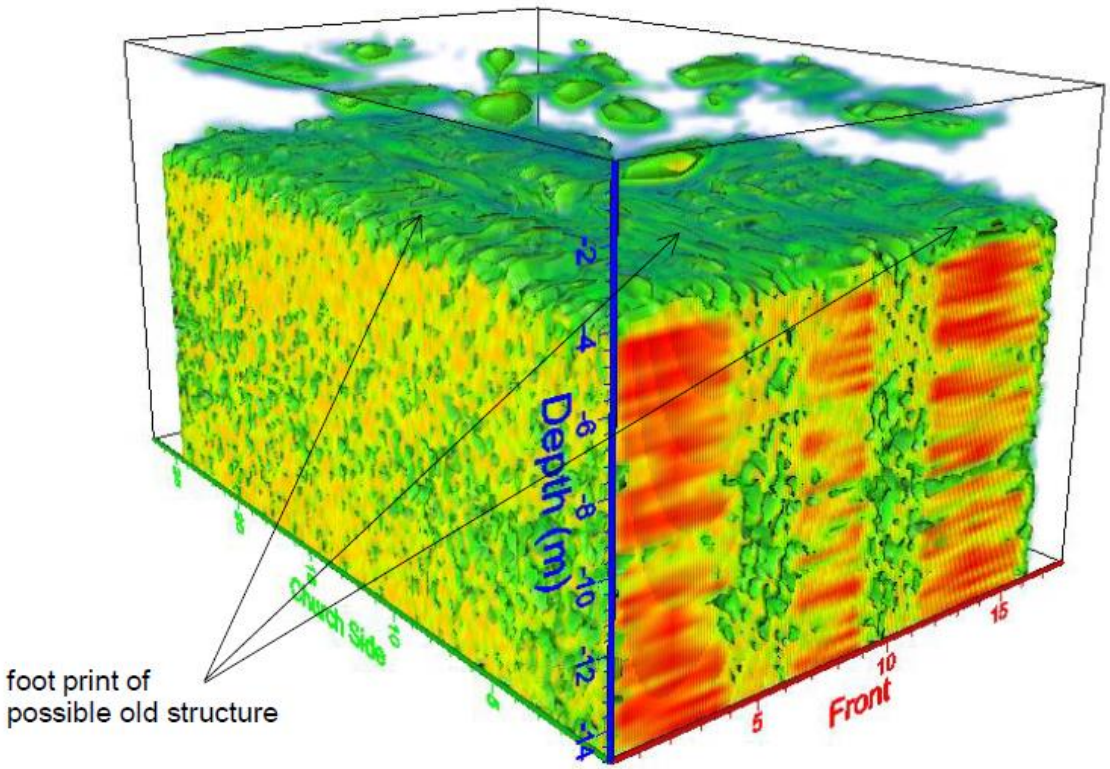

Figure 40 – GPR scanning of the soil.

Based on the GPR tests, the following main conclusions can be reported:

- The existence of a metal tie beam structure in a grid. The beams end at the altar.
- There are two drainage pipes. One is running under the west granite ground floor, and the water is evacuating from north to south. The other pipe runs from north to south along the width of the choir loft.
- Presence of moisture below the towers. The phreatic level is 2.50m below the ground.
- There are some soil drains at west side.
- There are no voids under the altar. This might indicate the presence of a cellar below the altar.

Figure 41 presents a map of the structure containing a summary of what was found in all the GPR tests.

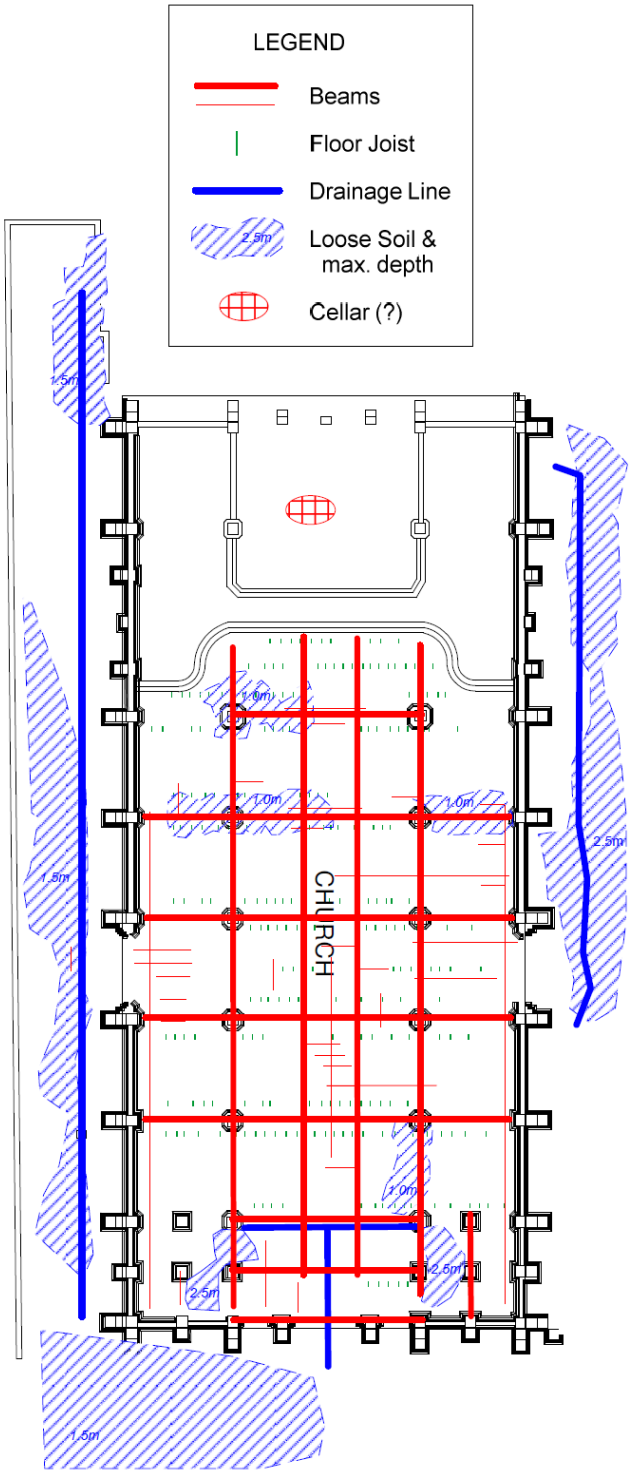

Figure 41 – Summary of the GPR results and findings.

3.3 Inclinometers

Testing with inclinometers was performed because surveying indicated patterns of open building joints. These patterns were possibly indicating an active movement of the building. For this purpose, four 2-axis inclinometers were installed, where the rotation in the two directions was measured. The inclinometers were installed in the four corner columns. Inclinometers 1, 2 and 3 registered similar maximum rotation values, maybe due to the fact that these columns are subjected to more or less the same wind loads. Inclinometer 4 was the one that registered the smaller values possibly because it is closer to the adjacent buildings on the northeast side. The rotations were measured during the months between November 2013 and February 2014, and the maximum rotation was 0.01º, obtained when the bells were ringing, see Figure 42.

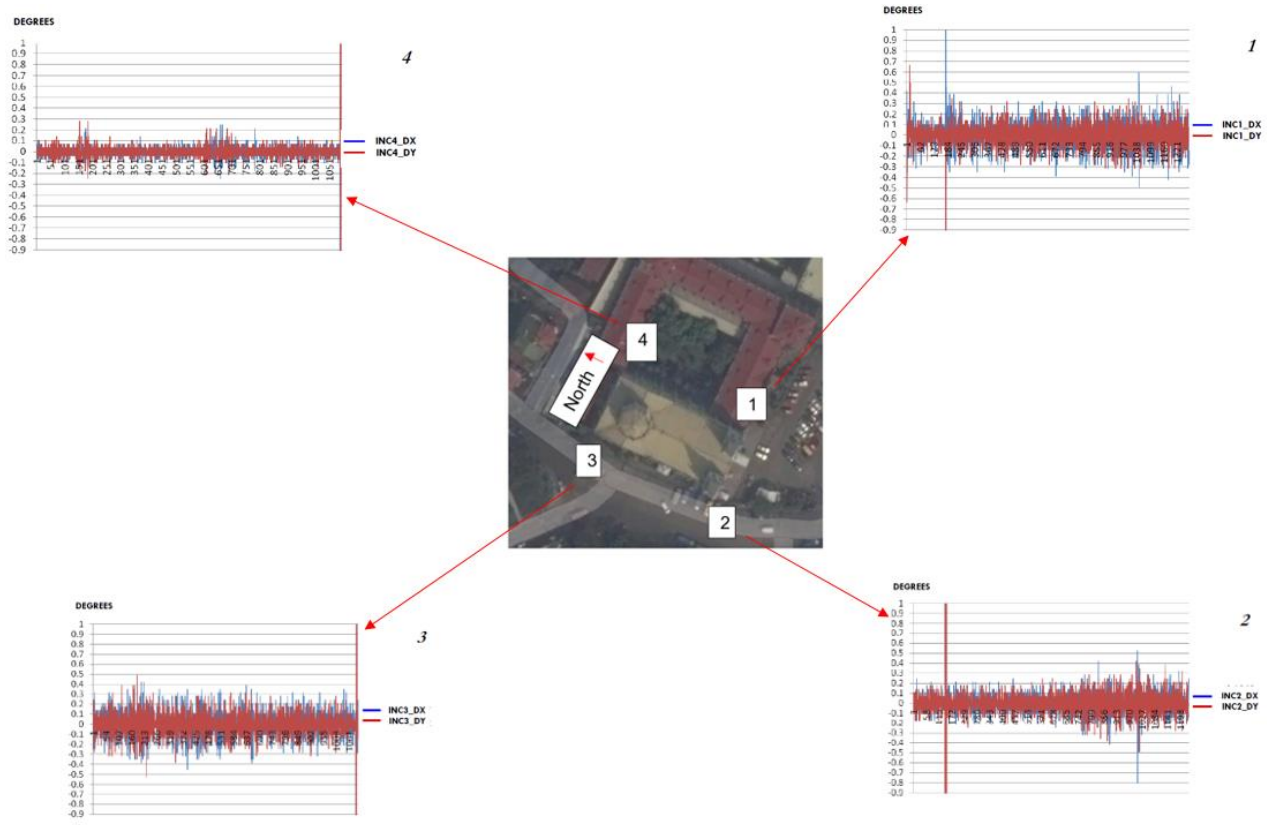

Figure 42 – Location of the inclinometers and the collected data.

3.4 Temperature and humidity monitoring

Temperature and humidity sensing in several interior points of the structure were done with the purpose of understanding if there were any condensation phenomena and their disposition on the structure, because condensation is a condition for the corrosion. The main nave was also analysed, with the goal of applying ventilation. Humidity and temperature contribute negatively to the trompe l'oeil painting life. According to previous reports (Conservation and Development Foundation 2014), data was recorded for two years using data loggers attached to walls with magnets. To monitor surface temperatures, digital laser thermometers were used, and the difference in morning and afternoon were recorded to calculate thermal expansion coefficients. The results are presented in Figure 43 and Figure 44, in which it is observed that the maximum measured temperature was equal to 35º (outside the wall).

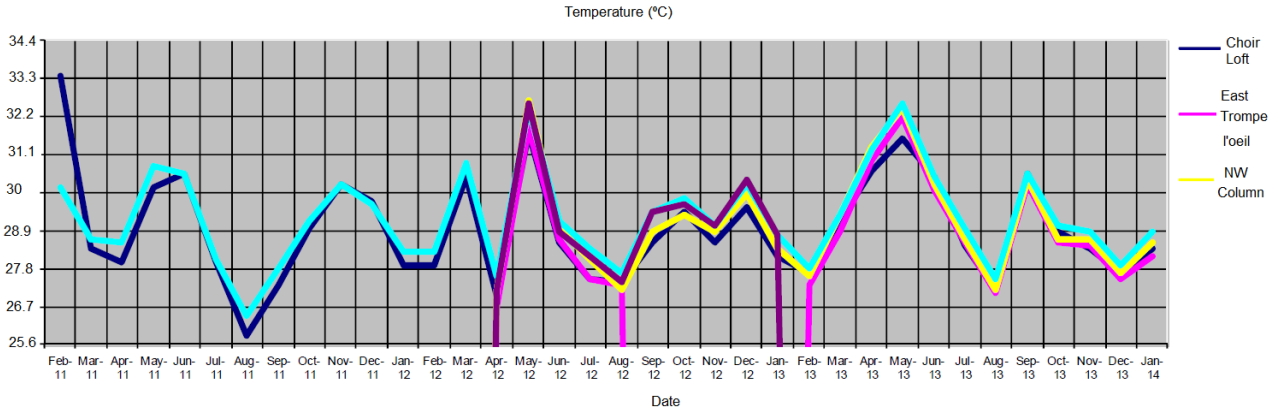

Figure 43 – Temperature evolution for two years.

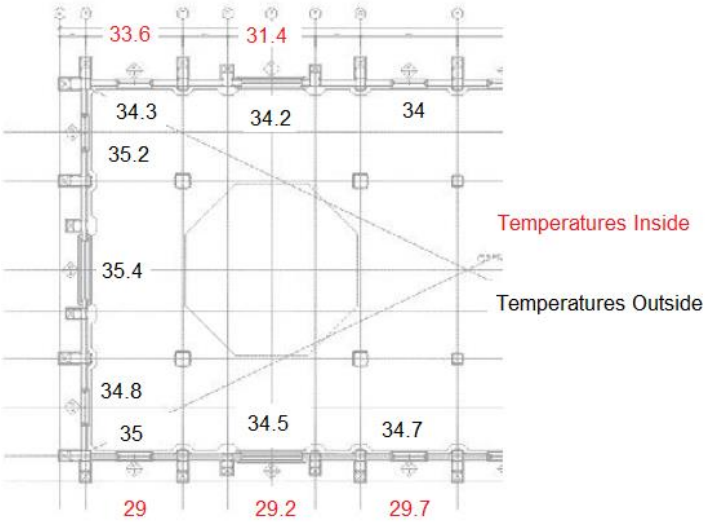

Figure 44 – Average temperatures for the inside and outside of the walls.

Analysing the relative humidity, and taking into consideration that it is recognized by experts that the percentage of relative humidity that can promote corrosion is 60% to 65%, and that the average relative

humidity is 68% (Figure 45), it can be stated that the San Sebastian environment is favourable to cause more damage due to this phenomenon. This can become more dangerous, if the effect of environmental pollutants and saline deposits are taken into account.

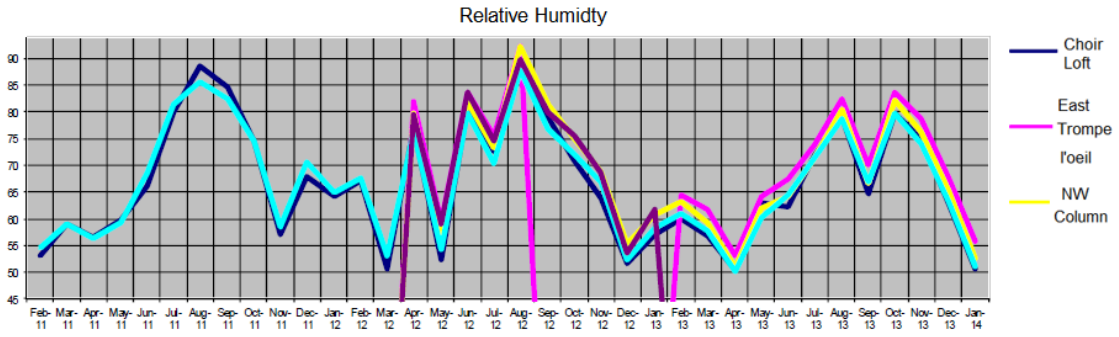

Figure 45 – Relative humidity values along two years (average equal to 68%).

3.5 Dynamic identification tests

Dynamic identification tests were performed with the aim of determining the dynamic properties of the structure, namely its frequencies, mode shapes and damping ratio.

There are several types of dynamic identification techniques. These methods can be divided into three groups:

- Input/output vibration tests, where the vibration response and the excitation that is applied to the structure are measured.
- Output only vibration tests, where the vibrations that occur to the structure are measured for the service conditions of the structure.
- Free vibration tests, where the vibration is measured when an initial displacement is applied and suddenly released.

The performed type of dynamic identification tests in the San Sebastian Church were the output only technique, where the source of excitation was the ambient vibration. In this case, the equipment used to perform such tests was 4 accelerometers (sensitivity equal to 10 V/g, frequency range from 0.15 to 1000 Hz, dynamic range ± 0.5g), several extension coaxial cables and one 24-bits data acquisition system with a software developed by the University of Minho.

The accelerometers are like a spring-mass-damper system, that produces an electric output proportional to the acceleration. This type of accelerometers is not able to measure the DC component, which corresponds to a response at 0 Hz, and it does not need an external power source.

In order to properly identify the dynamic properties of the structure, several configuration setups had to be prepared, where only horizontal accelerations were recorded. The amount of performed tests was

17, and the locations for the accelerometers were selected where the higher modal displacements were expected. In the configuration setups, accelerometers were placed at the top of the external walls, dome and bell towers. Furthermore, accelerometers were also placed at the bell towers and the dome at the roof level.

a) b)

Figure 46 – a) installing one accelerometer; b) used accelerometer.

Each setup involved 4 accelerometers, including the reference one that was located at the middle of the nave in the transversal direction, leading to a total of 51 measured signals of different points of the structure. Each setup lasted for 30 minutes, with a sampling rate of 200 Hz.

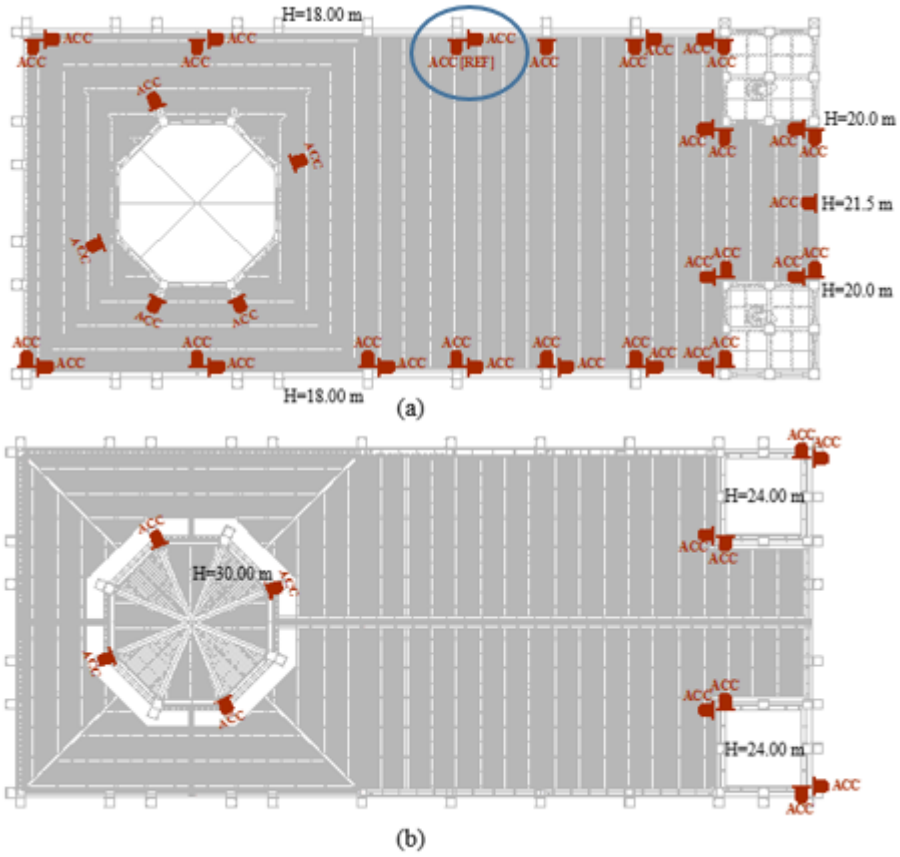

Figure 47 – Accelerometer setup: (a) Plan at roof level; (b) Plan at dome level.

([REF] corresponds to the accelerometer of reference)

To be able to identify the dynamic properties using vibration tests, there are several methods that can be used, namely, the Peak Picking, Circle Fit, Rational Fraction Polynomial or Complex Exponential. These methods are divided in groups according to the type of domain (frequency or time), to the formulation type (indirect or direct), to the type of estimates (global or local), to the number of the degrees of freedom of the system (SDF - Single Degree of Freedom or MDF - Multiple Degree of Freedom), to the number of the input/output signals (SISO - Single Input and Single Output; SIMO - Single Input and Multiple Output or MIMO- Multiple Input and Multiple Output) (Caetano 2000).

In this case, the two methods used were: The Enhanced Frequency Domain Decomposition (EFDD); and the Stochastic Subspace Identification Principal Component (SSI-PC). The EFDD method is a method that decomposes the signal in the frequency domain and can be divided in two steps. The first one, the FDD Peak Picking is performed. In the second one, the FDD identified mode shapes are used to identify the Single-Degree-Of-Freedom (SDOF) Spectral Bell functions and from these SDOF Spectral Bells the frequency and damping ratio can be determined. The SSI-PC method decomposes the signal in the time domain, where a parametric model is fitted directly to the raw time series data. The parametric

mathematical model has features that can be adjusted to change the way the model fits the data. The SSI-PC method is performed for each test setup. Afterwards, the modes for each test setup are determined and then the results of all test setups are merged to form the global set of modal parameters (Magalhães 2010).

The EFDD method allowed to estimate six modes, with the frequency ranging from 2.53 Hz up to 5.81 Hz (Figure 48). The first mode corresponds to a movement in the transversal direction of the church, and in this mode the longitudinal walls present a single curvature in plan. The second mode, with a frequency of 3.42 Hz, corresponds to a local mode of the tower's torsional mode. It is noted that the church can have an asymmetric dynamic behaviour, because there are some adjacent buildings at the east and north sides, and damage also influences the results. In mode 3, with a frequency of 3.81 Hz, the bells move in the longitudinal direction of the church. In the fourth mode, both bell towers move in the transversal direction of the structure, reaching the highest amplitude at the east tower. In the fifth mode, the church moves globally in the transversal direction, and the walls present a second curvature shape. Mode 6, with a frequency of 5.81 Hz, corresponds to the third global mode where the church moves in the transversal direction, and the walls present a triple curvature in plan shape. In the last estimated modes, both the bells were in phase (Figure 49). This method also allowed to determine the damping ratios. The damping ratios for the first and last modes are equal to 2.6% and 1.2%, respectively. This method was not able to determine the damping ratios for all modes.

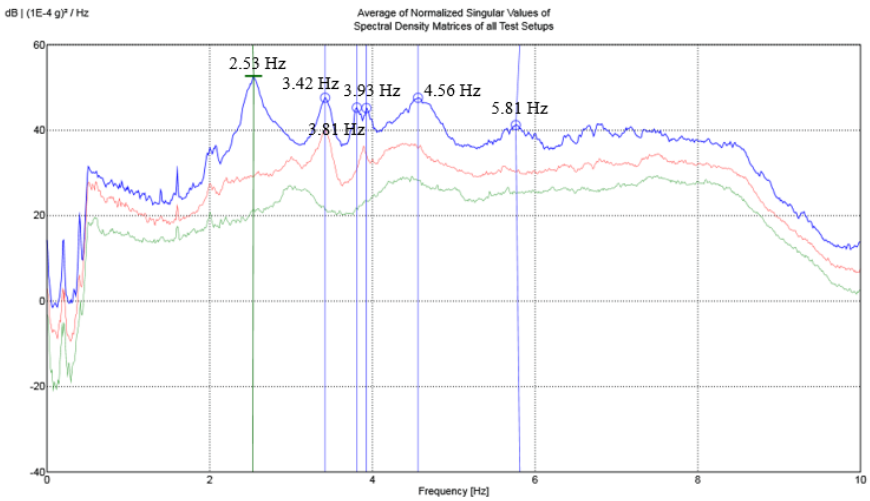

Figure 48 - Average of normalized singular values of the spectral density matrices of all test setups (EFDD method).

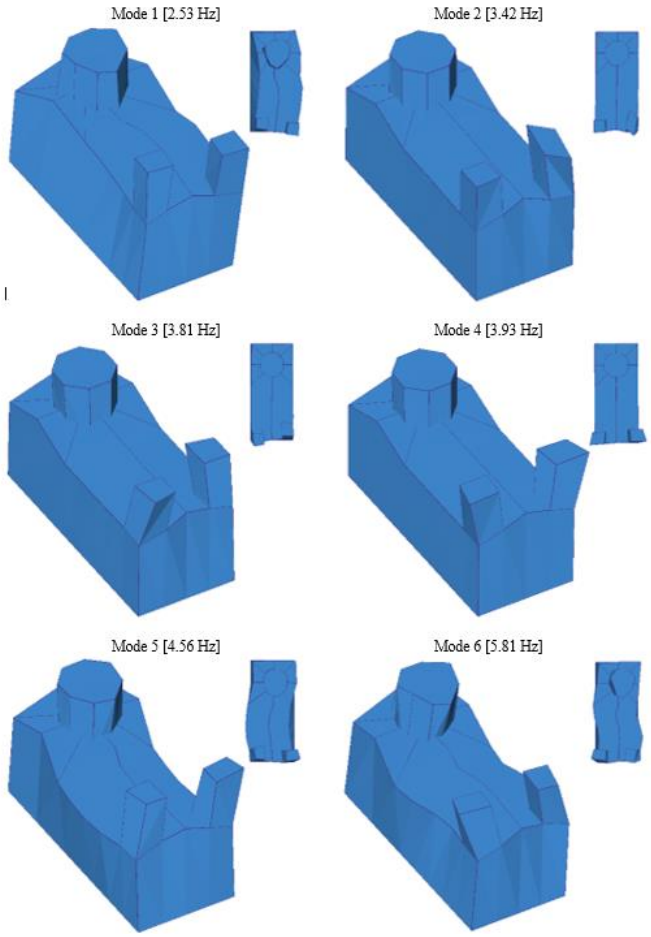

Figure 49 - Mode shapes estimated by the EFDD method.

The SSI-PC method also allowed to estimate six modes in a range of frequencies from 2.53 to 5.78 Hz (Figure 50). The mode shapes determined with this method were very similar to the ones obtained with the EFDD method. Therefore, modes 1,5 and 6 were the first three transversal global modes corresponding respectively to the transversal global modes with simple, double and triple curvatures of the longitudinal walls. The remaining modes were modes (2,3 and 4) corresponding to modes from the bell towers (Figure 51). The natural frequencies were obtained by the two methods are very similar to each other. The difference between the natural frequencies obtained in the two methods is less than 1%. Some set-ups might be more difficult to obtain since only four accelerometers were used and as expected some setups can present more difficulties to estimate all the modes. In particular, modes 2 and 3 were not clearly estimated according to the SSI-PC method in all setups. Additionally, it can be stated that the frequencies are very close to each other.

The SSI-PC method allowed to estimate the damping ratios for all modes, where it can be stated that the average damping ratio was equal to 2.7%. The damping ratio that was obtained for mode 1 was

equal to 2.5% and presented a variation of about 2.5%, according to values estimated by the EFDD method (2.6%).

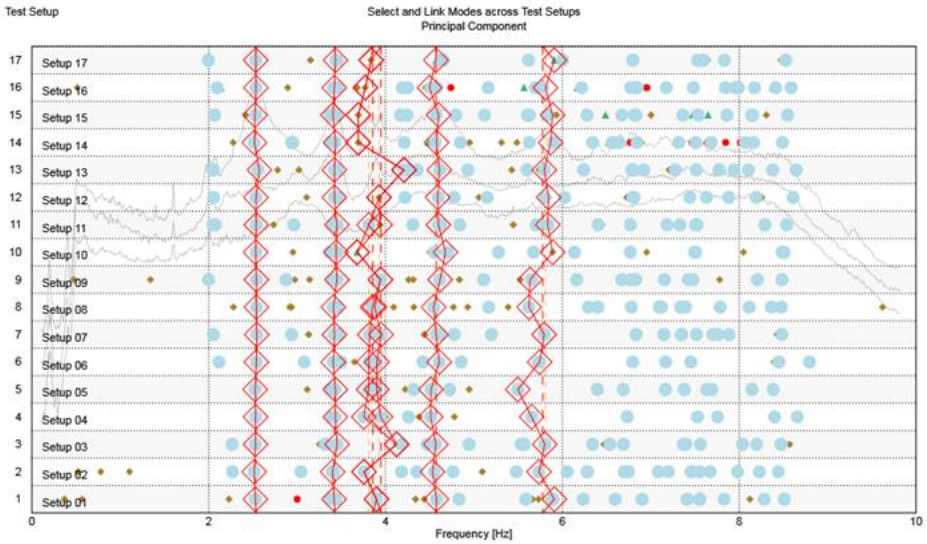

Figure 50 - Select and link modes across test setups (SSI-PC method).

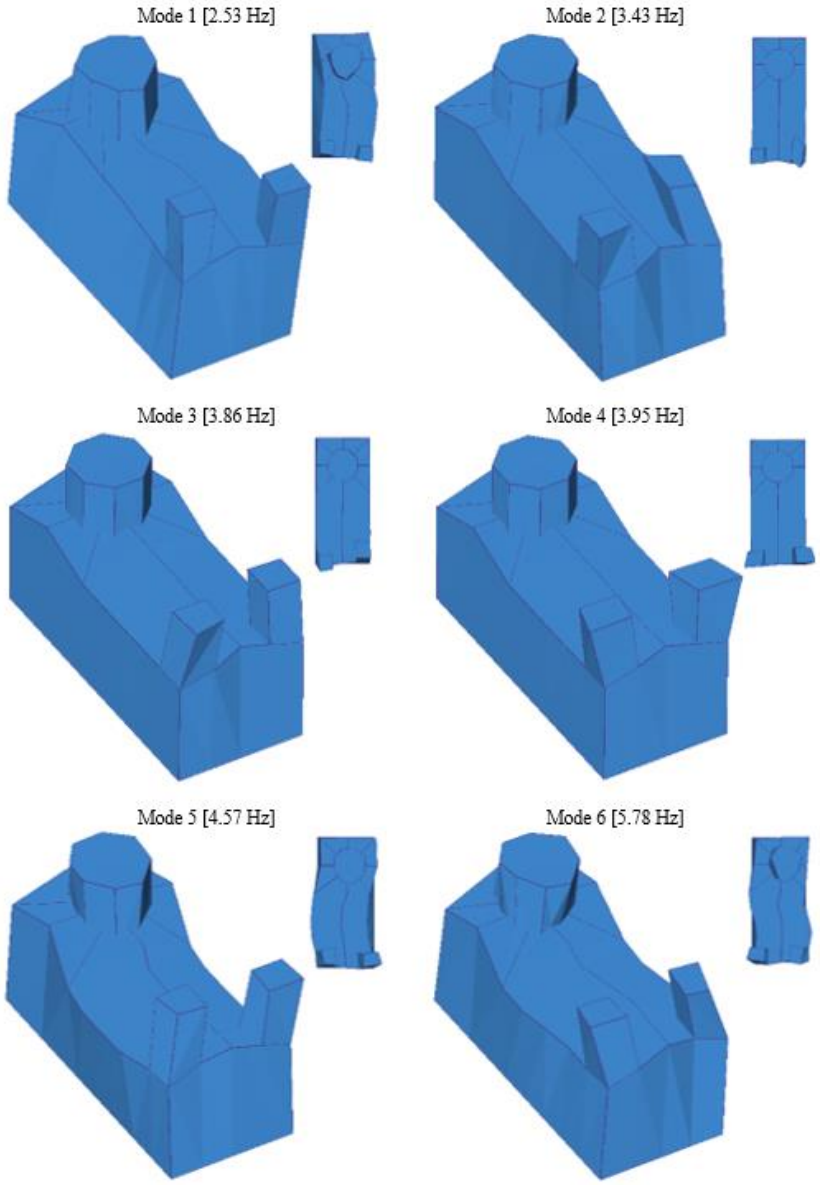

Figure 51 - Mode shapes estimated by the SSI-PC method.

Ultimately, the mode shapes estimated by both methods were compared based on the Modal Assurance Criterion values, and the results showed that the highest MAC values occur for mode 1, with a value of 0.996, which correspond to a perfect match for the first mode estimation by both methods. The average of the MAC values for all mode shapes is 0.70, in which the lowest presents a value of 0.39 for mode 2. The transversal global modes of the basilica present a MAC value on average equal to 0.84, which is a good match comparing the modes estimated by the EFDD and SSI-PC methods (Table 1).

Table 1 - Natural frequencies and damping ratios estimated by the EFDD and SSI-PC methods.

Mode	EFDD	SSI-PC			ΔFrequency
	Frequency	Damping ratio	Frequency	Damping ratio	[%]
	[Hz]	[%]	[Hz]	[%]	
Mode 1	2.53	2.6	2.53	2.5	0.2
Mode 2	3.42	-	3.43	1.7	0.2
Mode 3	3.81	-	3.86	2.3	1.3
Mode 4	3.93	-	3.95	2.0	0.6
Mode 5	4.56	-	4.57	3.1	0.3
Mode 6	5.81	1.2	5.78	4.4	0.6

4. PREPARATION OF THE NUMERICAL MODELS

The main objective of this work was to study the behaviour of the structure, when subjected to the gravitational and seismic loading. It is noted that previous versions of the church were destroyed by earthquakes. Thus, two numerical models with different assumptions were prepared, and pushover analysis for each model was performed. In the first model (Model 1), it was assumed that the outer columns of the structure would support the whole amount of vertical loads (Figure 52.a), which is a rather conservation assumption. In a second model (Model 2), it was assumed that the inner columns and the ribs would also contribute to the capacity of the structure, which is a more realistic assumption. Finally, the same analysis for the Model 2 was performed, but taking into account the damage caused by corrosion based on the survey performed in the past and available in the literature (Figure 52.b).

In general, the models consisted on the typical church frame which is located between the choir loft and the altar. Depending on the model, they can include the columns, the ribs and the truss that supports the roof. To take into account the area of the roof that the truss would sustain, the density of the rafters was changed to consider the weight of the corrugated steel roof.

In these models, several assumptions were made, such as the type of supports in the foundation, modelled as fixed in the three translation directions. The connections between the tie beam and the top of the columns were restrained in terms of rotations in the axial direction of the beam, aiming at preventing the out of plane rotation of the roof truss (Figure 52.c). In reality, the transverse elements in the structure assume this bracing effect.

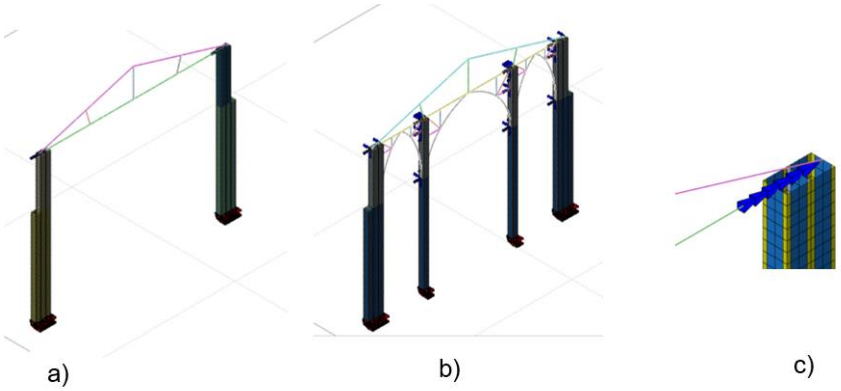

Figure 52: a) general view of model 1; b) general view of model 2; c) restraints at the top of the columns at the connection with the tie beam.

The columns of the structure were modelled using eight node quadrilateral iso-parametric curved shell elements, as shown in Figure 53, that in DIANA software are called CQ40S (Diana 2016). They are based on quadratic interpolation and Gauss integration over the two directions.

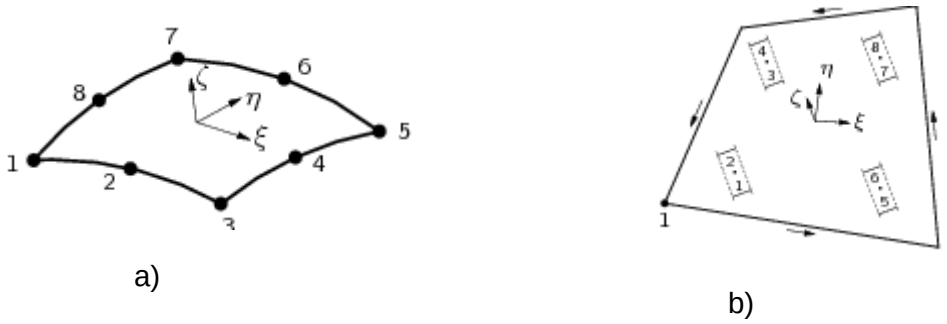

Figure 53 – Shell element: a)C40S elements; b) integration points for the CQ40S elements (DIANA Manual).

The integration along the thickness may be based on Gauss or Simpson, with comparable errors. For each shell element, the adopted number of integration points along the thickness for the nonlinear analysis was five (Figure 54), using the latter.

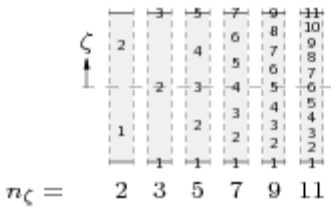

Figure 54 – The integration points along the thickness of a shell element (Diana 2016).

The material properties were assumed to have a behaviour based on the Von Mises law, with a yield stress value of 227MPa. This value was obtained by applying some safety factors (obtained multiplying the average experimental value given in the tests carried out by a reduction factor of 0.8 and was then divided by 1.15), since only a few tests were done on the steel that is part of the structure (Conservation and Development Foundation 2014). The Young's modulus was considered to be 200GPa. For the elements that belong to the structure of the roof truss, the three node and, three-dimensional class-III beam element known as CL18B, was used (Figure 55). The degrees of freedom that these elements take into consideration are the translations and the rotations in the three directions (Diana 2016).

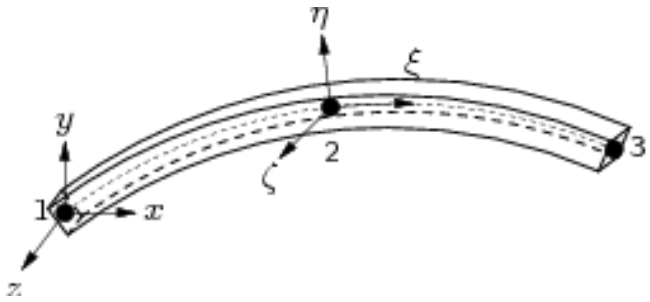

Figure 55 – CL18B element (Diana 2016).

To properly evaluate the stress distribution along the beam elements for the nonlinear analysis, the number of integration points along the thickness and the width also had to be carefully chosen (Figure 56). This number was chosen taking into account the cross-section of the beam element. For these elements, the used number of integration points along the thickness was five, as stated above, and along the length of the element, this number was three.

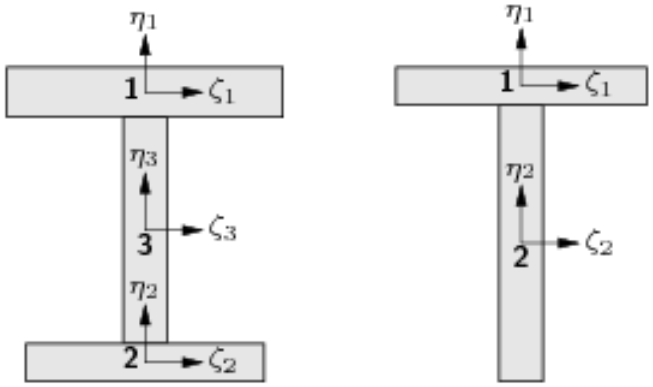

Figure 56 – The integration points of a beam element along the thickness of the element (Diana 2016).

4.1 Model 1

The first model consisted on a frame located between the choir loft and the altar, as discussed before, and it was composed of two columns, corresponding to the outer columns of the nave. In other words,

it was assumed that the vaults and the inner columns would not contribute to the capacity of the structure. It was also assumed that there would be no damage in the columns. Thus, it was possible to have a preliminary approximation on how the structure would behave under vertical and lateral loads.

The columns that are part of the structure of the frame were modelled as shell elements, with different thickness depending on the plans. The roof truss was modelled using beam elements, in which the cross-sections were applied according to the architectural drawings. Model 1 includes 5184 shell elements and 141 beam elements. In total, this model has 15501 nodes and 93006 degrees of freedom.

Figure 57 presents the structure that was considered for Model 1.

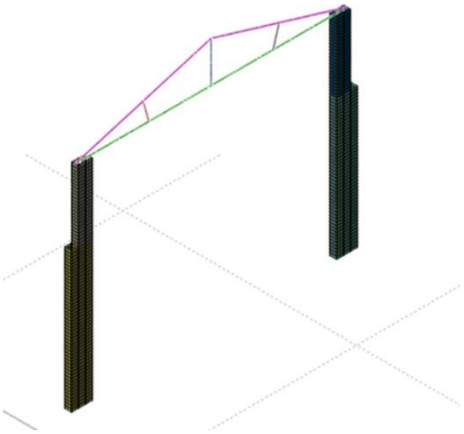

Figure 57 – Overall view on Model 1.

Model 1 was first evaluated through a linear static analysis for the gravitational forces. The results showed that the total self-weight of the structure is equal to 173.0 kN, which is in agreement with the estimated value (172.7 kN). The maximum vertical displacement is equal to 4.7mm and occurs at the middle span between the vertical central post and the lateral post, as it can be observed in Figure 58.a). Very large stresses are localized at the top of the columns in the connection between the truss and the

external columns, while the columns are subjected to very low stress valuesThe maximum vertical stress is equal to 4 kPa (Figure 58.b).

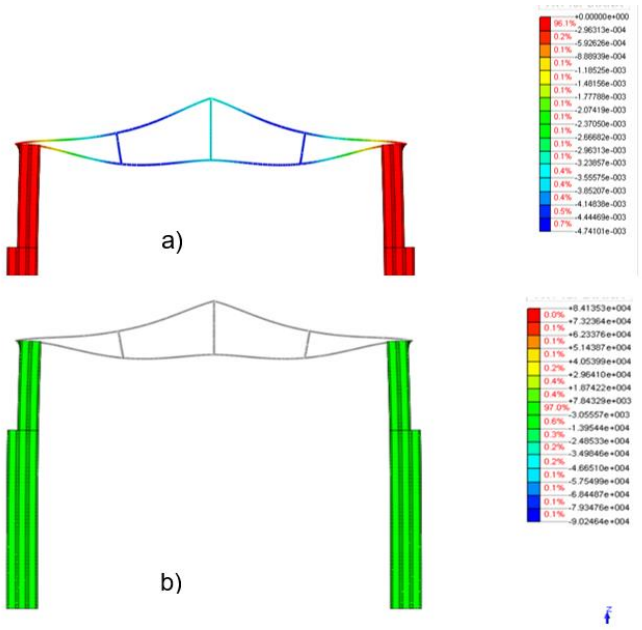

Figure 58 – a) Deformed shape of model 1 under self-weight; b) vertical stresses distribution in the structure.

4.2 Model 2

Contrarily to Model 1, Model 2 includes the inner columns (Figure 59), which is more realistic. This model takes into account the beams that are present at the top of the vaults, and also includes some beams that connect the columns to the beams at the top of the vaults (Figure 60). These elements contribute to the lateral stiffness of the structure, increasing its lateral capacity, and also the vertical capacity of the truss. Furthermore, Model 2 also took into account the weight of a slice of the vaults in the tributary area of the frame.

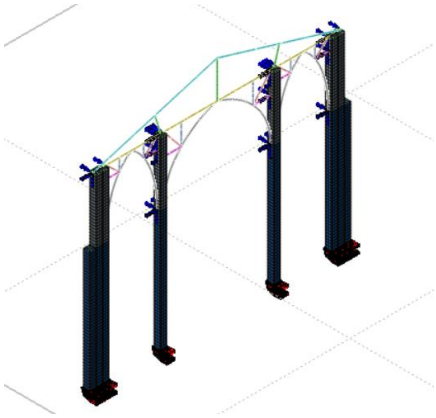

Figure 59 – Overall view on model 2.

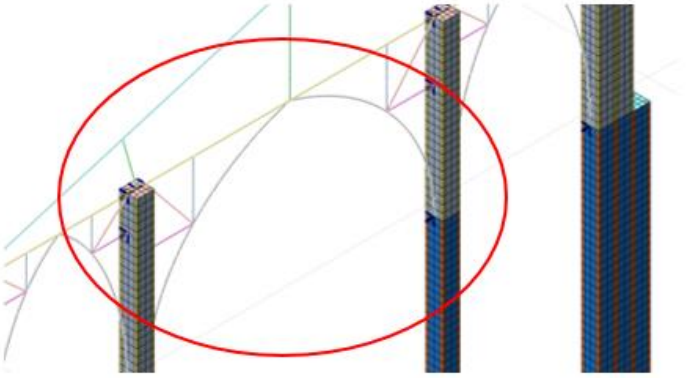

Figure 60 – Beam elements at the top of the vaults beams and reinforcement bars.

In the first model, a concentration of stresses was observed at the connections of the tie beam between the columns and the tie beams, as indicated in the previous section (see also Chapter 6). Therefore, a steel plate was added at the top of the columns. Model 2 includes 7712 shell elements and 390 beam elements. In total, this model has 23431 nodes and 140586 degrees of freedom.

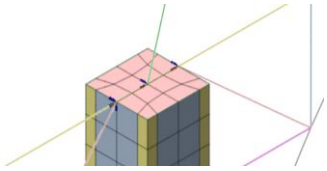

Figure 61 – Additional top steel plates included in model 2.

In this model, corrosion damage was also taken into account, and its influence on the vertical and horizontal capacity was evaluated. The corrosion damage was modelled as a uniform decrease on the thickness of all shell elements. The two levels of thickness reduction that were considered were 20% and 40%.

As previously carried out for Model 1, a linear static analysis considering the self-weight of the structure was performed for Model 2, aiming at validating the results and to be sure that the model was correct. Using this procedure, it was possible to verify if the model had any disconnected elements, and if the properties were properly assigned to the elements. To check if the model had any disconnected elements, the deformed shape of the structure under self-weight was used. Furthermore, to check if everything was correct with the assigned properties of the elements, the reactions were compared with an estimation of a hand calculation. The deformed shape of the structure is shown in Figure 62, in which it is observed that the maximum vertical displacement is equal to 1.2mm (reduction of about 75% with respect to Model 1).

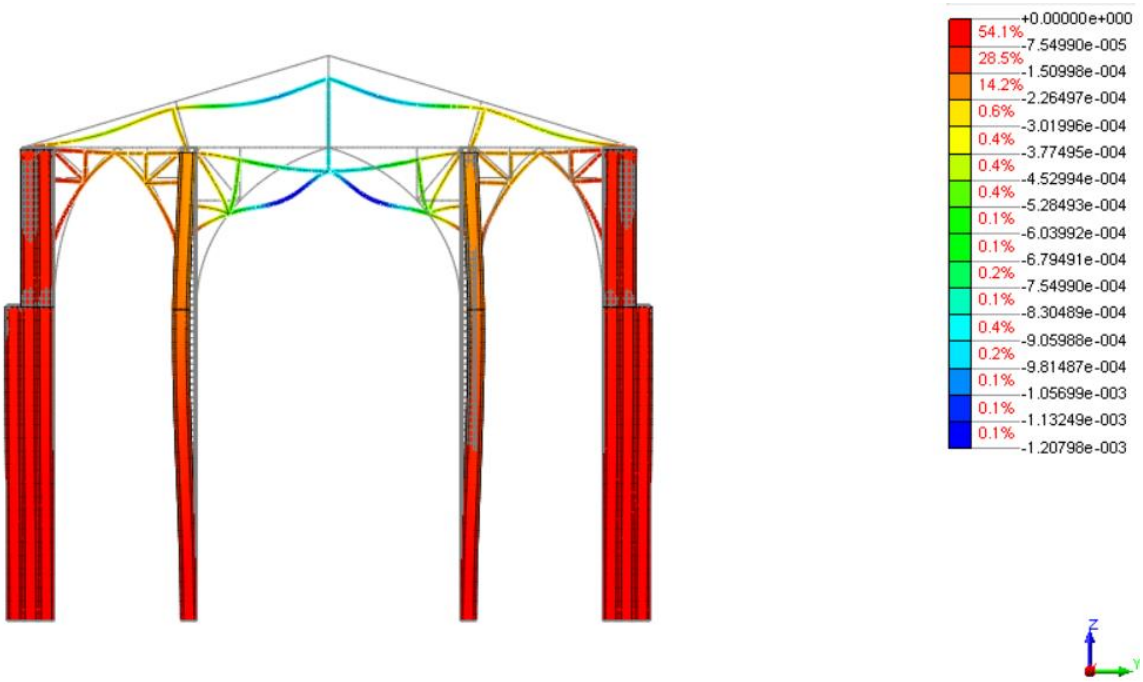

Figure 62 – Deformed shape of the structure. (Units : meters)

The deformed shape of the structure does not present any discontinuity, or any excessive displacement, meaning that the assigned properties were correct. As it was mentioned before, a hand calculation was carried out to determine the vertical reactions, and to be compared with the results obtained by the linear static analysis performed on the software DIANA. By hand calculations, the total vertical reaction is equal to 243.8kN. The total vertical reaction obtained from DIANA is equal to 243.9kN. These results lead to a difference in percentage of 0.1%. Comparing this two results, it can be concluded that Model 2 presents results according to the expected. The values that were chosen to the self-weight of the different sections of the elements were correct. The maximum vertical stresses at the bottom of the columns is 25.9kPa, with larger peaks at the connections.

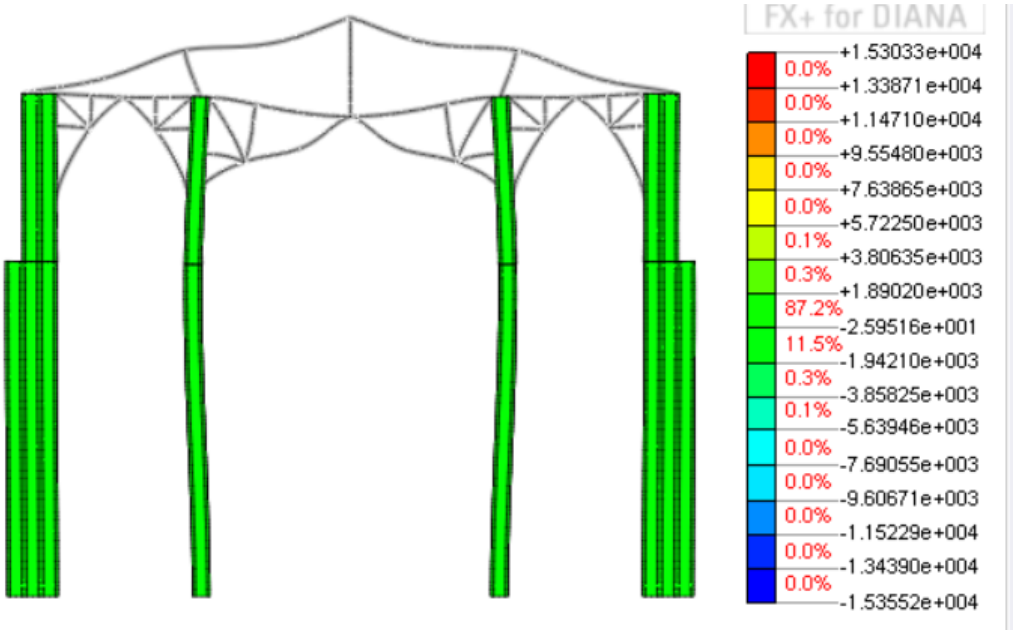

Figure 63 – Vertical stress distribution on the structure (kPa).

5. NUMERICAL ANALYSIS

5.1 Analysis for gravitational loads

5.1.1 Model 1

To apply the gravitational forces corresponding to the self-weight of the structure, the gravity acceleration was applied (9.81m/s^2). To analyse the vertical response of the structure, a nonlinear static analysis was performed. First, the gravitational loads were applied gradually in ten steps until the load factor was equal to 1.0. Then the analysis was carried out applying smaller steps until reaching the collapse.

Figure 64 presents the deformed shape for the maximum load capacity.

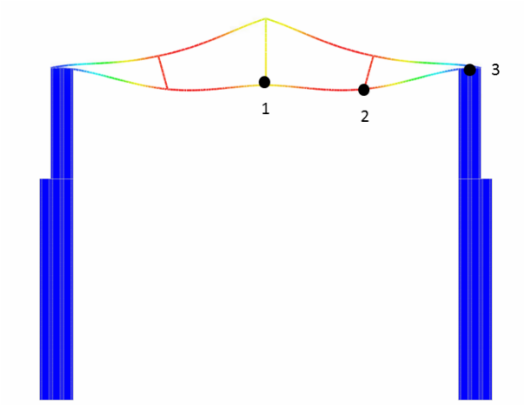

Figure 64 – Deformed shape of the structure.

In order to be able to evaluate the collapse load of the structure, several capacity curves were presented and compared. The capacity curves show that the maximum load factor is equal to 10.5, which corresponds to a high safety factor for the gravitational loads, see Figure 65.

As was expected, the top of the columns (Point 3) is the point where the vertical displacements are the smallest (3cm). These displacements get higher values when approaching the middle span of the frame, where the maximum vertical displacement is equal to 42cm.

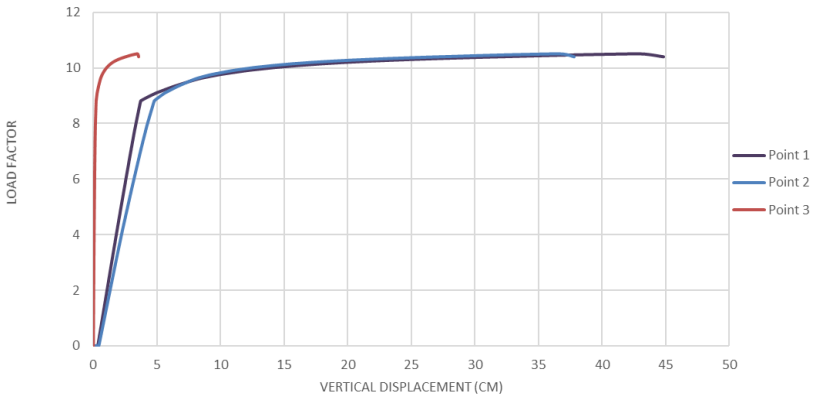

Figure 65 – Capacity curves of Model 1 for gravitational loads.

Besides the deformation, it is also fundamental to evaluate the damage of the structure. To do that, an analysis of the principal stresses must be done, to check where excessive stresses occur either in the external or internal fibres. Globally, the stresses on the structure do not surpass the maximum values that the material can resist, see Figure 66.

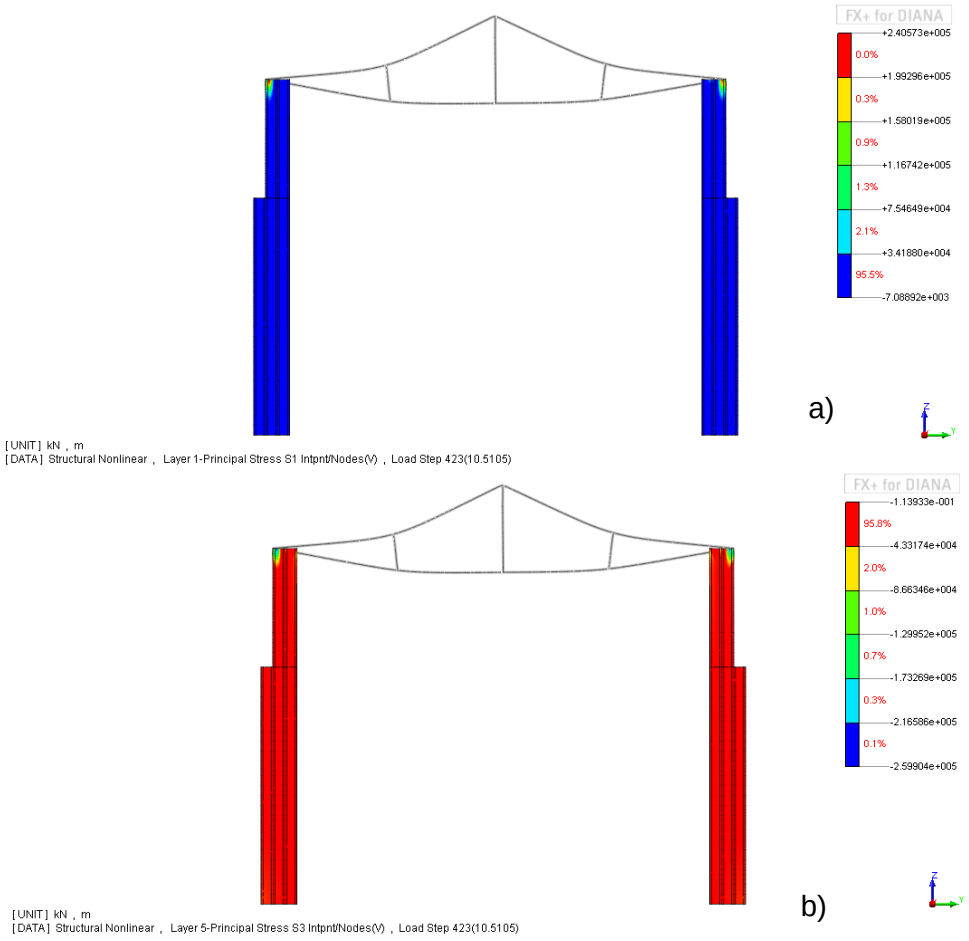

Figure 66 - Maximum principal stresses distribution for: a) the external fibres; b) internal fibres. (kPa)

Figure 67 and Figure 68 present the normal stresses in the YY local axis of the beam elements for the upper and lower fibres, respectively. The normal stresses distribution in YY local axis are within the expected shape, where the higher stresses occur in the central parts of the frame. The values of the stresses indicate that the failure might occur at the tie beam in the connection with the lateral posts.

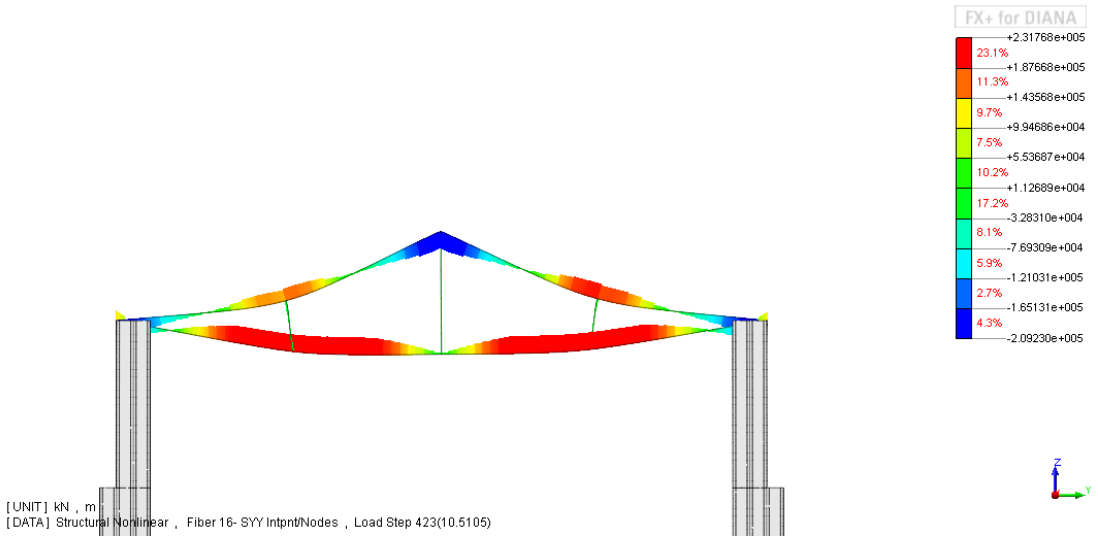

Figure 67 – Normal stresses at the upper fibre of the beam elements of the truss.(kPa)

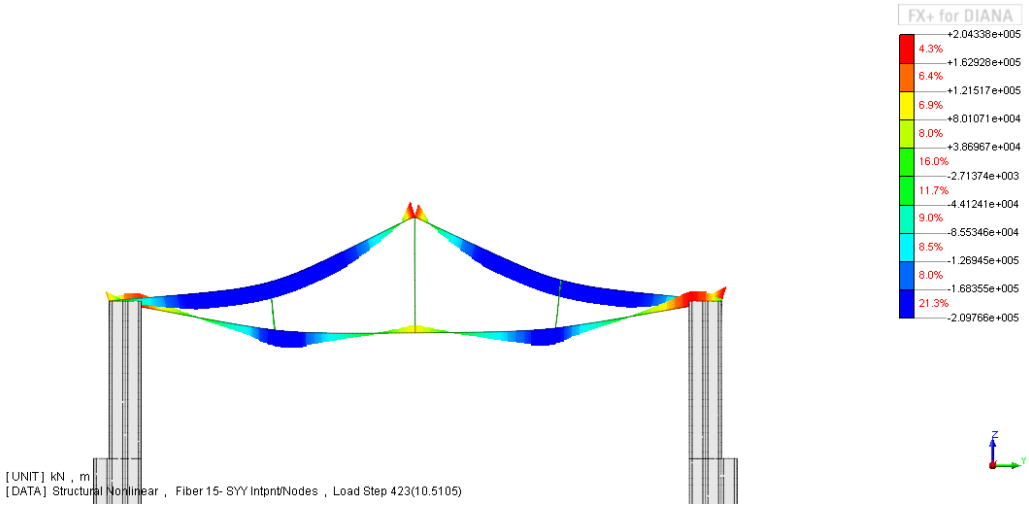

Figure 68 – Normal stresses at the lower fibre of the beam elements of the truss. (kPa)

Figure 69a) and b) presents the maximum tensile principal stress distribution for the last step of the analysis in the column/ truss connection. The results show that these connections present a concentration of stresses, which is according to the simplification assumed for its modelling (beam elements connected to the nodes of the shell elements). Based on these results, Model 2, which contains the inner columns and the beams of the vaults, has on top of the columns a steel plate that

reduces the stress concentration on this area. Figure 70 presents the Von Mises stress distribution on the connection between the tie beam and the top of the column, where the concentration of stresses is also observed, with local failure.

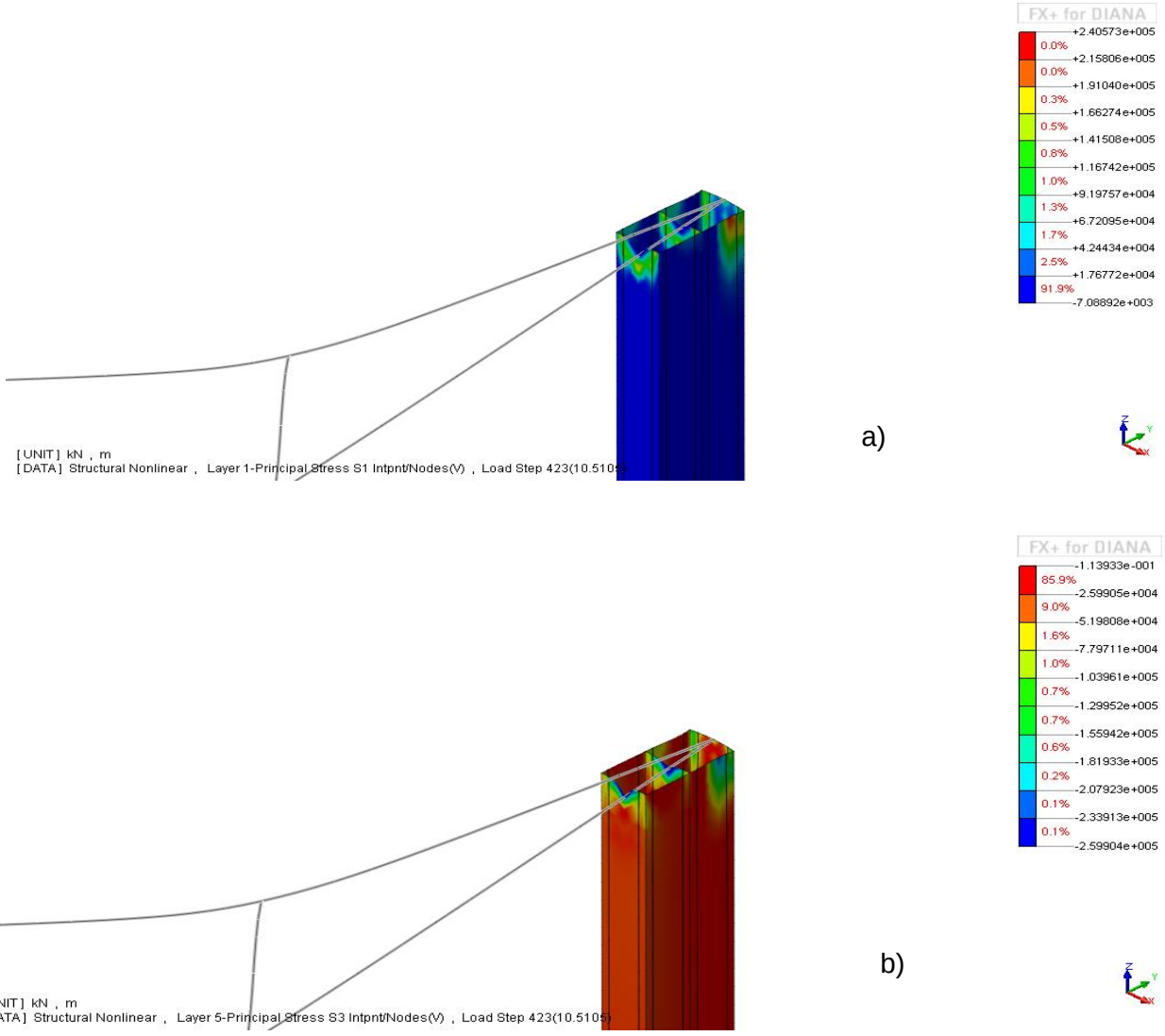

Figure 69 – Maximum tensile principal stresses distribution for: a) the external fibres; b) internal fibres. (kPa)

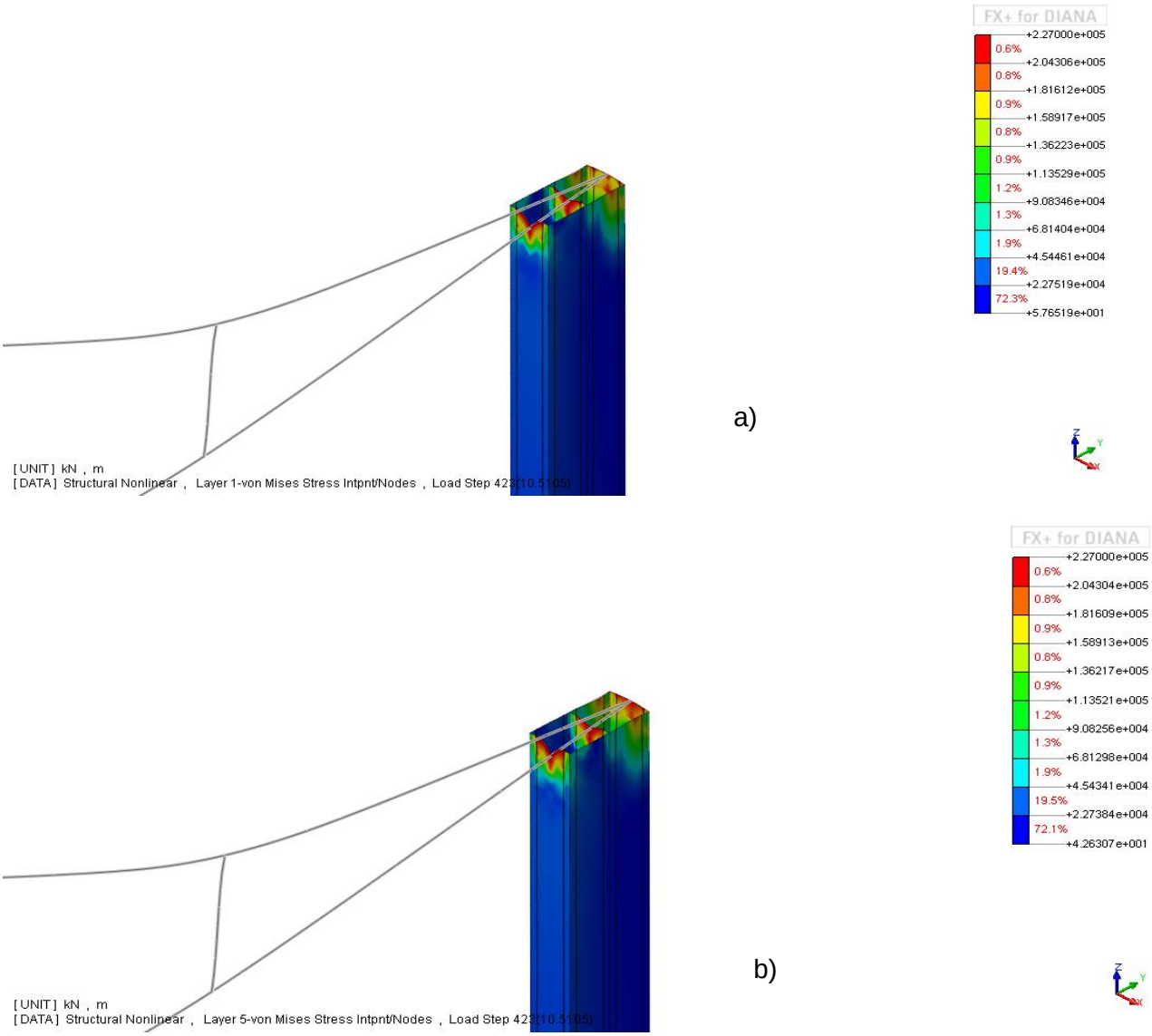

Figure 70 – Von Mises stress distribution for: a) the external fibres; b) internal fibres. (kPa)

5.1.2 Model 2

The procedure that was adopted for Model 1 was repeated for Model 2. The maximum vertical displacement occurs at the middle of the truss elements and is equal to 6cm, as it is depicted in Figure 71.

It is noted that the beams of vaults present a maximum vertical displacement equal only to 0.6cm.

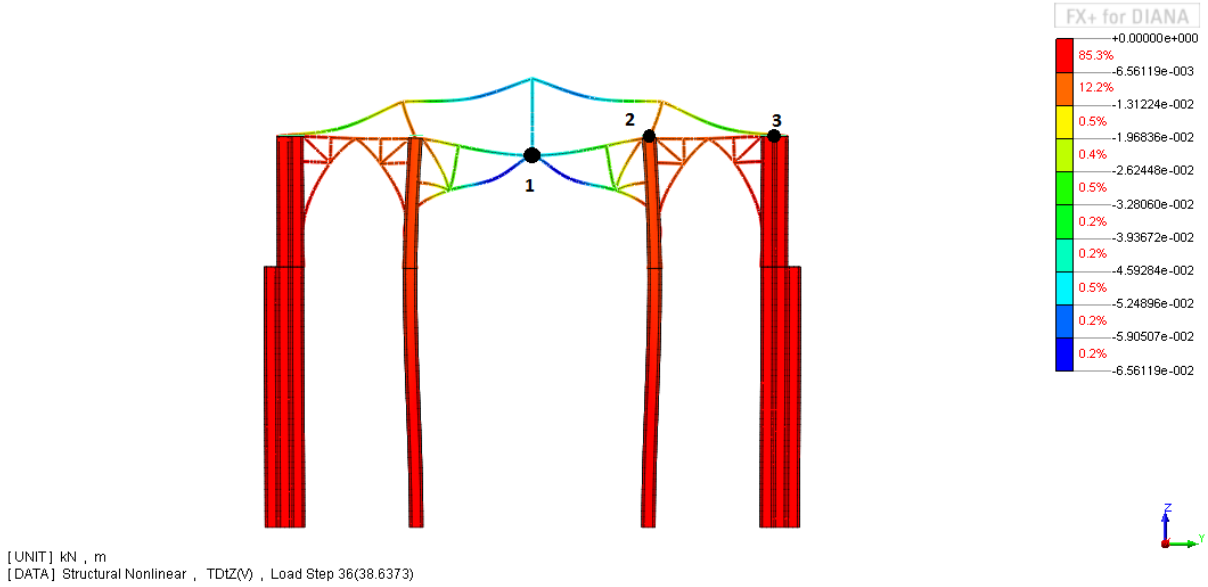

Figure 71 - Vertical displacements of Model 2. (m)

Figure 72.a) and b) present the maximum principal stress distribution on Model 2. The obtained values are within the expected range and the distribution of stresses along the structure is realistic in a way that there are not any parts of the structure where the stress state is not the expected.

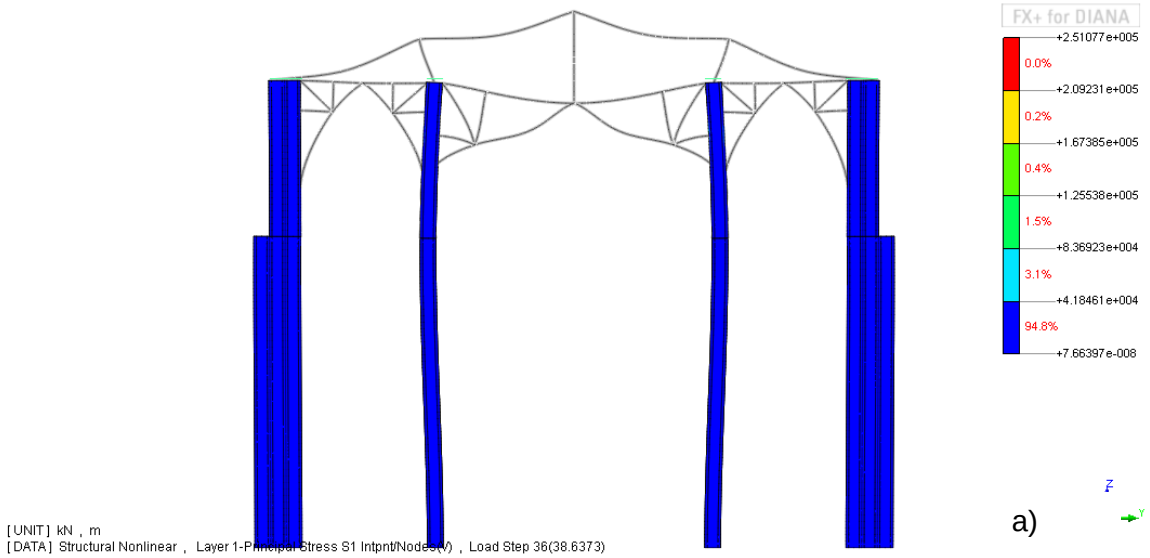

Figure 72 – Maximum principal stresses for a) the external fibres; b) internal fibres. (kPa)

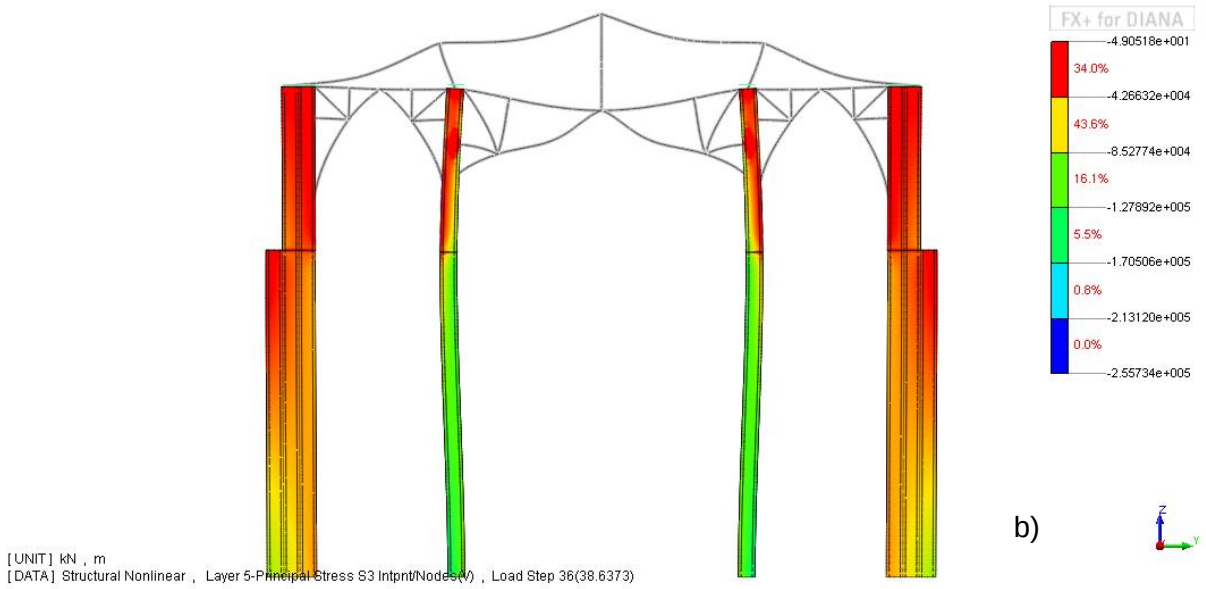

The capacity curve for the three considered points is presented in Figure 73, where it is observed that the maximum load factor is equal to 37 (3.5 times higher than the maximum load factor of Model 1).

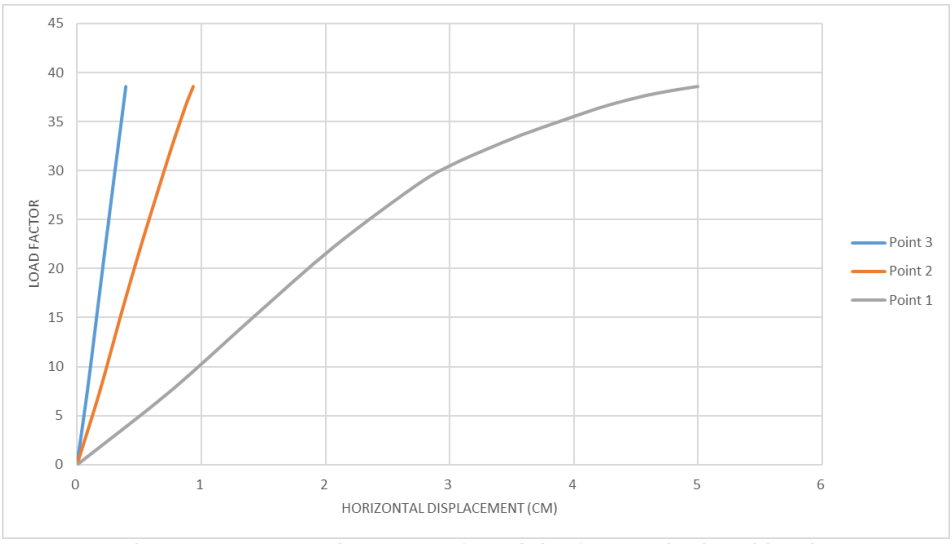

Figure 73 – Capacity curve of Model 2 for gravitational loads.

Figure 74 and Figure 75 present the normal stresses in the YY local axis of the beam elements for the upper and lower fibres, respectively. The normal stresses distribution in YY local axis are within the expected shape, where the higher stresses occur in the central parts of the frame. The values of the stresses indicate that the failure might occur at the middle span of the beams due to excessive tensile stresses, at the horizontal members of the reinforcement bars, in the part above the columns with the lateral posts, also for excessive tensile stresses, and at the middle of the central arch both for excessive compressive and tensile stresses.

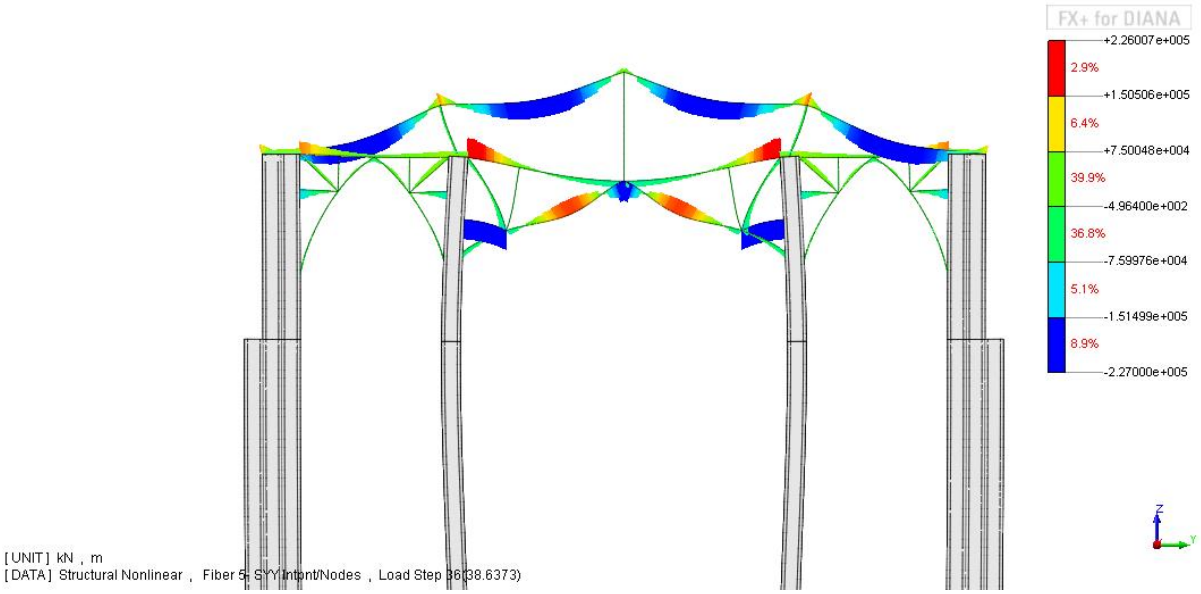

Figure 74 - Normal stresses at the upper fibre of the beam elements of the truss.(kPa)

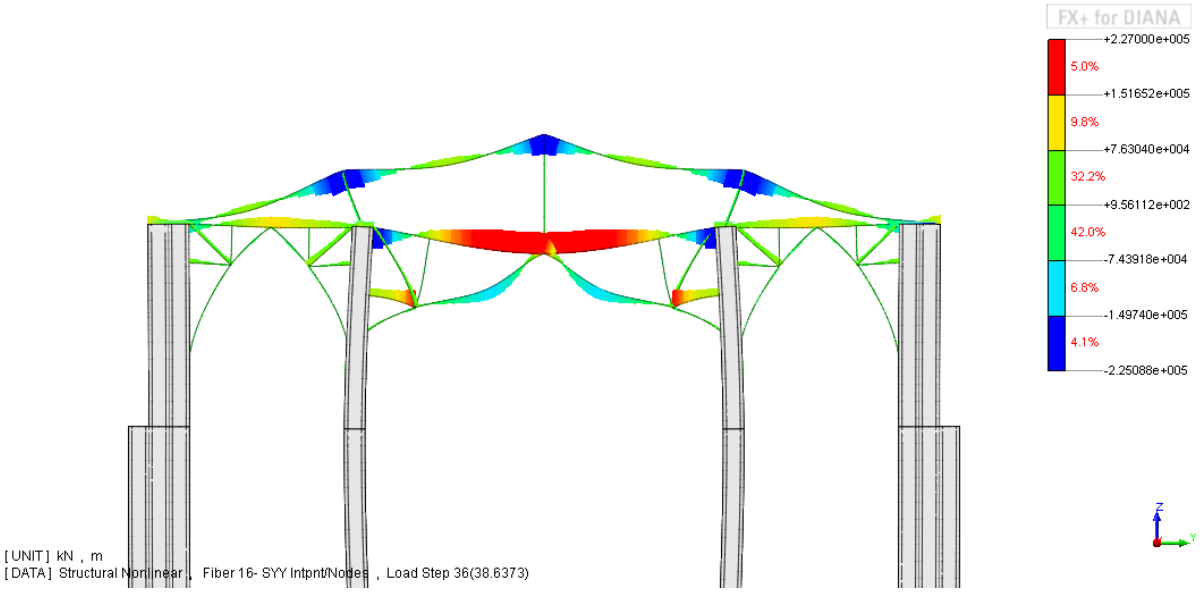

Figure 75 - Normal stresses at the lower fibre of the beam elements of the truss.(kPa)

As it was referred in the last section for Model 1, Model 2 includes at the top of the columns, steel plates in order to reduce the stress concentrations. Figure 76 presents the maximum principal stresses distribution there, and their values, where it can be observed that the values of the stresses are greatly reduced.

Figure 77 presents the Von Mises stress distribution on the structure, where it can be concluded that the columns might start to create a mechanism at the base where the stresses are higher and at the connections of the beam horizontal elements with the columns.

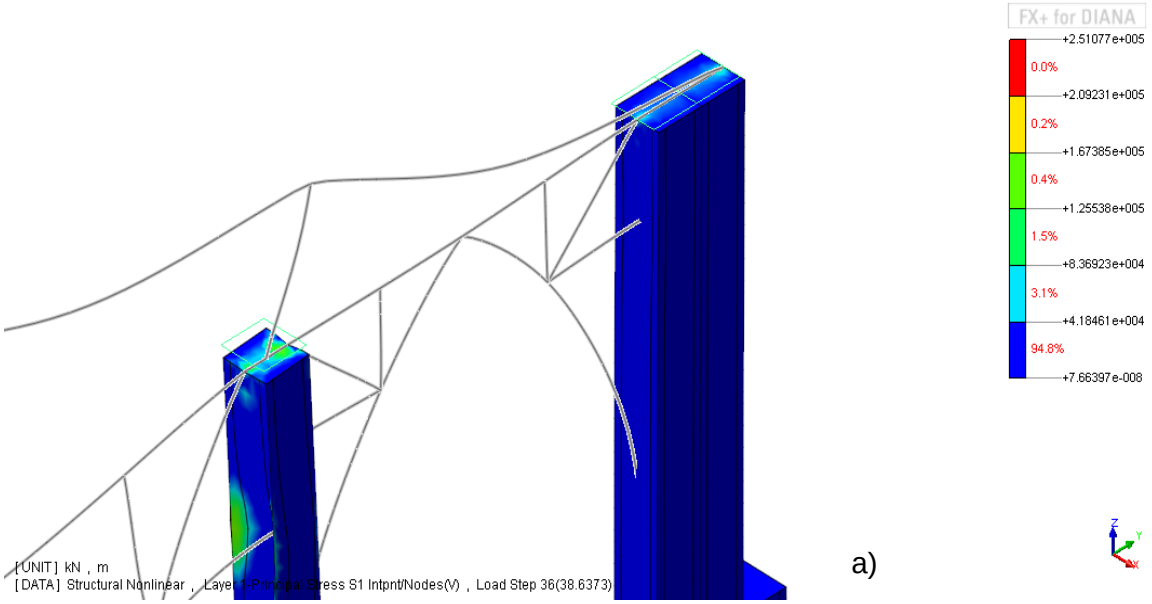

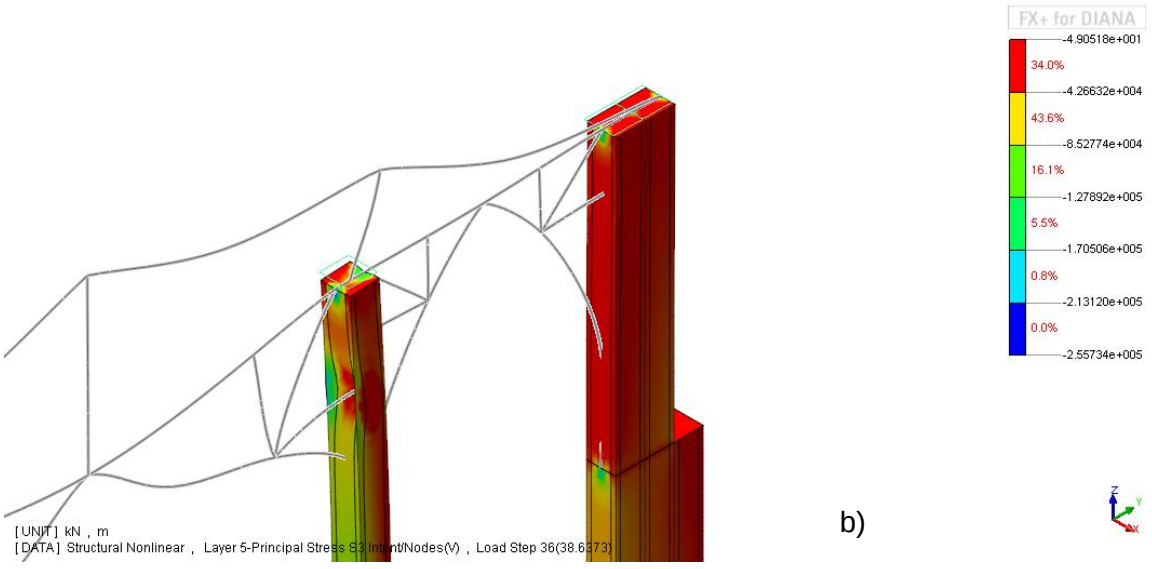

Figure 76 - Maximum tensile principal stresses distribution for: a) the external fibres; b) internal fibres. (kPa)

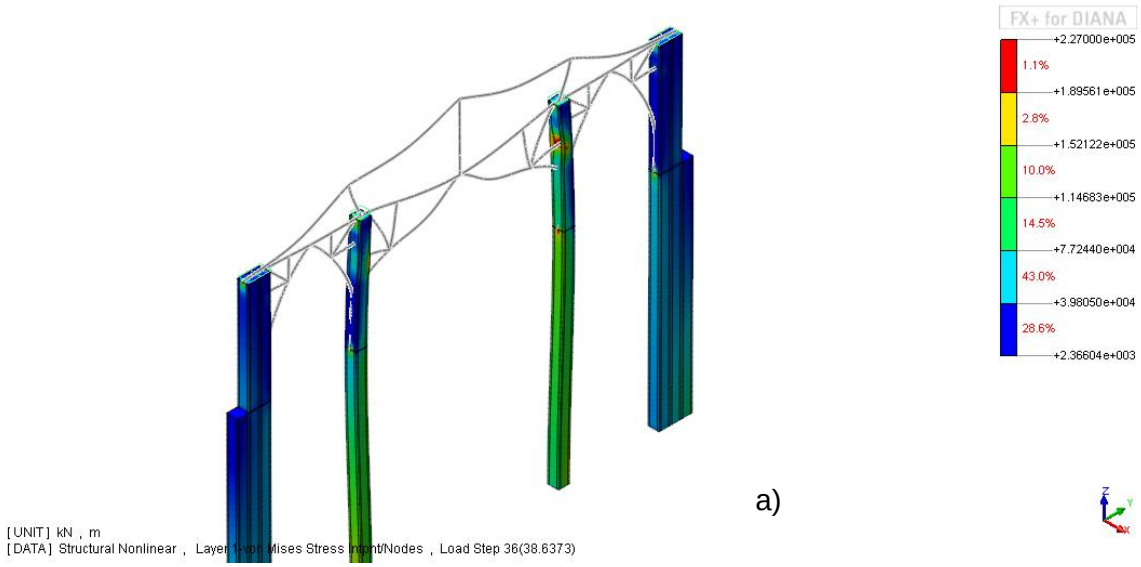

a)

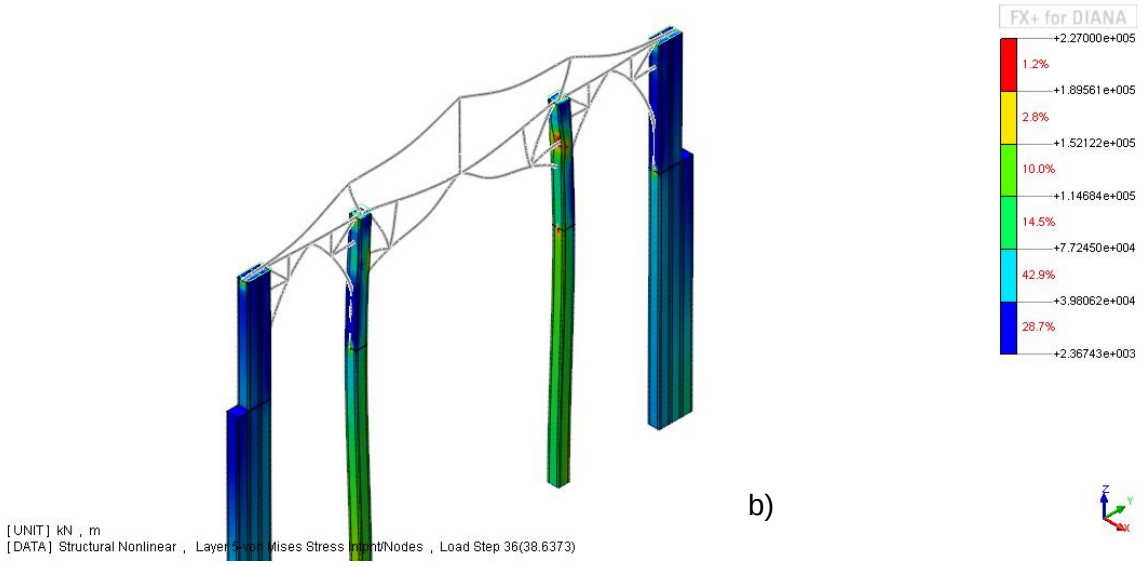

b)

Figure 77 - Von Mises stress distribution for: a) the external fibres; b) internal fibres. (kPa)

5.2 Analysis for seismic load

The Philippines is a country where there is a very high seismic activity. That is why it turns out to be relevant in this work to characterize the seismicity in that area. The western part of the Philippine plate is divided into five zones, based on the geologic character. These zones are the Nankai trough, the

Ryukyu arc system, Taiwan, the Luzon Strait between Taiwan and the northern Philippines, and the Philippines.

The Nankai trough is a recent trench, whose activity records present proofs of intense seismic activity presenting great earthquakes with large rupture zones and tsunamis dating back to the year 684 (Wyss 1979). The Ryukyu arc is a trench that it is not so recent, and presents a well-defined dipping seismic zone. The areas that include Taiwan, the Philippines, and the neighbouring regions seem to be integrated in a part of complex island arc systems. Parts of the latter experience frequent large shocks, but lack well-developed subduction zones.

The closest zone to the Philippines is the Luzon Strait, located between the northern Philippines and Taiwan, consisting in a series of ridges and troughs that are broken into big segments, which suggest that lateral shear is operating in this region (Wyss 1979). In this region, there is not any record of a large earthquake in the past years (Wyss 1979).

The Philippines' seismic activity is known to be characterized by frequent large, shallow earthquakes that occur across the different islands. The main sources of such events are the Manila trench, the Philippine fault system and the Philippine trench. The Philippine fault system is extended from Mindanao to central Luzon, where it divides into a number of subparallel faults that extend to northwestern Luzon. In the last years, the epicentres for the larger earthquakes seem to appear close to the fault trace, and some sections of the fault with 75km or more in length have not yet ruptured and seem to be a potential source of future large events (Wyss 1979).The Philippine trench has large earthquakes typically originated by shallow events.

Taking all this into consideration, studies were performed in the past by Wong et al, for a return period of 475 and 2475 years, for which the PGA values are 0.42g and 0.69g, respectively (Wong, Dawson, and Dober n.d.).

5.2.1 Model 1

The seismic response of Model 1 was evaluated through a pushover analysis with horizontal load distribution proportional to the structure's mass.

Figure 78 illustrates the horizontal displacement of the structure for the last step of the pushover analysis. The maximum horizontal displacement occurs, as expected, at the top of the columns, and is equal to 22cm.

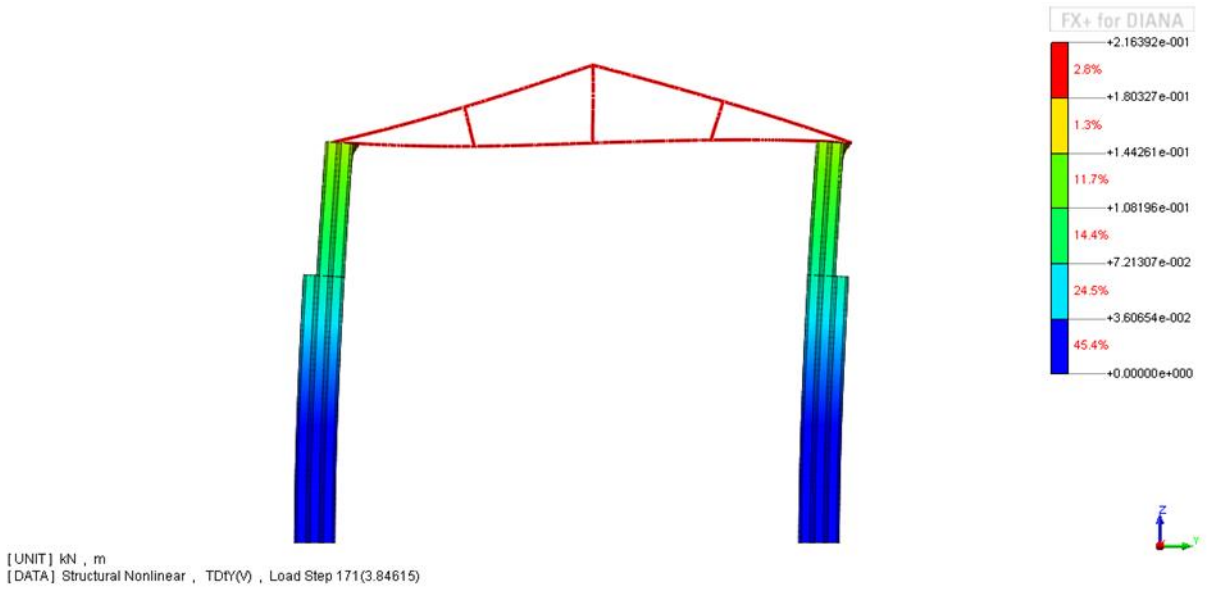

Figure 78 – Horizontal displacements for the seismic action. (m)

Figure 79 presents the capacity curve of Model 1 for the seismic action, in which it is observed that the maximum load factor is equal to 3.8g (a value much larger than the reference one for Manila [0.42g]).

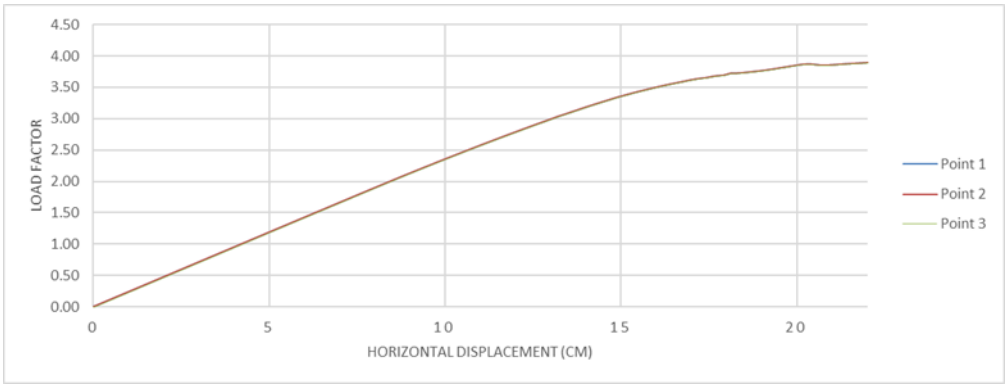

Figure 79 – Capacity curves of Model 1 for seismic action.

Figure 80.a) and b) present a general view on the maximum principal stress distribution on Model 1 for the seismic load. The obtained values are within the expected range and the deformation of the structure indicates local collapse at the connection between the truss and the columns.

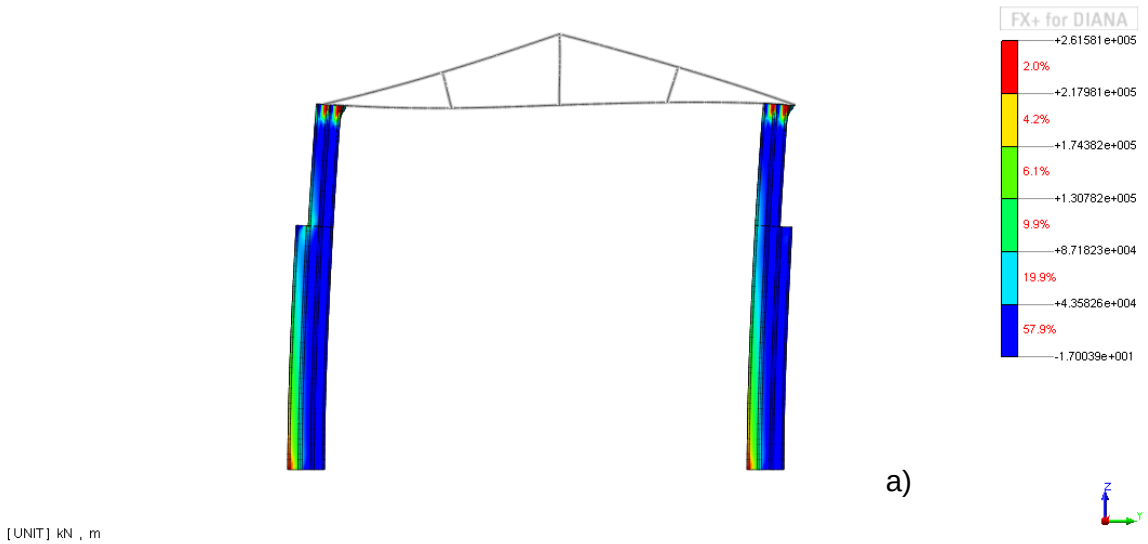

Figure 80 – Maximum principal stresses for: a) external fibres; and b) internal fibres.

The normal stresses distribution in YY axis of the beam elements, presented in Figure 81 and Figure 82, are within the expected shape, where the higher stresses would develop in the areas next to the connections with the columns frame. The values of the stresses indicate that failure might occur at the tie beam in the connection with the columns, although the stresses in the structure did not reach the limit values, confirming the failure at the connection.

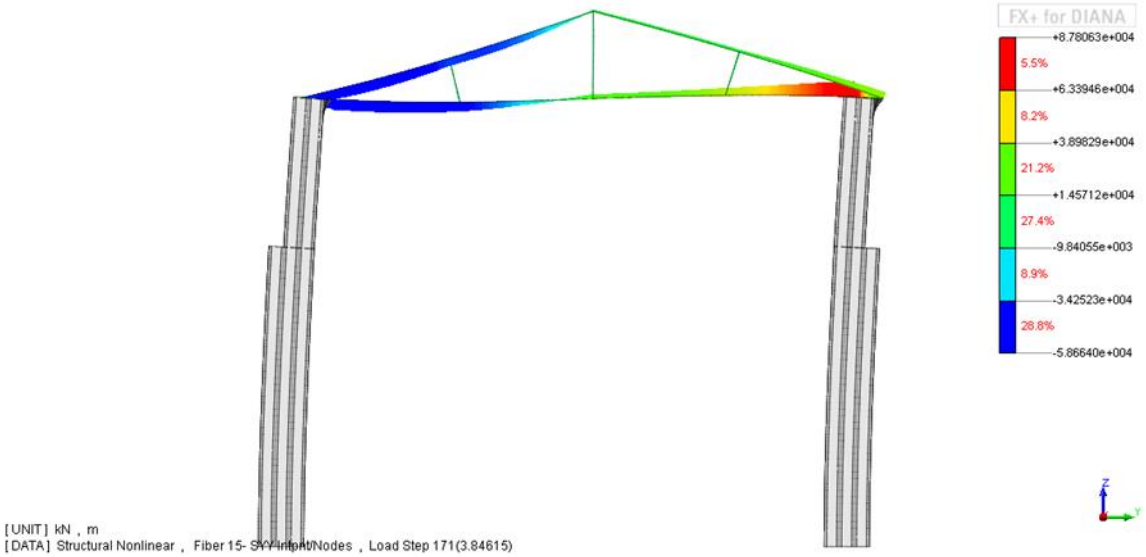

Figure 81 - Normal stresses at the upper fibre of the beam elements of the truss.(kPa)

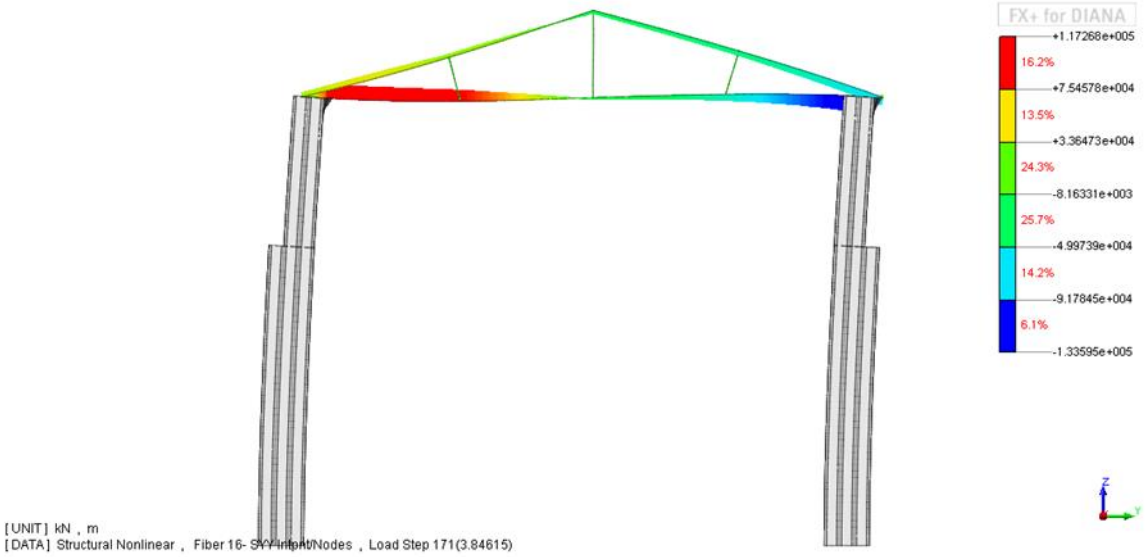

Figure 82 - Normal stresses at the lower fibre of the beam elements of the truss.(kPa)

The maximum stresses occur at the base of the columns, and slowly decrease as they head to the middle of the column, and when they reach the area next to the connection of the tie beam and the column, they increase again (Figure 83).

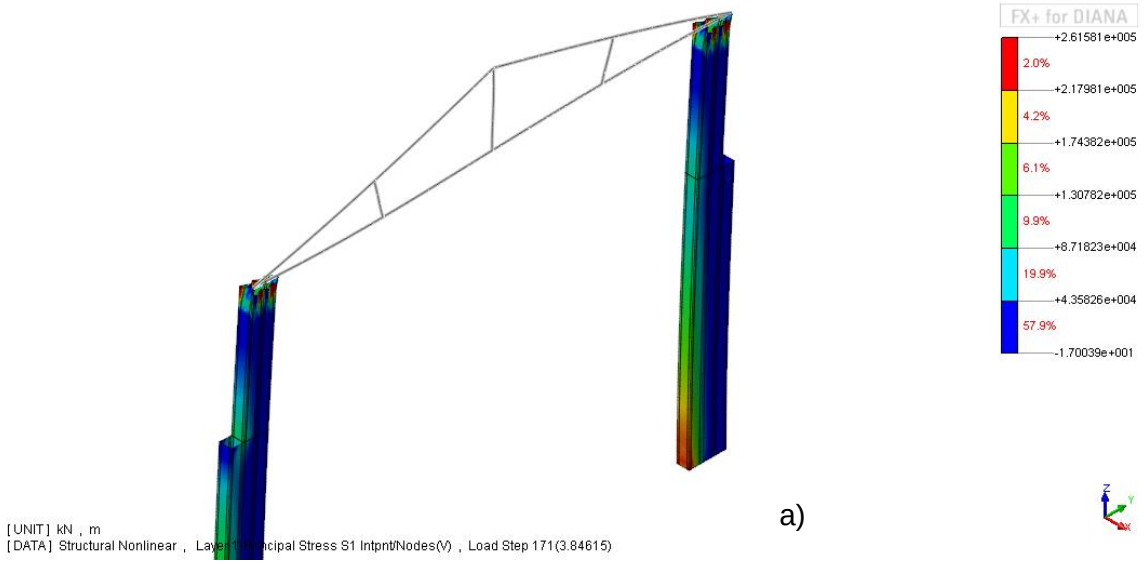

a)

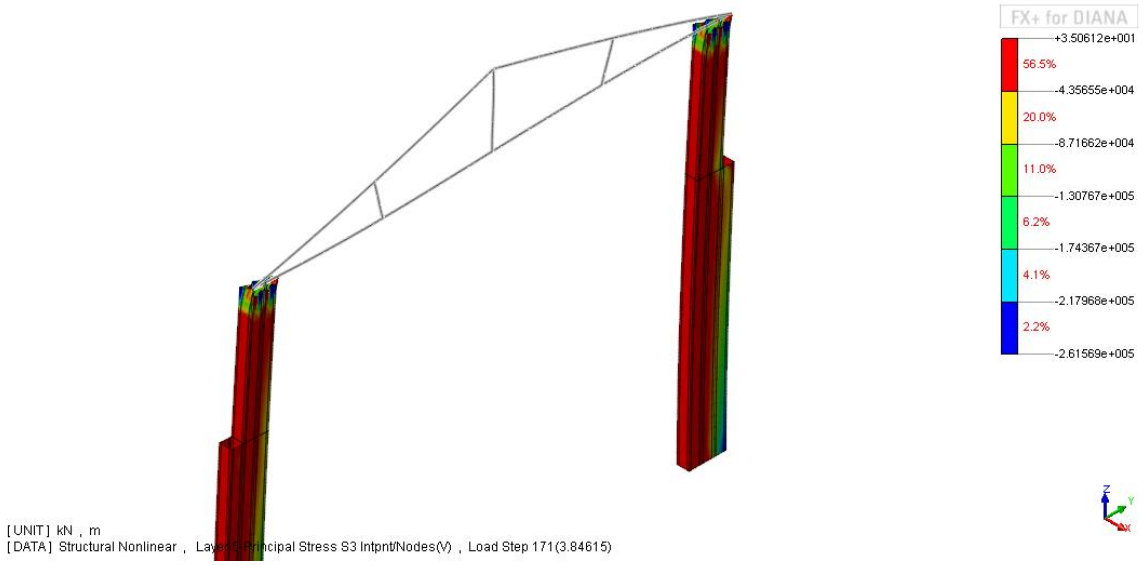

b)

Figure 83 - Maximum tensile principal stresses distribution for: a) the external fibres; b) internal fibres. (kPa)

Figure 84 presents the Von Mises stress distribution on the structure, where it can be concluded that the structure might start to create a mechanism at the base where the stresses are higher and at the connections of the beam horizontal elements with the columns.

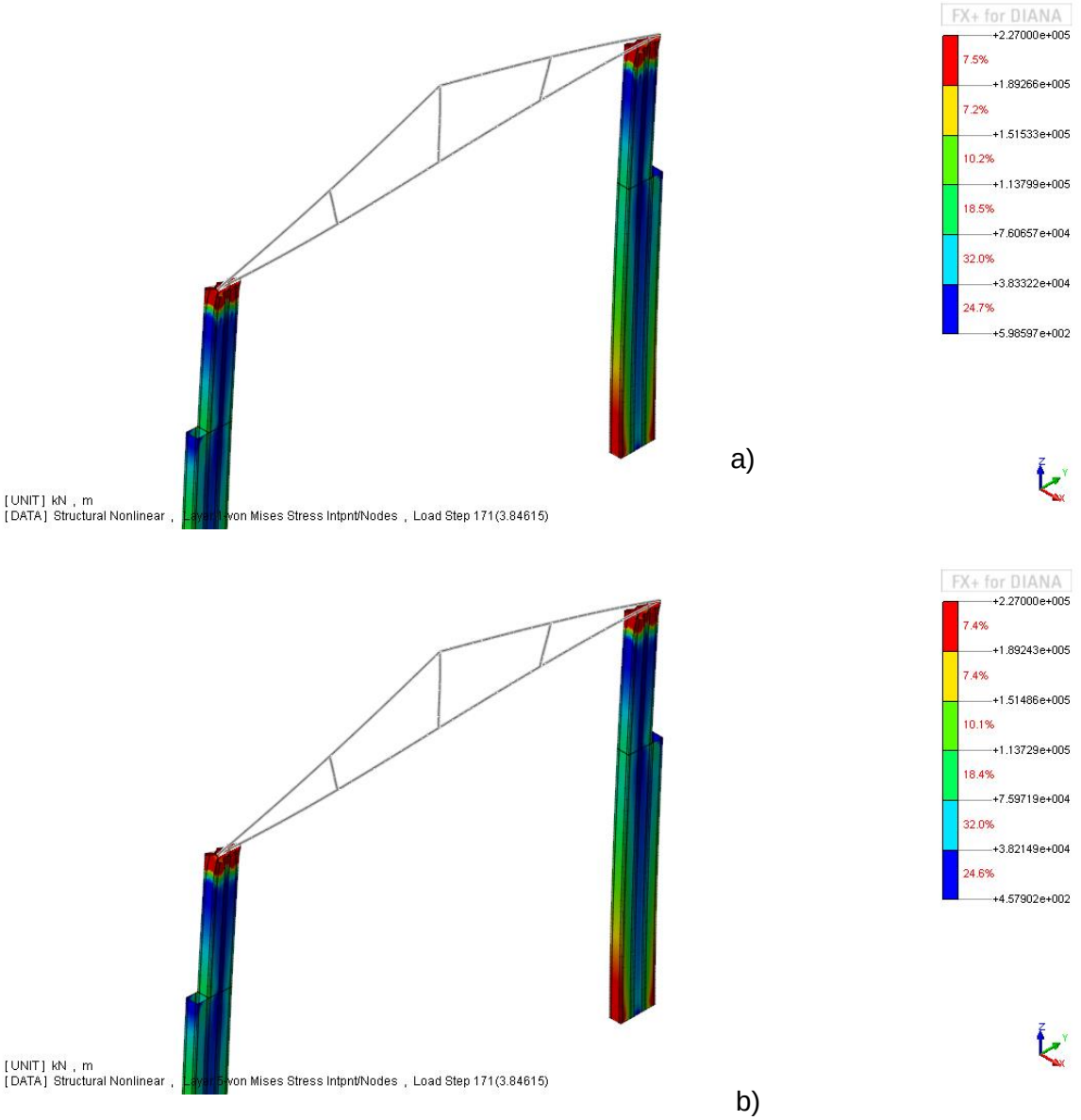

Figure 84 - Von Mises stress distribution for: a) the external fibres; b) internal fibres. (kPa)

5.2.2 Model 2

The seismic response of Model 2 was evaluated through a pushover analysis with horizontal load distribution proportional to the structure's mass.

Figure 85 illustrates the horizontal displacement of the structure for the last step of the pushover analysis. The maximum horizontal displacement occurs, at the beams of the vaults. In order to compare the values obtained with Model 1, the horizontal displacement obtained at the top of the columns was 26cm.

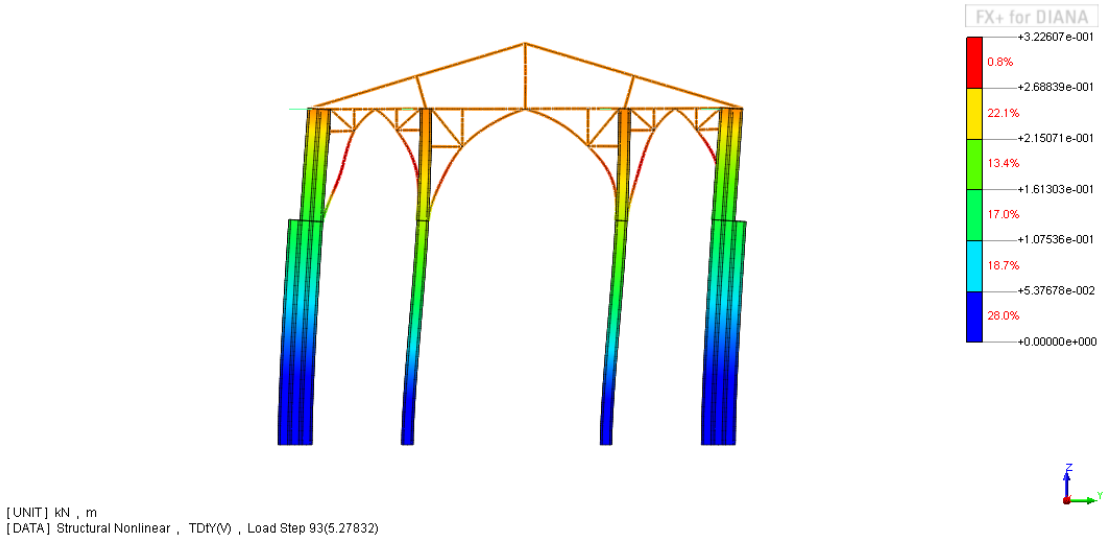

Figure 85 - Horizontal displacements for the seismic action. (m)

Figure 86 presents the capacity curve of Model 1 for the seismic action, in which it is observed that the maximum load factor is equal to 5.3g (again, a value much higher than the reference one for Manila [0.42g]).

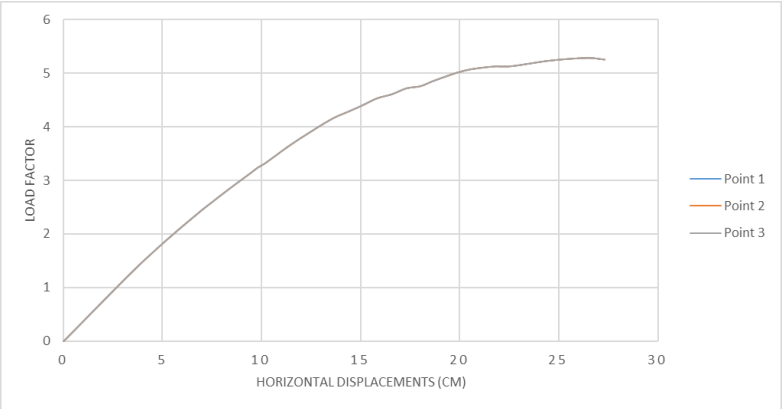

Figure 86 - Capacity curves of Model 2 for seismic action.

Figure 87.a) and b) present a general view on the maximum principal stress distribution on Model 1 for the seismic load. The obtained values are within the expected range and the deformation of the structure is according to the expected.

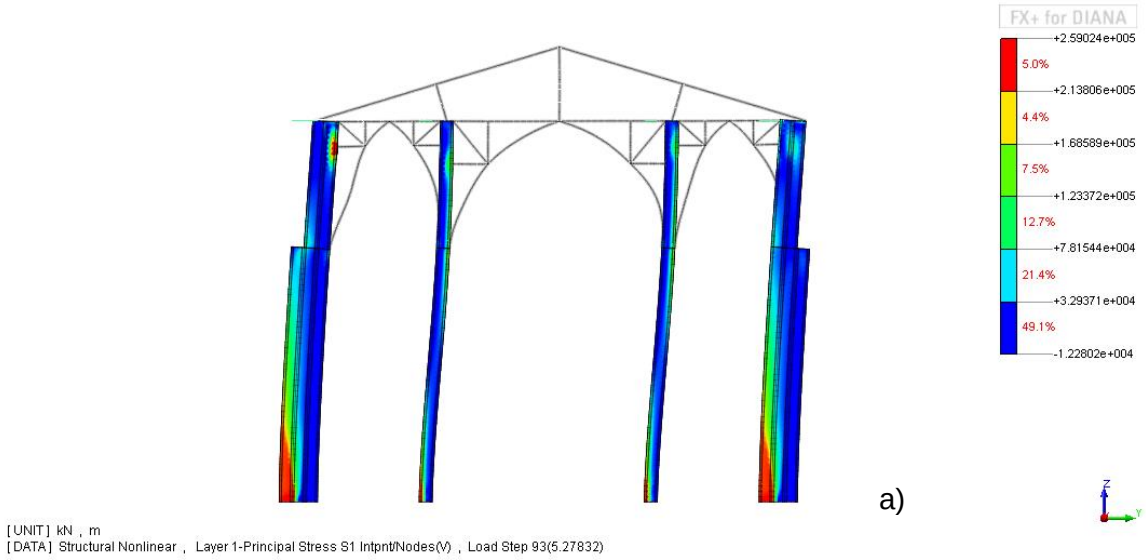

a)

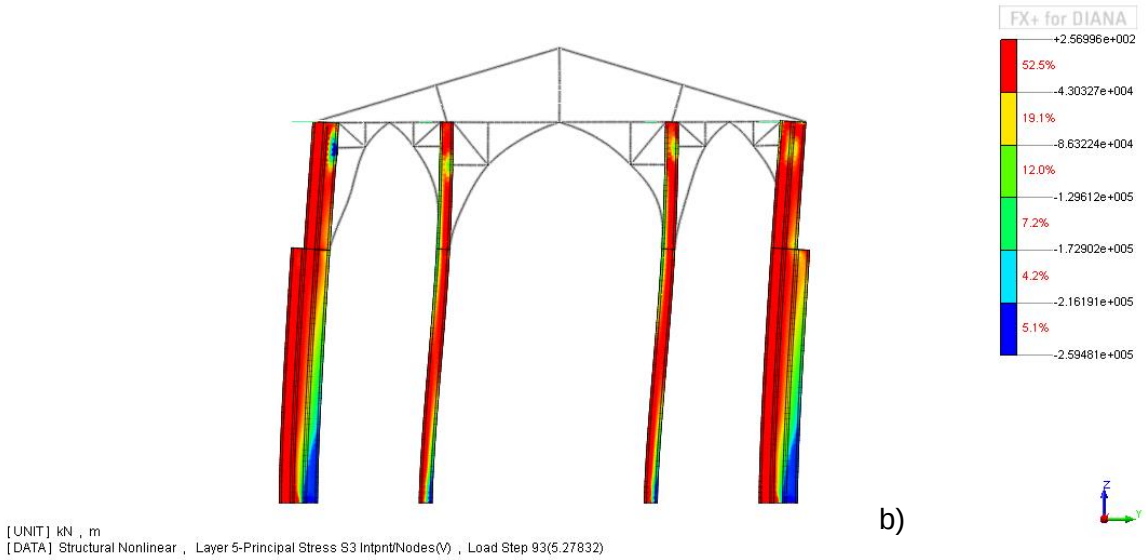

b)

Figure 87 - Maximum principal stresses for: a) external fibres; and b) internal fibres.

The normal stresses distribution in YY axis of the beam elements are within the expected shape, where the higher stresses would develop in the areas next to the connections with the columns frame, and in the middle of the arches (Figure 88 and Figure 89). The values of the stresses indicate that failure might occur at the connection of the beams of the vault with the reinforcement bars. The stresses along the tie beam have a significant reduction when compared with Model 1, since the span of these horizontal elements decrease significantly.

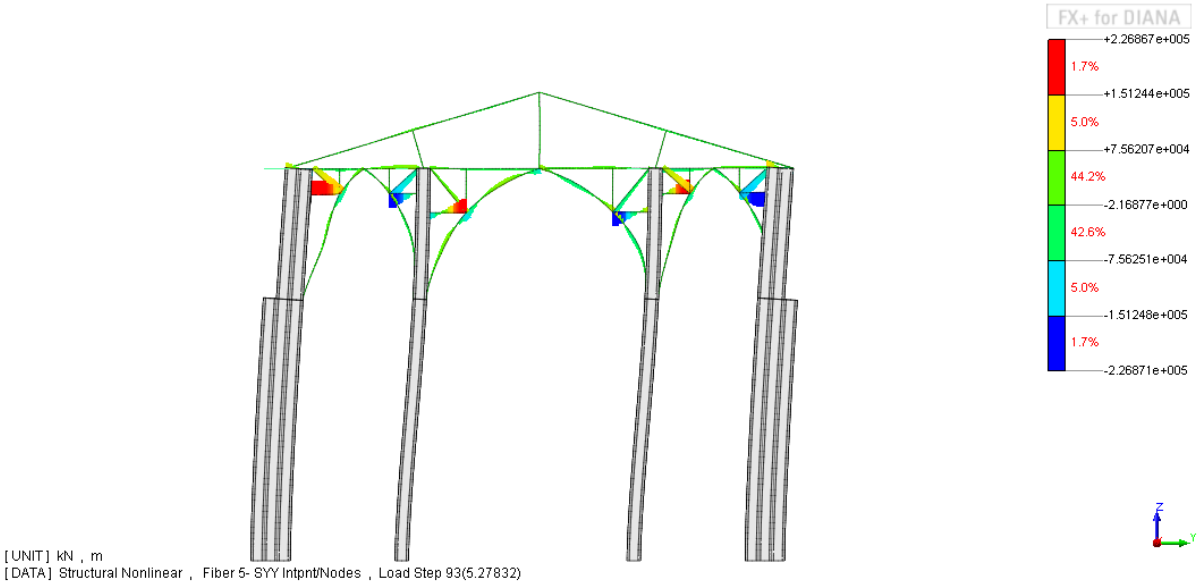

Figure 88 - Normal stresses at the upper fibre of the beam elements of the truss.(kPa)

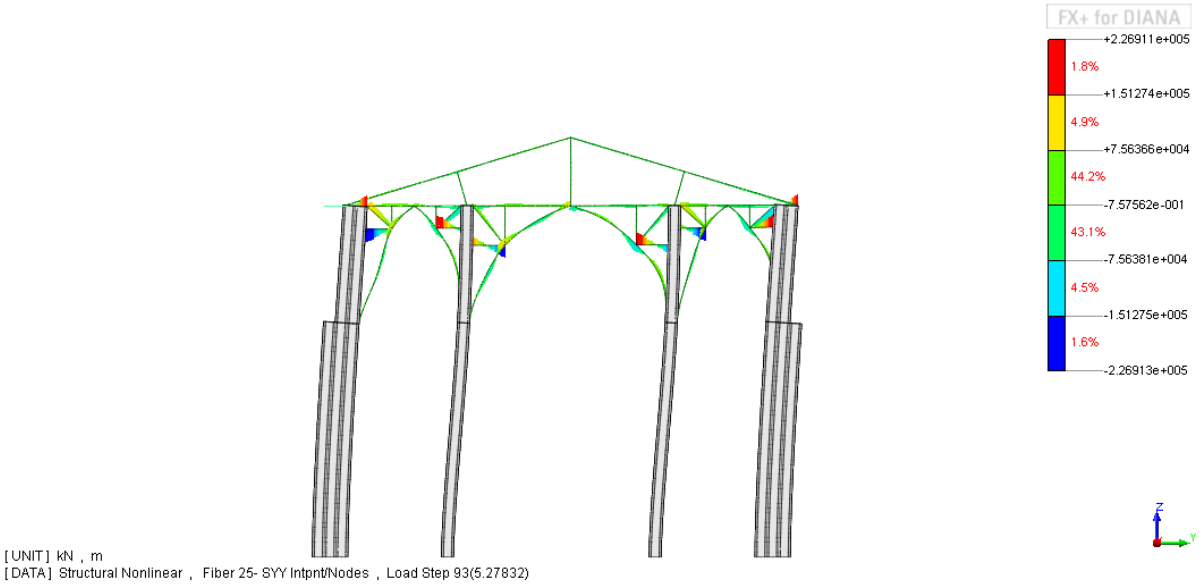

Figure 89 - Normal stresses at the lower fibre of the beam elements of the truss.(kPa)

The maximum stresses occur at the base of the columns, and slowly decrease as they head to the middle of the column, and when they reach the connection with the beam of the arch and the column, they increase again, due to stress concentration, but a reduction of the stresses at the top of the columns is noted (Figure 90).

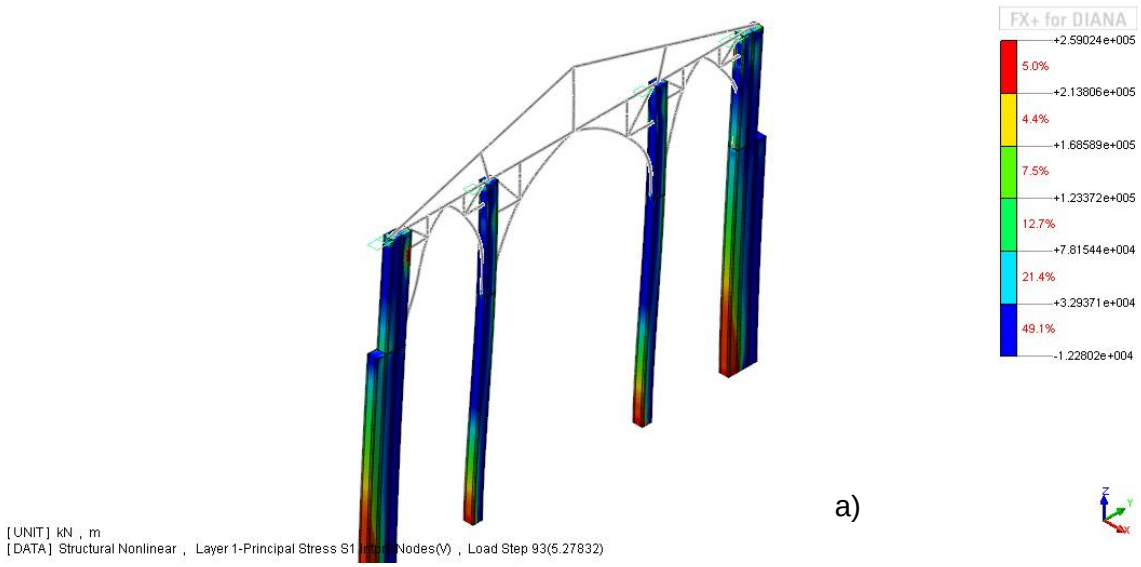

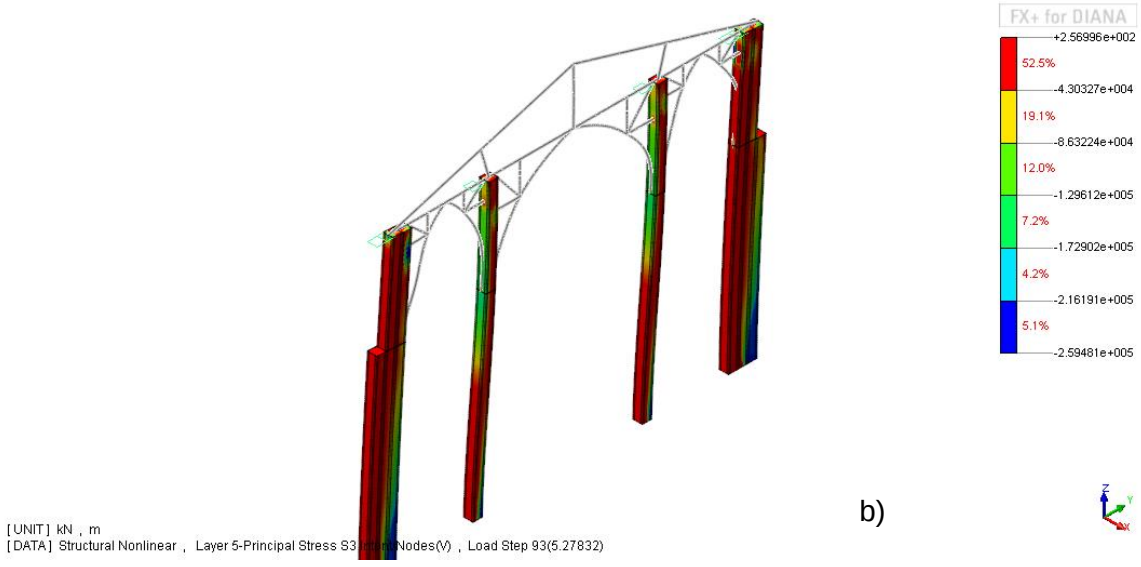

Figure 90 - Maximum principal stresses for: a) external fibres; and b) internal fibres.

Figure 91 presents the Von Mises stress distribution. It is noted that for the presented load step, the mechanism that correspond to the structure's collapse have started. The base and the connection between the horizontal reinforcement bars have a concentration of stresses that indicate the possible location of hinges and the beginning of the collapse mechanism, so a global failure mechanism is obtained.

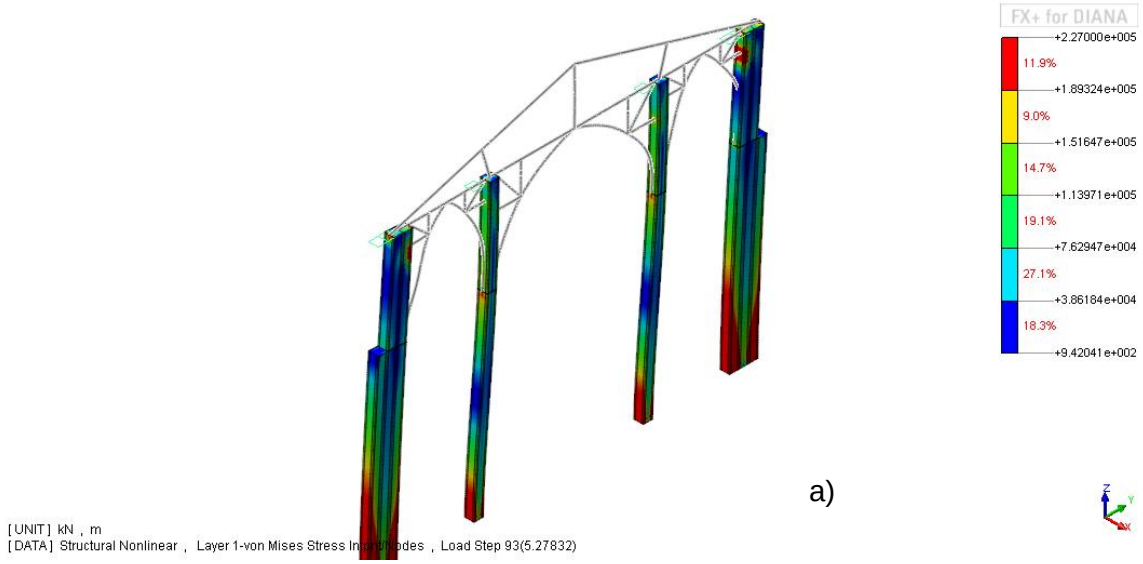

a)

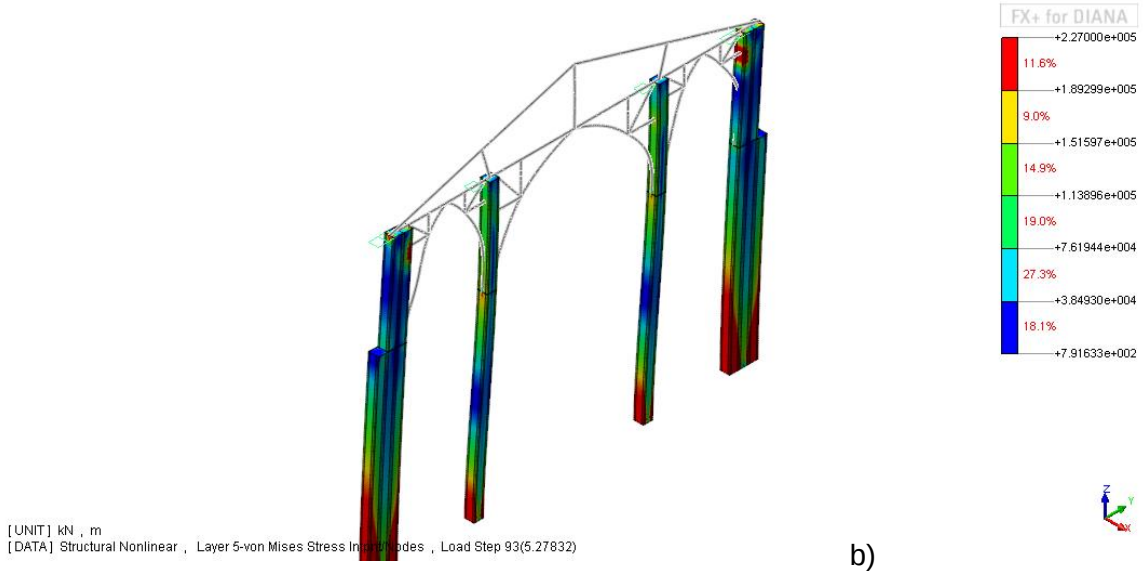

b)

Figure 91 - Von Mises stress distribution for: a) the external fibres; b) internal fibres. (kPa)

5.3 Discussion of the corrosion effects

In order to understand what effects the corrosion have on the structural behaviour, the pushover analysis for Model 2 on the two directions were performed, under different degrees of corrosion, namely, 20% and 40%. The corrosion damage was modelled as a reduction of the thickness of 20% and 40% for all the shell elements of the columns.

Figure 92 and Figure 93 present the capacity curves for the gravitational loads and seismic action, respectively, for the different levels of corrosion.

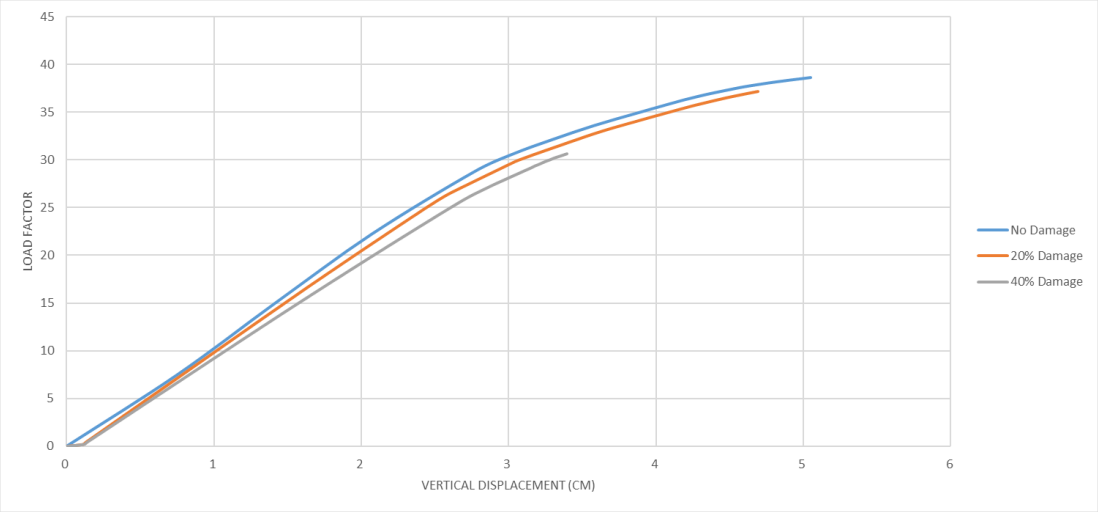

Figure 92 - Capacity curve for the gravitational loads taking into account different levels of damage.

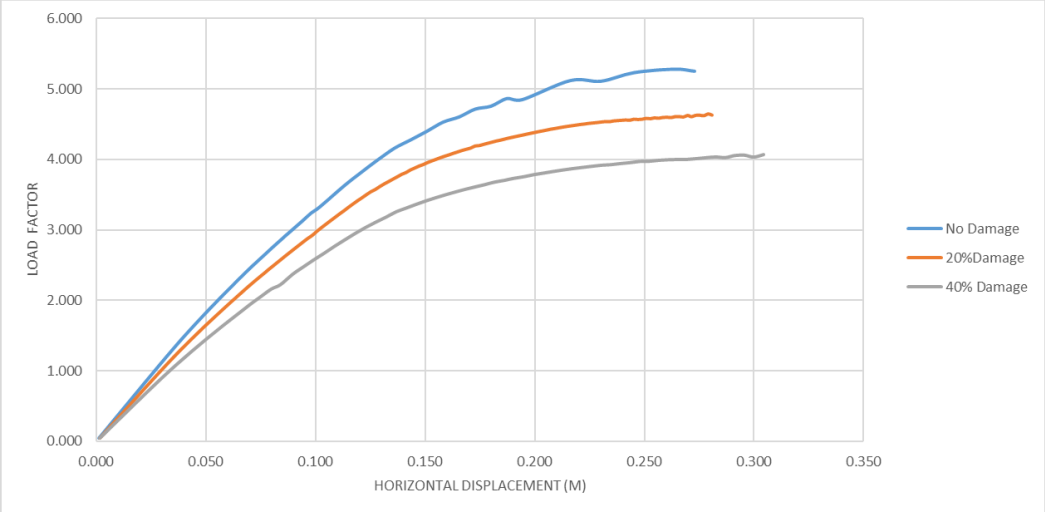

Figure 93 - Capacity curve for the seismic action taking into account different levels of damage.

Figure 94 presents the decrease on the capacity of the structure, depending on the damage on the structure. As it was expected, the capacity of the structure decreased as the damage increased, in which the maximum reduction of the load factor is equal to 22% with respect to the model without damage.

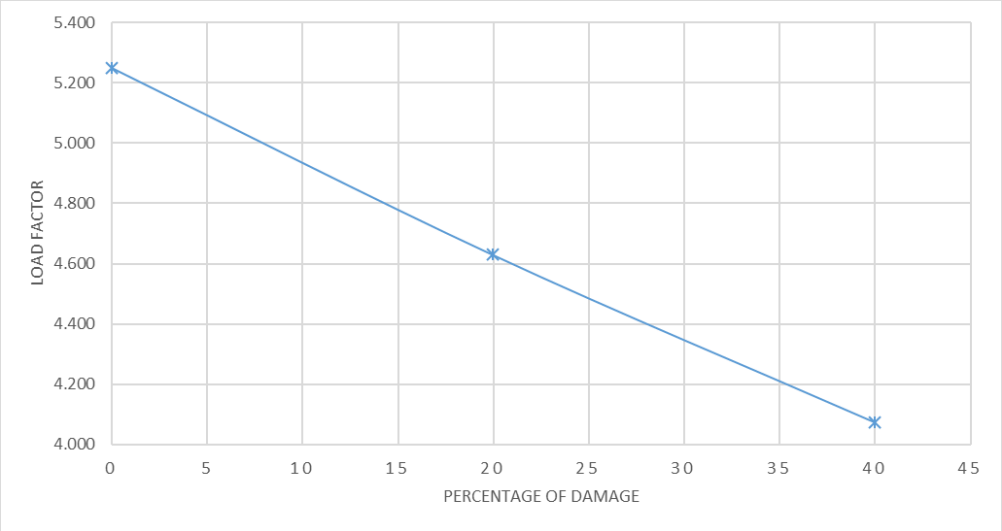

Figure 94 – Decrease on the horizontal capacity of the structure depending on the damage.

Figure 95 presents the decrease on the vertical capacity of the structure, depending on the damage on the structure. As it was expected, the capacity of the structure decreased as the damage increased, in which the maximum reduction of the load factor is equal to 21% with respect to the model without damage.

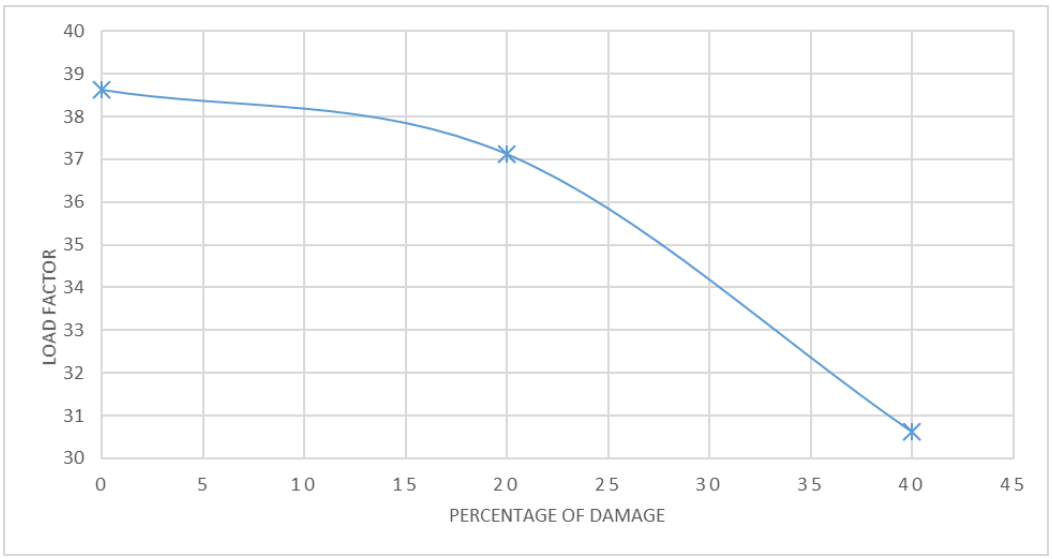

Figure 95 - Decrease on the vertical capacity of the structure depending on the damage.

6. CONCLUSIONS AND FUTURE WORKS

It is a duty of the society in general to protect the architectural heritage. Heritage means cultural identity, means a part of history of mankind in the World. It is because of this that the mentality needs a change. In other words, it is not only on the richer countries that heritage must be preserved. The governments should prioritize, and act as fast as they can. Policies regarding assessment of heritage should change to avoid losses due to catastrophic events.

The San Sebastian Church is a historical building with unique features. The materials used on the structure, its location, the reason why it was built that way are factors that make it special.

Several experimental testing was done on the past, namely, column cross-section reduction tests to determine the column cross-sectional losses; Ground penetrating radar was used to know how were the soil conditions, it was used to check the existence of steel beams below the floor, to check the existence of drainage lines and to confirm the possibility of the existence of a cellar; Inclinometers were used to determine if any relevant movement was happening; Temperature and humidity monitoring was also performed, since humidity is a factor that fastens the corrosion process. Furthermore, dynamic identification tests were carried out, and the natural frequencies and the mode shapes were estimated.

Regarding the results obtained in this work, several conclusions can be stated:

- Model 1 had a maximum load factor of 10.5 for the gravitational loads, and failure occurred locally at the beam connection with the lateral posts.

- Model 2 had a maximum load factor of 37, and failure occurred at the middle span of the rafters, with excessive tensile stresses. The central arch also presented excessive compressive and tensile stresses. However, it is noted a great reduction on the values of the stresses at the tie beam.

- Model 1 for the seismic load presented a maximum load factor of 3.8, a much higher value than the reference one in Manila (0.42g). In this model, the collapse occurred at the connection between the truss and the columns. For this model, the mechanism formation would start at the base and at the beam connections.

- Model 2 for the seismic load presented a maximum load factor of 5.3, a much higher value than the reference one in Manila (0.42g). In this model it is noted at the lower beam of the roof, a decrease on the stresses, due to the span reduction, and a global failure mechanism was obtained.

In what concerns the diagnosis of the structure, a detailed inspection of all structural elements including damage detection and evaluation is recommended.

The choir floor should be also studied, and their structural elements should be characterized. The thickness of the vaults should be determined, since its thickness might affect the lateral stiffness of the

structure, and depending on the thickness, its inclusion on the numerical model should be evaluated. An inspection to the dome should also be carried out, aiming at verifying their geometry properties.

Finally, a global model of the church should be prepared and calibrated, aiming to evaluate the global seismic performance of the church and identifying the most vulnerable elements. The global model should be calibrated based on the natural frequencies and mode shapes estimated by the identification tests.

7. BIBLIOGRAPHY

Caetano, Elsa. 2000. “Dynamics of Cable-Stayed Bridges : Experimental Assessment of Cable-Structure Interaction.”

Conservation and Development Foundation, San Sebastian Basilica. 2014. “San Sebastian Basilica - Final Conditions Assessment Report.”

Daniels, David J. 2004. *Ground Penetrating Radar*.

Diana, TNO. 2016. “User ’ S Manual Theory.”

Ivanova, Blagovesta, Radi Ganev, and Miloš Drdácký. 2013. “International Journal of Architectural Heritage : Conservation , Analysis , and Restoration Historical and Condition Survey of the St . Stefan Bulgarian Metal Church in Istanbul.” (April 2013): 37–41.

Leggio, Christine N. 2012. “Investigation of the Deterioration of the Trompe L ’ Oeil Interiors of San Sebastian Basilica , Manila , Philippines.”

Magalhães, Filipe. 2010. “OPERATIONAL MODAL ANALYSIS FOR TESTING AND MONITORING.”

Mendes, Nuno, Rui Tiago Seabra, and Paulo Lourenço. 2016. “Dynamic Identification Tests of the Sebastian Basilica, Manila, Philippines.” (June).

Romanillos, Emmanuel Luis A. 2001. *The Augustinian Recollects in the Philippines, Hagiography and History. Manila, Philippines : Recoletos Communications Inc. , 2001.*

Wong, Ivan, Timothy Dawson, and Mark Dober. “EVALUATING THE SEISMIC HAZARDS IN METRO MANILA , PHILIPPINES.”

Wyss, Max. 1979. *Earthqueke Prediction and Seismicity Patterns*.